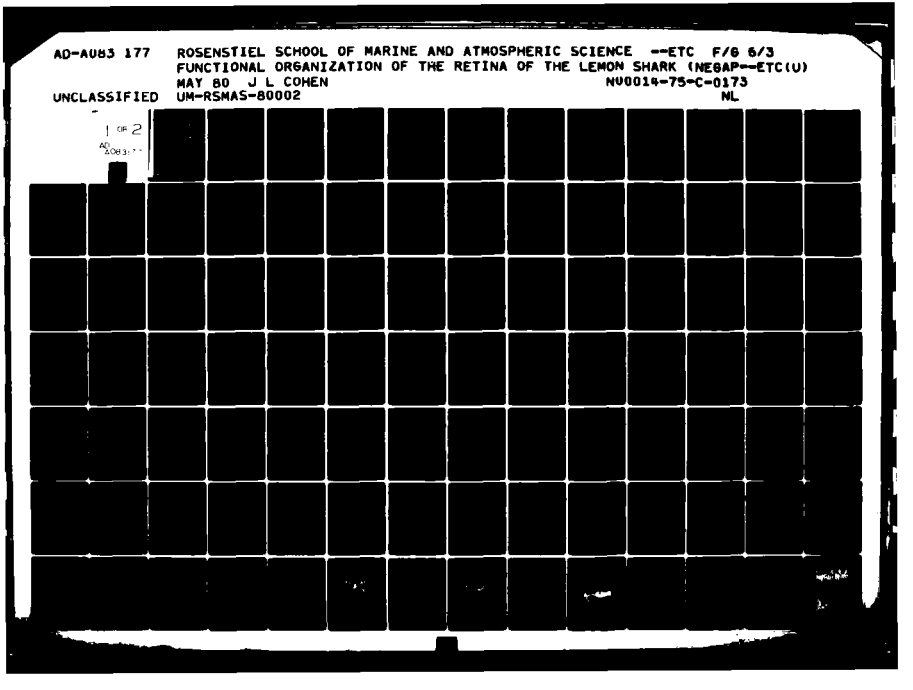
AD-A083 177 ROSENSTIEL SCHOOL OF MARINE AND ATMOSPHERIC SCIENCE --ETC F/G 6/3
FUNCTIONAL ORGANIZATION OF THE RETINA OF THE LEMON SHARK (NEGAP--ETC(U)
MAY 80 J L COHEN N00014-75-C-0173
UNCLASSIFIED UM-RSMAS-80002 NL
1 OF 2
AD A083177

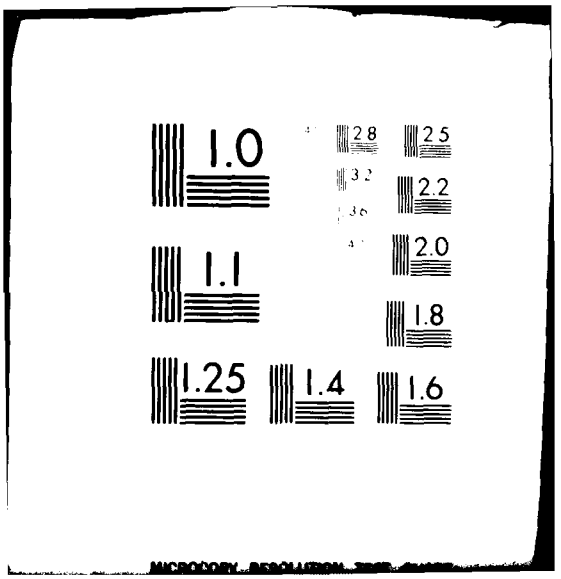
1.0
2.8
2.5
3.2
2.2
3.6
2.0
1.1
1.8
1.25
1.4
1.6

UNIVERSITY OF MIAMI

ROSENSTIEL SCHOOL OF MARINE AND ATMOSPHERIC SCIENCE

LEVEL II

UM RSMAS-80002

Technical Report

May, 1980

FUNCTIONAL ORGANIZATION OF THE RETINA OF THE LEMON SHARK (NEGAPRION BREVIROSTRIS, POEY): AN ANATOMICAL AND ELECTROPHYSIOLOGICAL APPROACH

by

Joel L. Cohen

The Office of Naval Research
Contract N00014-75-C-0173

MIAMI, FLORIDA 33149

UNIVERSITY OF MIAMI
ROSENSTIEL SCHOOL OF MARINE AND ATMOSPHERIC SCIENCE
4600 Rickenbacker Causeway
Miami, Florida 33149

TECHNICAL REPORT

May 1980

FUNCTIONAL ORGANIZATION OF THE RETINA OF THE LEMON SHARK (NEGAPRION BREVIROSTRIS, POEY): AN ANATOMICAL AND ELECTROPHYSIOLOGICAL APPROACH

by

Joel L. Cohen

A Report to the Office of Naval Research
of Research Supported by
Contract N00014-75-C-0173

UM-RSMAS-80002

William W. Hay
Dean

COHEN, JOEL LEONARD (Ph.D., Marine Biology)

FUNCTIONAL ORGANIZATION OF THE RETINA OF THE LEMON SHARK (NEGAPRION BREVIROSTRIS, POEY): AN ANATOMICAL AND ELECTROPHYSIC APPROACH. May, 1980.

Abstract of a doctoral dissertation at the University of Miami.

Dissertation supervised by Drs. Samuel H. Gruber and Duco I. Hamasaki.

Light microscopy of the retina of the lemon shark reveals two populations of photoreceptor cells in the ratio of 5 rods to 1 cone. Electron microscopy confirms that the conically tapering photoreceptors are in fact cones. Golgi stained material reveals cells typical of a vertebrate retina. Three varieties of interplexiform cells (i.e. a class of retinal cell with the cell body located in the proximal portion of the inner nuclear layer and with processes going to both plexiform layers) were described for the first time for an elasmobranch.

Extracellular recordings of lemon shark ganglion cells revealed three types of responses; ON, OFF and ON-OFF. Area-threshold curves reveal a receptive field of 0.85 to 1.45 mm in diameter which corresponds to 5.13 to 8.76 degrees of visual angle.

Measurement of spectral sensitivity revealed both rod and cone components of the OFF cell mechanism. OFF cells were also found with pure cone input. The peak sensitivity in the dark adapted state was at 519-522nm. Upon light adaptation the peak shifted to 547nm. Chromatic adaptation had no effect on the spectral sensitivity curves, implying only one cone input.

ON-center cells had both input from rods and cones. In the dark these two receptors acted together to produce a spectral sensitivity at 519-522 nm. Upon light adaptation the peak of the spectral sensitivity curve shifted to 547 nm.

Chromatic adaptation had no effect on these spectral sensitivity curves.

The on component of the ON-OFF center cells had the same spectral sensitivities and receptor inputs as the ON-center cells. The off component of the ON-OFF center cells had the same spectral inputs and sensitivity as the OFF-center cells.

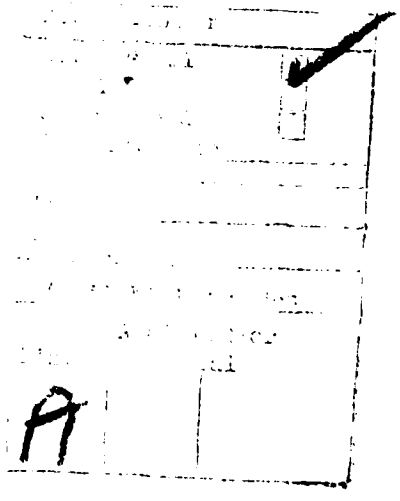

ACKNOWLEDGMENTS

I would like to extend my sincere appreciation to the chairman of my dissertation committee, Dr. Samuel H. Gruber, for giving me the opportunity to do this study.

Special appreciation and thanks are given to Dr. Duco I. Hamasaki, co-chairman of my committee for his scientific judgment and encouragement during this study.

I would also like to sincerely thank the members of my committee, Drs. Arthur A. Myrberg Jr., William Evoy and Daniel K. Odell, for their help and encouragement during this project.

I am especially grateful to the following people: Mr. Robert Hueter for the many hours of discussion during the course of this study, for his beautiful drawings, as well as for his friendship; Dr. Tom Robertson for his encouragement and assistance during many tiring hours of experiments; Mr. Tom Walmsley for technical assistance; Mr. Alan Baldridge and Ms. Mary Danio, librarians, for all the help they gave me; Dr. Douglas Anderson for allowing me to use his laboratory facilities; Mr. E. Barry Davis for the many hours of assistance he gave me; Ms. Barbara French for her skills as a photographer; Ralph Fernandez, Hank Poor, Shelly Schrager, and Ross Schwelm for assistance with the writing of the computer programs; and Ms. Ruth Trencher for her generosity and kindness.

Finally, I would like to extend my warmest thanks to all my friends, who gave me the encouragement and support that allowed me to accomplish this study.

This study was supported by Office of Naval Research contract N 000 14-75-C-0173Subl.

TABLE OF CONTENTS

LIST OF FIGURES

CHAPTER ONE

INTRODUCTION

General Remarks

The visual apparatus of vertebrates consists of the eye, visual pathway, and the higher neural center. The optical system of the eye forms an image of an object in space onto the retina. The retina changes the image, which is composed of photons of light, into a neural signal. The neural signal undergoes some preliminary form of processing within the retina before it is sent, via the optic nerve and tract to higher visual centers in the brain. Here it undergoes final processing so that the image can be perceived by the animal. The extent of the processing that the neural signal undergoes within the retina and higher visual centers depends, in part upon the type of animal under investigation. In general, the retinas of lower vertebrates carry on a series of processing comparable to that seen in the visual cortex of higher mammals (Lettvin et al., 1959; Maturana et al., 1960).

Duplexity Theory

After studying the retinal anatomy of many varieties of animals, Schultze (1866) noticed that those animals active during daylight hours possessed many cones and few rods, while the animals active at night had mostly rod retinas. He came to the conclusion that animals possessed two receptor systems, one for daytime and the other for night vision. Furthermore, he suggested that cones are for daylight vision, while rods are for night vision.

Since the time of Schultze, this observation has come to be known as the Duplexity Theory. It states that rods are responsible for achromatic, hazy vision in dim light, while cones operate under bright light conditions to give sharp,

chromatic vision (Walls, 1942).

Most animals, do not possess retinas with pure rod or pure cone populations. Their retinas usually contain a mixture of both rods and cones. As a result, these animals can extend the time period over which they can be active. But having a duplex retina requires a trade-off: inherent in the Duplexity Theory, is the fact that an animal's visual system is designed for either sensitivity or acuity (Walls, 1942). These in turn depend upon the structure of the entire visual system, including eye, retina and visual pathway.

One set of facts that contributed to the Duplexity Theory was the observation by Purkinje (1825), that the apparent brightness of red and blue objects differed according to the levels of light intensity. At dawn a blue object will appear brighter than a red object compared to during the day. This shift in sensitivity of wavelength with changes in level of adaptation became known as the "Purkinje Shift." Munz and McFarland (1973) suggested that the Purkinje shift is an adaptation for twilight vision. They showed that underwater, twilight is more monochromatic than sunlight with higher sensitivity in the shorter (blue) wavelengths. The Purkinje shift toward shorter wavelengths during scotopic (night) vision is therefore an adaptation for twilight vision where the blue wavelengths of light predominate.

Retinal Anatomy

The vertebrate retina possesses five major types of neurons, the nuclei of these neurons are arranged in three nuclear layers, while synaptic contacts between cells are confined to two plexiform layers. The photoreceptor cells can be divided into two classes; rods and cones. Both types of receptors are composed of an outer segment, inner segment and synaptic terminal.

The retinas of a large number of elasmobranchs contain both rod and cone photoreceptors. This was not always thought to be the case. Early investigators

of elasmobranch retinas reported that the elasmobranch had pure rod retinas (Schultze, 1866; Verrier, 1930; Franz, in Walls, 1942). This view prevailed even to recent times (Gilbert, 1961, 1963; Ali and Anctil, 1975).

However, cones have been found in twenty five species of elasmobranchs (Walls, 1942; Gruber and Cohen, 1978). While they vary morphologically from slender rod-like cells in Squalus (Stell, 1972) to truly cone-like in Negaprion (Gruber et al., 1963), they are all of the single cone type. In other animal groups however, morphologically distinct classes of cones have been found.

The double cone is found in holostean and teleostean fishes, amphibians, reptiles, birds, one monotreme, marsupials, but not in any placental mammal (Walls, 1942). One member of the double cone resembles a single cone and is called the principal cone. The second, or accessory cone has a distended myoid that curves around the inner segment of the principal cone (Rodieck, 1973).

The outer segment of the photoreceptor cells is filled with lamellar membraneous structures oriented perpendicular to the axis of the photoreceptor. In cones, which have a conically tapering outer segment, the lamella arise as an infolding of the plasma membrane. This continuity with the plasma membrane is not seen in the rods. The lamella of the rods are distinct from the plasma membrane and appear as a series of stacked discs or saccules (Rodieck, 1975).

The transduction of photons of light to a neural signal takes place in the outer segment, where the visual pigment is located as part of the saccules (Hubbell and Bownds, 1979).

Evidence that photoreceptor cells were derived from ciliated ependymal cells can be seen in the outer segment. It is connected to the inner segment by a ciliary stalk which, in cross section contains nine pairs of tubules arranged in a circle. The central pair, usually found in motile cilia is not found in photoreceptors (Rodieck, 1973).

The distal part of the inner segment, known as the ellipsoid contains mitochondria, which indiates that the metabolic activities of the receptor cell takes place here; mitochondria of cones are more numerous and more densely packed than those in rods (Dunn, 1973). This suggests that the cones have a higher metabolic rate than rods.

Proximal to the ellipsoid is the parabaloid, a glycogen containing region of the inner segment. The function of the parabaloid is not known (Rodieck, 1973).

The most proximal part of the inner segment is a region known as the myoid. It is found in fishes, amphibians and birds. The myoid changes length according to the state of adaptation. The function of this photomechanical movement is to move the outer segments into the villous processes of the pigment epithelium. This would shield the outer segments of the rods from light. The cones migrate in the direction of the external limiting membrane in light (Walls, 1942).

According to Ali and Wagner (1975) the retinomotor response in fishes is found only in teleosts with the exception of the holostean, Amia calva. Wang (1968) however, found movement of the cones in the nurse shark, Ginglymostoma cirratum, while Cohen and Gruber (unpublished observations) found no movement in lemon shark photoreceptors.

Nuclei of photoreceptors are generally located vitread to the external limiting membrane and form the outer nuclear layer. The thickness of this layer varies from two to many layers of nuclei. Cone nuclei of the nurse shark straddle the external limiting membrane, while those of the stingray, Dasyatis, were situated on the receptor side of the membrane (Hamasaki and Gruber, 1965).

Information flows vertically in the retina from outer to inner plexiform layers by means of bipolar cells. Information is carried laterally by the

horizontal and amacrine cells. This is suggested both by anatomical and electrophysiological evidence (Rodieck, 1973).

Processes from bipolar and horizontal cells extend toward photoreceptor terminals and synapse with them in the outer plexiform layer.

Bipolar cells have their nuclei located in the inner nuclear layer. Cajal (1892) recognized two types of bipolar cells in teleosts: giant and small. Each type connects to either rod or cone cells respectively. Stell (1967) showed that small bipolars of the goldfish synapse exclusively with cones, while the giant bipolars synapse with both cones and rods.

Witkovsky and Stell (1973) using the smooth dogfish, Mustelus canis, which possesses few cones, classified its bipolar cells according to the location in the outer plexiform layer where their axons terminate. Using this classification scheme they described five types and subtypes of bipolar cells. Type a1 was monostratified and its axons terminated in the distal 1/3 of the IPL. The horizontal distance the axon spanned was the longest for any of the bipolar cell types, being 400 to 600 μm. It possessed a Landolt's club that was cylindrical or bulbous in shape (Landolt's clubs were first described for amphibians and their function is unknown according to Hendrickson (1966)). Type a2 bipolar cells terminated in the distal 1/2 of the IPL, were multistratified and had a filamentous or flask-shaped Landolt's club. Type b bipolar cells were the only class of bipolar cells possessing bulbous terminals. They lacked a Landolt's club. Their axons proceeded vertically or obliquely from the perikaryon to the middle of the inner plexiform layer. Two forms of bipolar cells terminate in the proximal 1/3 of the IPL. Type c1 was monostratified, while c2 was multistratified. No Landolt's club was associated with either c type of bipolar cell.

Axonal and dendritic spans of elasmobranch bipolar cells far exceed those

found in mammalian retina such as cat or monkey. Boycott and Dowling (1969) found bipolar cells in the monkey with spans from 5 to 30 µm; Boycott and Kolb (1973) found a range of 20-50 µm in cat. Bipolar cells processes of Mustelus spread from 25 to 600 µm (Witkovsky and Stell, 1973). Parthe (1972) found giant bipolar cells with dendritic spans of 350 µm in the teleost Eugerres.

Horizontal cells are thought to be responsible for mediating lateral interaction in the distal portion of outer nuclear layer (Werblin and Dowling, 1969). Horizontal cells have their perikarya or cell bodies located in the inner nuclear layer. The defining characteristic of a horizontal cell is that all of its processes terminate in or about the outer plexiform layer (Rodieck, 1973).

Horizontal cells in elasmobranchs are noteworthy for their large size. Yamada and Ishikawa (1965), described the horizontal cells of Mustelus cells; external and internal. Membrane specializations between horizontal cells of the same layer were also seen.

Using Golgi impregnated material, Stell and Witkovsky (1973) found three rows of horizontal cells in the smooth dogfish, Mustelus. These were designated as the first row or external (H1), second row or middle (H2) and third row or internal (H3) horizontal cells. External horizontal cells were cuboidal and measured 20-25 µm vertically and up to 200 µm horizontally, these horizontal cells to make contacts with rods. Second row horizontal cells were flattened cells with fusiform perikarya. These cells also contact only rods. H3 horizontal cells were stellate. In Mustelus, cones contact only internal horizontal cells. This is the reverse of what is found in teleosts, which also possess very large horizontal cells. In the goldfish, external horizontal cells make contacts only with cones (Stell, 1967).

Toyoda et al. (1978), using the electron microscope as well as intracellular recording, reported that in the stingray, Dasyatis, the inputs to the middle (H2)

and internal (H3) horizontal cells were the same as in Mustelus. Only rods were in contact with middle (H2) horizontal cells and only cones contacted internal (H3) horizontal cells. But they found that both rods and cones contact the external (H1) horizontal cells.

Amacrine cells are neurons lacking an axon. Their perikarya are located along the proximal region of the inner nuclear layer and their processes terminate in or about the inner plexiform layer (Rodieck, 1973). Recent reviews on vertebrate retinal anatomy in general (Dunn, 1973) and elasmobranch retinal anatomy in particular (Gruber and Cohen, 1978) attest to the limited knowledge of amacrine cells in lower vertebrates.

Stell and Witkovsky (1973) described amacrine cells in the retina of Mustelus with unusually long processes that are monostratified. Two processes up to 2.5 mm in length originate from the small, fusiform perikaryon and descend from opposite poles to the IPL where they bifurcate.

Ganglion cells are tertiary neurons whose axons leave the eye to form the optic nerve. They are the only pathway by which information from the retina reaches the brain. They are normally confined to their own layer which is proximal to the inner plexiform layer. However, cells termed displaced ganglion cells can be found in the inner plexiform and inner nuclear layer. They are normally classified according to their dendritic spread (Rodieck, 1973).

Neumayer (1897), investigating the retinas of elasmobranchs showed that in the rays Raja, the ganglion cell layer is not well defined. Ganglion cells were found in both the optic nerve and inner plexiform layers. Four categories of ganglion cells were found. One type was monostratified, while a second was multistratified. A third type had a diffuse dendritic spread throughout the IPL. A fourth type had dendrites which did not read the IPL, but were found in the

ganglion cell and optic nerve fiber layer. Very large ganglion cells were also described.

Stell and Witkovsky (1973) investigated the ganglion cells of Mustelus canis using Golgi, reduced silver and Methylene blue staining. They found ganglion cells with perikarya among the optic nerve fibers. Ganglion cells of various size and form were found but only giant ganglion cells were described. Of these, three classes were distinguished; 1) ordinary, 2) displaced and 3) intermediate giant ganglion cells.

Ordinary giant ganglion cells were found near the proximal margin of the inner synaptic layer. The cell bodies were semilunar, measuring 10-12 μm deep and 30-40 μm wide. Dendrites branched up to 1 mm in length from the cell toward the inner plexiform layer.

Displaced giant ganglion cells had perikarya located among the amacrine cells. They were also semilunar and measured 15-18 μm deep and 25-35 μm wide. dendritic fields measured 2.03 mm by 1.89 mm.

The intermediate ganglion cells had flattened perikarya of the same dimensions as the ordinary variety. They were confined to the inner plexiform layer. Their dendrites did not stain well so details of their structure are absent.

Shibkova (1971) investigated the retinas of the dogfish, Squalus acanthias and the ray, Raja clavata, and found that giant ganglion cells composed only a small percentage of the neurons in the ganglion cell layer.

Giant ganglion cells of the type found in Mustelus (Stell and Witkovsky, 1973) were also found in the retina of the hammerhead shark, Sphyrna lewini (Anctil and Ali, 1974).

Ali and Anctil (1974) reported small ganglion cells scattered throughout the inner plexiform and the optic nerve layers in the electric ray (Narcine brasiliensis). Larger ganglion cells were found near the inner nuclear layer as

well as in the ganglion cell layer. Large ganglion cells were also found in the inner plexiform and nerve fiber layer of the freshwater stingray, Paratrygon motora.

Retinal Organization

Neural signals proceed from cell to cell by means of synapses. Two principal types of synaptic contacts have been described in vertebrate retinas. The first, the ribbon synapse is characterized by an electron dense bar or ribbon in the presynaptic cytoplasm surrounded by synaptic vessicles. The ribbon is always oriented at right angles to the plasma membrane and is associated with multiple postsynaptic elements (Dowling, 1970).

Conventional synapses are characterized by an accumulation of synaptic vessicles on the presynaptic side of the membrane and an increase in membrane density on both pre and postsynaptic elements. Only one post synaptic element is associated with conventional synapses (Dowling, 1970).

Rod and cone synaptic terminals can be differentiated morphologically. Rod terminals, called spherules, are spherical in shape and smaller than cone terminals, which are called pedicles. In addition, spherules have fewer invaginations than the pedicles.

Invaginations in photoreceptor terminals contain several postsynaptic contacts surrounding a synaptic ribbon. Usually two lateral processes surround a single central process. The central process is normally a bipolar cell dendrite (Stell, 1967; Boycott and Kolb, 1973) but can also be a horizontal cell dendrite (Stell, 1976). The lateral processes originate from horizontal cells. This arrangement is seen in fish, turtles, cats and primates and is considered to be the usual case for all vertebrate classes (Rodieck, 1973).

In addition to the invaginating synaptic contact, bipolar cells may make superficial contacts to the base of the cone pedicle (Dowling and Boycott, 1966;

Dowling and Werblin, 1969; Lasansky, 1971).

Synapses between horizontal cell dendrites onto bipolar cells have been reported for the catfish, mudpuppy, and rabbit (Naka, 1976; Dowling and Werblin, 1969; Dowling et al., 1966).

Photoreceptors were thought to function independently of one another (Naka and Rushton, 1966). Recently, electrophysiological and anatomical evidence has accumulated to show that this is not necessarily true. Electrical coupling has been described between rods and between cones in toad retina (Gold and Dowling, 1979). It was also shown between rods of turtle (Copenhagen and Owen, 1976) and between cones of carp, between rods, cones and rods and cones of carp, catfish, toad, turtle, rabbits, and monkeys (Witkovsky et al., 1974; Gold and Dowling, 1979; and Raviola and Gilula, 1973).

The inner plexiform layer represents the retina's second synaptic layer. In this layer are found the axon terminals of bipolar cells and the dendrites of amacrine and ganglion cells.

As in the outer plexiform layer both conventional and ribbon synapses are found in the inner plexiform layer. However, ribbon synapses are found only in bipolar cell processes (Rodieck, 1975).

At the ribbon synapse, the bipolar cell is presynaptic to an amacrine cell. The amacrine cell in turn may then be presynaptic to this same bipolar cell axon. This is termed a reciprocal synapse (Dowling and Boycott, 1966).

Conventional synapses between amacrine and bipolar cells, bipolar and ganglion cells, amacrine and ganglion cells and amacrine and amacrine cells are also found in the inner plexiform layer of all vertebrates studied. These contacts often occur in series and are termed serial synapses. For example, an amacrine cell synapses onto an adjacent amacrine cell, which in turn synapses onto a third amacrine cell.

Witkovsky and Stell (1973) found that 30% of the ribbon synapses in the IPL of Mustelus had only one post synaptic element. This was also seen in the skate retina, Raja (Dowling, as reported in Witkovsky and Stell, 1973). Bipolar cell ribbon synapses with two postsynaptic elements showed variation in the orientation of the ribbon to the membrane. Counts of synaptic contacts showed that reciprocal synapses occurred only a small percentage of the time.

Regions of close apposition between adjacent cells, known as gap junctions, were observed in Mustelus. Specialized junctions have been seen between bipolar cell axons and ganglion cell perikarya in monkey and human retina (Dowling, as reported in Witkovsky and Stell, 1973).

Ganglion Cell Responses

Ganglion cells are the only neurons in the retina that exclusively use only regenerative, all or none action potentials to transmit information to the next neuron.

Using the eyecup preparation of the frog, Hartline (1938, 1940a, b) was the first to study the activity of single retinal ganglion cells. Three types of ganglion cells were described, according to their responses to a flashing light. ON units (20%) responded with a transient burst of activity when the light stimulus was turned on and the activity was maintained for the duration of the stimulus. Fifty percent of the units produced discharges at ON-OFF but had no maintained discharge during illumination. OFF responses (30%) discharged only when the stimulus was turned off.

Hartline (1938) defined the receptive field (RF) of a ganglion cell as the area of the retina which must receive illumination to cause a change in the firing pattern of a particular ganglion cell. The different classes of responses (ON, OFF, ON-OFF) described were found throughout the retina irrespective of stimulus size or state of adaptation. Barlow (1953) showed that the ON-OFF

units possessed an inhibitory surround which decreased the responses of the receptive field to stimuli.

Kuffler (1953) recorded directly from ganglion cells in the cat's retina. By introducing the electrode through a puncture in the eyeball, he was able to preserve the natural optics of the eye. By moving a spot of light to different positions on the retina he recorded different responses.

From the same ganglion cell, the receptive field was partitioned into concentric zones. In the central zone, called the receptive field center (RFC), either an ON or an OFF response was recorded. Outside the RFC, was a zone which yielded a response of opposite sign; i.e. for an ON center cell, illumination of this surround region resulted in inhibition at light ON and excitation at light OFF. An overlapping zone between the two produced ON-OFF responses, these zones were mutually antagonistic. If a spot of light placed in the center of the receptive field produces an ON response, simultaneous stimulation of the surround will cause a reduction in the ON response.

Lettvin et al. (1959) using the intact frog found five classes of ganglion cells. They termed class 1 sustained contrast detectors. These responded only if the sitmulus was a sharp edge, either lighter or darker than the background. These cells were considered analogous to Hartline's ON units. The second class of cells were called net convexity detectors. These fibers responded to a small object passing through their receptive fields. Straight edges did not elicit a response, but the corner of a square target did. The greater the convexity of the object, the greater the intensity of the response. Class 3 ganglion cells were termed moving edge detectors and corresponded to Hartline's ON-OFF units. These units responded to any edge moving through their receptive fields. The fourth type of ganglion cell was called the net dimming detector and was analogous to OFF units. These cells responded to reductions in the amount of

illumination in the receptive field. These four classes of units appear to detect different features of the stimuli. As such they show that the retina of lower vertebrates is capable of complex operations.

Lettvin et al. (1959) recorded from a small group of fibers which did not seem to have a distinct receptive field. These units increased their rate of firing with decreased light intensity until a maximum firing rate was reached in total darkness. These units were termed dark detectors.

Investigations on elasmobranch ganglion cells have confirmed the presence of the same three classes of ganglion cell responses described by Hartline (1940a).

Stell et al. (1970, 1971, 1975) investigated the ganglion cell responses of the smooth dogfish Mustelus. Most of the units recorded were ON units. An annular stimulus failed to evoke responses in most cases, but a bar evoked OFF and ON-OFF responses. Spectral sensitivity for both excitatory and inhibitory processes was 500-510 nm. Receptive field centers up to 1.5 mm in diameter were found. Upon light adaptation the size of the receptive field centers decreased.

Receptive fields of 1.5 mm diameter with an annular surround extending to 3 mm were found for the ray, Raja (Dowling and Ripps, 1970).

Responses of ganglion cells to different wavelengths of light have been classified as either non-opponent or opponent. Non-opponent cells respond with the same activity (e.g. ON-response) to all wavelengths of light in the center and surround. Opponent cells have responses that depend on the wavelength of the stimuli.

Wagner et al. (1960, 1963) described opponent and non-opponent cells in the retina of the goldfish. One type of spectrally opponent cell was inhibited with spots of red light (650 nm) but excited by green light (500 nm) that stimulated a

slightly larger area of the retina. A second type of cell responded with excitation to red light and inhibition to green light.

Daw (1968) extended the study on goldfish opponent ganglion cells. By using an annulus in addition to spots of light, he was able to show that many of these cells had antagonistic surrounds that extended up to 5 mm in diameter. He called these type O cells. Stimulation of the periphery with red and green annuli produced ON and OFF responses respectively. Type O cells are therefore double opponent cells and implies that goldfish ganglion cells receive input from at least two types of cones.

Daw (1968) found that some cells lacked a surround, and these were termed type P. A third type of color opponent cell, type Q, was similar to type O cells, except the red mechanism exerted a stronger effect than did the green mechanism.

Spekreijse et al. (1972) found an additional group of color coding cells in the retina of the goldfish. In these ganglion cells, the sign of the response to red and blue stimuli was the same, while stimuli of intermediate wavelengths (green) gave the opposite response.

Beauchamp and Lovasik (1973) found a blue mechanism in goldfish that had the same response sign as the green mechanism and opposite that of the red. The results of Spekreijse et al. (1972) were attributed by Beauchamp and Lovasik (1973) to the sensitivity of the secondary or beta band peak of the absorbance spectrum by the red sensitive pigments. The beta band is a secondary absorbance peak of a visual pigment and is due to the cis-bond of the chromophore part of the pigment molecule. It has a maximum peak at 400-420 nm dependent on the λmax of the pigment (Rodieck, 1973).

Similar opponent cells were also seen in the carp (Witkovsky, 1965). Opponent color cells have been recorded in the rhesus monkey (DeMonasterio and

Gouras, 1975), macaque monkey (Gouras, 1968), and ground squirrel (Michael, 1968). Spectrally opponent ganglion cells have not been found in elasmobranchs.

Purpose

External cues in the environment affect the behavior of animals. Animals receive information from the external environment through their sensory systems. Therefore, an important step in understanding an animal's behavior, is understanding the limits of its sensory systems. This approach was emphasized by Tinbergen (1951) who related the importance of sensory physiology to the study of animal behavior.

If visual cues play a role in the behavior of the lemon shark, it is important therefore, to know the range of stimuli to which the visual system is capable of responding to.

Previous studies on the retina of the lemon shark, have shown the presence of two, morphologically distinct classes of photoreceptors; rods and cones (Gruber et al., 1963). According to the Duplexity Theory, vision is mediated by these two classes of photoreceptors. Rods are said to act at low luminance and provide achromatic vision, while cones act at high luminance and provide for color vision. It was the purpose of this dissertation to determine whether the retina of the lemon shark has the capability for chromatic, daylight vision.

One way to establish the possibility of color vision is to determine whether information necessary for color vision is present in the ganglion cells of the retina, and that at least some photoreceptors operate at photopic levels.

A necessary prerequisite for color vision is the presence of at least two independent receptor systems having photopigments with different absorption spectra. Recording from ganglion cells, was therefore an important technique since determination of their spectral inputs provides indirect evidence of the absorption spectra of this input.

It was also the purpose of this study to gain some insight into the processing of visual information in the retina of the lemon shark, so as to compare it with other animals. While most studies of the visual system of aquatic animals utilized fresh or salt water bony fish, this study utilized the lemon shark, a cartilaginous fish, which possesses a duplex retina, i.e. containing rods and cones. Possession of a duplex retina with a high ratio of cones to rods sets it apart from most elasmobranchs utilized in vision research. The goldfish and carp have become the 'typical fish' for studies on vision in aquatic animals, yet they are not very visual animals. In the same regard, the dogfish (Squalus acanthias) and the smooth dogfish (Mustelus canis) have become the 'typical elasmobranch' in similar types of studies even though they too are not visual animals.

It appears from my observations that the lemon shark has a morphologically and physiolgoically duplex retina. Two photoreceptor systems can be seen in histological preparations and the presence of two spectrally distinct mechanisms was also demonstrated. While color opponent mechanisms were not seen, it was shown that at least one photoreceptor system operates under photopic conditions, as well as under dim light conditions.

This dissertation has two sections. The first section discusses the anatomy of the retina of the lemon shark. The methods include both light and electron microscopy as well as various staining methods to differentiate not only cell bodies, but also their dendritic and axonal extensions. It is my feeling that contemporary sensory physiology requries an anatomical foundation. For example, animals active during the day were found to have retinas that were morphologically different from those animals active at night. The finding of cone-dominated retinas in the diurnal animals and rod-rich retinas in the nocturnal animals was the basis for the Duplexity Theory.

Electrophysiological studies later showed that animals which possessed a duplex retina had a shift in the peak of their spectral sensitivity curve when going from light to dark adapted conditions. In addition, a discontinuity often marked the transition of various functions when going from light to dark-adapted states. These 'phenomena' were easily explained as the transition from cone to rod function because of the anatomical foundation previously laid down, i.e. the presence of two types of photoreceptors, rods and cones.

The basic foundations, necessary for this study have already been laid down. Examination of the lemon shark retina by light microscopy has shown the presence of two types of photoreceptors that resemble rods and cones (Gruber et al., 1963). But would the segregation of these receptor cells into rods and cones still hold up when they were examined with the electron microscope? This was a piece of information important to my dissertation.

All animals that have color vision, possessed cone photoreceptors. It was therefore important to my dissertation that the photoreceptors purported to be cones could indeed be shown to be cones, using a variety of criteria.

To study the way information transmitted in the retina, it was necessary to classify the cell types that make up the retina. This has never been done before for the lemon shark and was especially important since previous visual studies on elasmobranchs utilized species whose retinas were dominated by rod photoreceptors. Since there were great differences in the ratio of rods to cones between the lemon shark and the other species of elasmobranchs, it was vital to determine if there would also be differences in the population of cells that compose the remaining retinal layers.

While my study was not meant to be the definitive study on the lemon shark retina, it was meant to serve as a foundation upon which further studies might be built on. Therefore, the basic building blocks of such studies, anatomy and physiology, were provided.

CHAPTER TWO

METHODS AND MATERIALS

Animals

Immature lemon sharks (Negaprion brevirostris), 1-1.5 years old, approximately 60-80 cm, total length, were obtained from a private collector in the Florida Keys. The animals were caught by a cast net. This produced minimal injury to the animals compared to other capture methods, such as hook and line. The sharks were transported to the marine laboratory (60 km) by placing them in plastic bags. The bags were filled with enough seawater to cover the gills of the shark, ice cubes were then added, the bag inflated with 100% oxygen and tied off. The sharks tolerated the trnasportation well as noted by their immediate recovery in the holding tank. The animals were kept in a 6000 liter recirculating seawater system and were allowed some time to acclimate to their new surroundings. All sharks were fed cut pieces of fish and usually started eating within a few days of their arrival. This attests to their excellent physiological and stress-free condition.

Preparation

After one hour dark adaptation, eyes were removed under dim red light. The anterior segment, including the lens, was cut off with a razor blade and discarded. The vitreous was removed by using filter paper to lift it up. The vitreous was then cut with scissors. The remaining eyecup (retina, choroid and sclera), was trimmed to 1 cm^2 and placed on a pedestal located inside a chamber. This procedure took 2-3 minutes. A Ringer's soaked wick placed under the eyecup, and connected to a silver-silver chloride wire, served as the indifferent electrode.

The chamber (Fig. 1) was constructed of solid brass and coated with silicone rubber. A moat surrounded the pedestal and was connected to a reservoir. the reservoir and connecting moat were fileld with elasmobranch Ringer's solution (16.38 g/l NaCL, 0.89 g/l KCl, 1.47 g/l $CaCL_2$-H_2O, 0.38 g/l $NaHCO_3$, 1.00 g/l dextrose, 21.6 g/l urea, 0.07 g/l NaH_2PO_4-H_2O) (Cavanaugh, 1975). A mixture of 95% oxygen and 5% carbon dioxide was bubbled into the reservoir. the pH of the Ringer's solution was 7.2. The chamber rested upon a piece of vibration dampening and placed inside a light-tight, Faraday cage.

Recording System

Extracellular action potentials were recorded with insulated tungsten electrodes. The electrodes were electrolytically sharpened by repeatedly dipping a 0.05 cm diameter tungsten wire in a saturated potassium nitrate solution, while passing an alternating current between the wire and a carbon rod. The electrode was examined periodically and the procedure was repeated until a sharp tip, as determined by observation under a microscope, was produced. The electrode was then coated with insulating material (INSL-X) and baked in an oven until hard (Hubel, 1957).

The recording system consisted of a high impedance preamp (WPI, M4A) connected to another preamplifier (Tektronix, 122) where the signals were amplified and filtered. The high cutoff filter was set at 1000 Hz while the low cutoff filter was set at 80 Hz with a time constant of 0.002 seconds. The signal was displayed on a storage oscilloscope (Tektronix 5115). Action potentials were monitored via an audio amplifier connected to the oscilloscope. For permanent records, photographs were taken from the oscilloscope screen with an oscilloscope camera (Tektronix M-5).

Optical System

The optical system consisted of two channels of light, one for test stimuli and the other for background illumination (Fig. 2), the light source for both channels was a 150 watt tungsten halogen bulb (OSRAM $64633) which was underrun at 14 volts, 9 amps by a regulated D.C. power supply (Electro Products Lab). Only achromatic lenses and first surface mirrors were used in this system.

The filament of the lamp was imaged on electromagnetic shutters (SH) (Vincent Associates) by lenses L1 and L4. Heat absorbing filters were placed in the optical path to eliminate infrared radiation. The beams were then collimated by lenses L2 and L6. The light then passed through the iris diaphragm (AP) which controlled the size of the image. The diaphragm was mounted on a moveable stage which was used to position the test stimulus. The diaphragm in channel 2 was modified so that specific size openings could be chosen. The size of the openings, as measured on the retina, were determined with a calibrated stage micrometer placed in the position normally occupied by the retina. The beams from the two channels were combined by a mixing cube (MC). A final lens, L3, imaged the aperatures of the diaphragms onto the retina.

The intensity of the test spot and the background illumination was controlled by thin film neutral density filters (Ditric Optics) which were tilted slightly to eliminate differences in density resulting from multiple reflections.

The stimulus wavelength was selected by the use of narrow band (1/2 amplitude bandwidth = 10 nm) interference filters (IF) (Ditric Optics). The following wavelengths were used: 430 nm, 460 nm, 490 nm, 500 nm, 510 nm, 520 nm, 540 nm, 560 nm, 580 nm, 610 nm, 630 nm, 660 nm.

For the chromatic adaptation experiments the following color filters were used: blue-green (Bausch and Lomb 90-1-570), yellow (Bausch and Lomb 90-2-520), red (Kodak Wratten #92) and orange (Kodak Wratten #23).

The duration of the stimulus was controlled by means of a grass (Model S44) stimulator connected to the control boxes of the electromagnetic shutters. Selenium photocells (Edmond Scientific) were used to monitor the duration of the stimulus.

Calibration

Spectral transmissions, peak wavelength and bandwidth of the interference filters, neutral density and broad band color filters were measured on a recording spectrophotometer (Cary 15 and Unicam 800).

The spectral radiance of the stimulus was measured with a radiometer which utilized a pin photodiode that had a flat response across the spectrum. The detector was positioned in the system in place of the eye and a reading of the spectral radiance (in μwatts/cm^2) at each wavelength was recorded. Figure 3 shows a graph of the energy output of the lamp at each wavelength. The output of the lamp at 610 nm was 2.47 x 10 12 photons/cm^2.

Comparing the value etched on the neutral filters with the spectrophotometric calibration, I found a significant discrepancy between the measured values and those stated on the filters. Thus, density values for all combinations of the neutral density filters, were calculated using the data from the spectrophotometer. These values were then tested by measuring the transmission of the filters with the radiometer. There was excellent agreement between the calculated values and those measured with the radiometer. These calculated 'actual' neutral density values were used in all of the calibrations subsequently performed.

Procedures

The animal was dark adapted for 45-60 minutes. The eye was then removed under dim red light. After the anterior segment was cut away and the eye

trimmed, it was placed in the chamber. A plexiglas cover, with an opening for the electrode and light stimuli was placed over the chamber.

The electrode was lowered into the vitreous and centered on a 0.67 mm spot of 610 nm light. The retina was allowed to dark adapt an additional 30 minutes. The electrode was slowly lowered to the retinal surface as the retina was stimulated with 500 msec flashes of dim 610 nm light. Usually, as soon as the electrode touched the retinal surface, either spontaneous activity or a light activated response was seen. If no activity was found, or if an injury potential was recorded, the electrode was lifted and a different part of the retina was tested.

Spectral activity in the dark adapted state was determined as follows. A criterion respnose was defined as 1-2 spikes. The stimulus intensity (neutral density filter) value needed to give the response 50% of the time was designated at the threshold response.

The criterion response was determined for a 0.67 mm spot at each wavelength, starting at 610 nm. The order of wavelengths was 630 nm, 660 nm, 430 nm, 460 nm, 490 nm, 500 nm, 510 nm, 520 nm, 540 nm, 560 nm. The threshold response was found by removing neutral density filters from the stimulating beam until a threshold response of 1-2 spikes was seen on the oscilloscope screen and heard on the audio monitor. This procedure was repeated until the response for the starting wavelength was replicated.

The size of the receptive field center was then determined with white light. The threshold response was determined for spots of light of increasing diameter, concentric to the electrode. This is known as the area threshold method (Stell et al., 1975). The diameter of the spot sizes as they appeared on the retina ranged from 0.35 mm to 3.05 mm.

To determine if the lemon shark retina possesses both a scotopic (dark)

system where only the rod photoreceptors should operate and a photopic (light) system where only the cones should operate, the eye was adapted with a steady background of white light. This raised the thresholds to the photopic system and allowed the cones to operate. If two systems were present, white light adaptation might move the spectral peak horizontally towards the red end of the spectrum from that of the dark adapted spectral sensitivity. This is because adaptation with white light should raise the threshold of the rod system to a point where it saturates and therefore no longer operates. The resulting spectral sensitivity curve should be that of the cone photoreceptors which does not have to differ from that of the rods.

The eye was then light adapted with a relatively large diameter (2.1 mm) spot of white light. A test flash of 610 nm was used to follow the threshold change over the time course of the light adaptation until no further change in threshold was seen. The stimulus intensity at threshold was determined for each wavelength. The presentation of stimuli differing in wavelength was repeated until the threshold responses at the initial test wavelength could be replicated. If the response to all wavelengths was of the same sign (ON or OFF) the retina was stimulated with large diameter stimuli (0.5 cm) of 460 nm, 540 nm and 610 nm to quickly determine if wavelength dependent or color opponent.

Responses could be evoked from the surround of the receptive field. Cells having the sign of the response (ON or OFF) dependent upon the wavelength are termed color opponent cells. The opponency can be between the center and surround of the receptive field. If a cell is a color opponent type, a large diameter spot of light, which stimulates both the center and surround simultaneously should elicit a response from either the center or surround, according to the wavelength. However, there should be a wavelength where the spectral sensitivity of the center and surround overlap. At this point, a lare

diameter stimulus should elicit a response from both center and surround, i.e. ON-OFF.

To determine if there were more than one cone input to the ganglion cells, it was necessary to use chromatic adaptation. By adapting with light that is more effective to one cone system than the other, the responses seen will be that of the cone system less sensitive to the adapting light. If only one system were present, the spectral sensitivity curve would only be moved vertically; its shape will remain unchanged. For example, using a blue-green filter should depress the sensitivity of any cone pigment system with sensitivities in the blue-green region of the spectrum. This would allow any cone pigment system with sensitivities not in the blue-green region of the spectrum, but for example with maximum sensitivity in the red region of the spectrum, to respond. Use of a yellow filter would likewise depress sensitivities in the yellow to red portion of the spectrum and would allow any pigment system that had maximum sensitivities in other parts of the spectrum, for example in the blue-green portion, to appear.

For the chromatic adaptation experiments, broad band cut-on and cut-off filters were used (see previous section). Backgrounds were turned on and thresholds followed until stable. A criterion response was determined at each wavelength. This was done until repeatable responses could be obtained from the initial wavelength.

The ERG was monitored by increasing the time constant of the preamplifier. The loss of the ERG meant that the condition of the preparation was deteriorating. If this occurred, the experiment was terminated. The experimental protocol for a single unit took 6-7 hours to complete. Successful experiments on the eye would typically last 12-14 hours.

Data

To obtain the spectral sensitivity curves, the neutral density threshold values were corrected first for actual neutral density and then quantized. As can be seen from Figure 3, the output of the lamp is nonlinear across the spectrum. More energy is emitted in the red end than in the blue end. To correct for differences in the lamp output and differences in the energy of quanta at different wavelengths. a correction factor was calculated which, when subtracted from the threshole intensity measurement, would yield a relative log quantal threshold. The reciprocal of the threshold, sensitivity, was used in the construction of the spectral sensitivity curves.

The correction factor was calculated as follows:

1. The reading of the lamp, taken with a radiometer, placed in the position normally occupied by the retina in uwatts/cm^2 was converted to a base 10 logarithmic value.
2. Each log spectral radiance value was then subtracted from the spectral radiance value at 430 nm. This step corrected for differences in the energy of a quantum at each wavelength, since there is more energy in a quantum at 430 nm than at 660 nm.
3. Each wavelength was divided by 430 nm to obtain a ratio.
4. The resultant was converted to a $\log_{10}$ value.
5. The value obtained in (4) was subtracted from the value obtained in (2). This corrects for differences in quantal output of the lamp in the blue and red end of the spectrum.

The following example will illustrate the effects of the correction factor. Curve A in Figure 4 shows an example of raw data. Curve B shows the same data after completion of step 2. Curve 3 shows the data after correction for differences in quantal output in the blue and red ends of the spectrum.

Since the data are in relative terms, they were normalized at 580 nm. This was done by choosing one set of data and transforming all other sets of data so as to bring their 580 nm point up to the 580 nm point of the chosen set of data. This value became the weighting factor and was added to the data at all wavelengths. The mean: $\pm$ 1 standard error of the mean (SEM) was then calculated. Since neutral density values are logarithmic, the corrected threshold values were plotted as the log relative quantal sensitivity. Sensitivity being the reciprocal of threshold. However, this was plotted versus the reciprocal of wavelength, i.e. the frequency.

To objectively determine the peak (λmax) of the spectral sensitivity curve, a computer program was written to fit the data points to a Dartnall nomogram (Wyszecki and Stiles, 1967). The Dartnall nomogram allows the construction of the absorbance spectrum of any visual pigment that is based on the aldehyde of vitamin A1 (retinal). When plotted on a frequency or wavenumber (wavenumber = 1/wavelength) basis, the absorbance spectrum of visual pigments all have the same shape, the only difference being the point of maximum sensitivity. Thus, curves constructed from the nomogram can be compared to the experimentally determined action spectrum to obtain the wavelength of maximum sensitivity (max). A segmented, straight-line approximation to the set of data curve points of the Dartnall nomogram was shifted and scaled for closest horizontal fit to the measured points and the appropriate displacement used to determine the peak of the curve. This program was run on a Univac 1100 computer.

Light and Electron Microscopy

Eyes were fixed in either one of two ways. In the first method eyes were removed and cold (4°C) 2.25% phosphate buffered gluteraldehyde (pH 7.3) was

injected into the globe through a 25 guage needle. The eyes were then immersed in additional fixative.

For the second method, animals were anesthetized with MS-222 and perfused through the heart with elasmobranch Ringer's solution, followed by cold ($4^{o}C$) 2.25% phosphate-buffered, gluteraldehyde (pH 7.3). eyes were subsequently removed and stored in fixative for 2 hours and immediately postfixed in either 1 or 2% osmium tetroxide. They were then dehydrated in alcohols and embedded in epoxy resin (Epon 812, Kodak).

Thick sections (1-2 µm) were cut on a microtome Sorvill MT-1. Thin sections for transmission electron microscopy (TEM) were cut on the MT-1 or on an ultramicrotome LKB. Sections for light microscopy were stained with toluidine blue or phenylalaninediamine (Pease, 1963). Those for TEM were stained with lead citrate and uranyl acetate and photographed on an electron microscope (JELCO). Measurements of histological material were made using a calibrated ocular micrometer. The values reported were not corrected for shrinkage.

Golgi Stain

Eyes were removed from animals anesthetized with MS-222 and cut into pieces. The pieces of eyecup were immersed in a solution containing a mixture of 2.25% gluteraldehyde, 0.90% paraformaldehyde, 0.40% OsO_4 and 1.35% NaCl. This solution was buffered to pH 7.1 with 0.1 M sodium cacodylate. Pieces of eyecup were then washed with 0.1 M potassium dichromate for two days. The tissue was then rinsed in several changes of distilled water and transferred through several changes of 0.75% silver nitrate, where it remained immersed for two days. The eye was washed again in distilled water. Fixation in osmium-potassium dichromate and silver nitrate was repeated to increase the intensity of the stain.

The tissue was then dehydrated through a graded series of alcohols and embedded in 30% nitrocellulose. Sections were cut at 90 µm on a sliding microtome (AO). Following this, the serial sections were again dehydrated in a series of alcohols and left in cedar wood oil for a week before mounting. Drawings of cells were made using a microscope fitted with a camera lucida.

CHAPTER THREE

RESULTS

Anatomy

Most of the elasmobranchs which have been used in vision research have retinas which are anatomically rod dominated. This is in contrast to the lemon shark which has a duplex retina, containing large numbers of both rods and cones. The duplex retina is typical of the majority of vertebrates.

The lemon shark retina, as in other vertebrates can be divided into seven cellular and synaptic layers. These will be described in the following sections.

The retina of the lemon shark, including pigment epithelium and internal limiting membrane has a mean thickness of 206 µm.

Retinal Epithelium

The outermost (sclerad) part of the lemon shark retina, which is called the pigment epithelium in other vertebrates is 15.0 µm thick and made up of cuboidal cells, however, pigment granules are lacking in these cells. Therefore this layer should more appropriately be termed 'retinal epithelium' (Rodieck, 1975).

Photoreceptor Layer

Adjacent to the retinal epithelium is the photoreceptor layer (Fig. 5). This layer has a mean thickness of 60.5 µm as measured from the distal tip of the outer segment to the external limiting membrane. Each photoreceptor consists of two parts; an outer and an inner segment. The outer segment contains a series of lamallae stacked one on top of another. On these lamellae are located the photopigment molecules (Rodieck, 1973). The inner segment contains mitochondria and other organelles.

With the light microscope, I identified two types of photoreceptors in the retina of the lemon shark. The rods have a cylindrical outer segment that

extends from the termination of the outer segment to the external limiting membrane. Staining with toluidine blue brings out a dense region, the ellipsoid, located at the distal portion of the inner segment. The diameter of both outer and innner segment is approximately the same.

Cone photoreceptors are shorter than rods. The cone outer segment is tapered and reaches the level of the ellipsoid of the rods (Fig. 5). The diameter of the outer segment, measured mid-way along its length is 2.5 µm. The cone ellipsoid is larger and more darkly staining that that of rods. The width of the cone inner segment is 5.1 µm.

Gruber et al. (1963) found a rod to cone ratio of 12:1 throughout the retina of the lemon shark. I found a rod:cone ratio of 5:1 in the dorsal part of the lemon shark retina in the present study.

Previous studies on lemon shark photoreceptors have only made use of the light microscope (Gruber et al., 1963). Detailed differences in photoreceptor types can only be visualized using the electron microscope. In this study, I used the electron microscope to examine the fine structure of lemon shark retina, and in particular, the photoreceptors.

The discs of the rod outer segment are enclosed completely by a plasma membrane (Fig. 6). In the cone, indentations can be seen in the plasma membrane surrounding the outer segment (Fig. 7). By following the membrane, I noted that the indentations are caused by the continuity of the membrane with the discs. The discs are thus open to the extracellular space, a situation opposite to that found in the rods. The outer and inner segments are joined by a connecting cilium.

The darkly staining ellipsoid portion of the inner segment of rods and cones contains large numbers of mitochondria when viewed with the electron microscope. Differences in staining between the rod and cone ellipsoids are due

to the greater number of mitochondria per unit area in the cones than in the rods. In addition to the mitochondria, I saw smooth endoplasmic reticula, microtubules, and subsurface cisternae in the inner segment.

The rods and cones I found in the lemon shark retina are morphologically similar to those described in other vertebrates by Dunn (1973).

A dark band separates the inner segments of the photoreceptors from the nuclei of the outer nuclear layer. Because of its dark appearance, the band resembles a membrane and is even termed the external limiting membrane (ELM). Electron microscopy has shown that the band represents the sites of attachment between the photoreceptor cells and the Muller fibers (Rodieck, 1973).

Outer Nuclear Layer

The outer nuclear layer (ONL) consists of the nuclei of the photoreceptors. They form three layers of cells in the lemon shark (Fig. 5). Stained with toluidine blue, the cone nuclei appear lighter in color than rod nuclei and could thus be differentiated from them. The shape of the rod nuclei is ovoid, while the cone nuclei are teardrop shaped. I saw cone nuclei in the lemon shark at all three levels of the outer nuclear layer. This differs from the nurse shark, Ginglymostoma cirratum, where the nuclei occur adjacent to the external limiting membrane (Hamasaki and Gruber, 1965).

Outer Plexiform Layer

The outer plexiform layer (OPL) contains the synapses between photoreceptor, bipolar and horizontal cell dendrites. The photoreceptor terminals are well differentiated in the lemon shark. Figure 8 shows a typical rod terminal from the lemon shark retina. It is spherical, hence it is called a spherule. It is smaller than the cone terminal and the cytoplasm is filled with

spherical vessicles. Invaginating junctions containing bipolar and horizontal cell dendrites were seen at the basal portion of the spheriule, a dense bar or ribbon surrounded by parallel rows of synaptic vessicles was also seen (Fig. 8). The ribbon is separated from the surrounding membrane by a dense band of electron dense material known as the 'arcuate density' (Rodieck, 1975).

The cone terminal, or pedicle, is larger than the rod spherule (Fig. 7). The basal portion of the cone pedicle is flattened. Synaptic invaginations are more numerous in the cone pedicle than in the rod spherule. Ribbon synapses, which I saw in the spherule, were also seen in the pedicle.

Inner Nuclear Layer

The inner nuclear layer (INL) contains the perikarya of horizontal, bipolar, and amacrine cells. Also included in this layer are the nuclei and processes of the interplexiform cells which may be a type of bipolar cell.

As in other vertebrates, the INL of the shark retina is stratified. The horizontal cells occupy the distal portion, while the bipolar, amacrine and interplexiform cells occupy the proximal part.

Interspaced between the nuclei are Muller cells. These possess long, radially spreading fibers that run from the internal limiting membrane to the external limiting membrane. The nuclei of the Muller fibers are found in the INL and can be recognized by their fusiform shape.

Horizontal Cells

Three layers of horizontal cells are found in the retina of the lemon shark (Fig. 5). These have been called by Stell and Witkovsky (1973) the first row or external (H1), second row or middle (H2), and third row or internal (H3) horizontal cells. In the lemon shark, the horizontal cells are massive cells with a mean length of 42.1 µm (range: 25.4-53.3 µm). In Golgi stained material,

dendrites of these extend toward and reach the region of the photoreceptor synaptic terminals in the OPL (Fig. 9).

In gluteraldehyde fixed tissue, stained with touidine blue, I saw prominent ovoid (shaped) nuclei in the horizontal cells of each layer. These nuclei were located eccentrically in each cell. A prominent, darkly staining nucleolus was also seen. In transversely sectioned material the horizontal cells of the external (H1) and internal (H3) layers appear much thicker than those of the middle (H2) layer.

With the electron microscope, I was able to see that adjacent horizontal cells of the same layer interdigitate and overlap at their ends. Numerous membrane specializations occurred along the borders of adjacent horizontal cells (Fig. 10). In one type of membrane specialization, a space between the two membranes appears to widen at the junction. A symmetrical distribution of electron dense filamentous material lines both sides of the opposing membrane at this point. This type of junction termed Zonula adherentia (Peters, Palay and Webster, 1976) represents points of attachment between cells.

A second type of membrane specialization or junctional complex is structurally symmetrical. It consists of a narrowing of the membrane without obliteration of the gap between them. These are gap or electrical junctions and represent points of low electrical resistance where communication between cells is possible (Peters et al., 1976). Kaneko (1971) demonstrated the presence of a low resistance junction in the dogfish, by passing current between adjacent horizontal cells.

Bipolar Cells

The nuclei of the bipolar cells are situated in the proximal half of the inner nuclear layer. These form a layer two to three cells thick. Nuclei of bipolar

cells, in gluteraldehyde fixed tissue, stained with toluidine blue appear dark blue. A darker staining, centrally located nucleolus was also seen.

In general, input from distal neurons is received by dendrites spread along the OPL (Rodieck, 1973). Output from the bipolar cells is sent via axons that terminate at different levels in the inner plexiform layer and synapse onto ganglion cells.

Very little information about bipolar cells can be obtained from thick sectioned material. Only location, size of nuclei, along with relative number and position can be ascertained. With the Golgi stain, however, these cells can be completely visualized and classified because their dendritic arborizations and axonal processes can be seen. Only a small proportion of the cells in any given retina are stained by the Golgi procedure which is one of its advantages. If all cells were stained, details would be obscured. While classification of Golgi stained cells is possible, contacts between nerve cells can only be inferred, synaptic contacts can only be identified with the electron microscope. The classification scheme used here is a modification of the bipolar scheme used by Witkovsky and Stell (1973) for Mustelus.

I found much variability in cells classified according to categories such as stratification of axons, location of perikarya, presence of Landolt's clubs, etc. Therefore classification of bipolar cells, as discussed in this paper, is based on position of axon terminals, within distal, middle, or proximal portions of the IPL. Studies on other species utilizing the EM-Golgi technique have shown separation of rod and cone pathways through rod and cone bipolar cells that terminate in specific parts of the IPL (Nelson et al., 1978; Famiglietti et al., 1978). Classifying the bipolar cells of the lemon shark is a first step in deciding whether rod and cone pathways are also separate for the lemon shark retina, as they are in cat and carp. Differences between types of bipolar cells in the lemon shark

and the smooth dogfish (whose retina served as the basis for the present classification system), will be discussed later. Due to the capriciousness of the Golgi procedure, one is never sure that all types of a particular cell have been found. Thus, the cell types reported here should not be assumed to be the complete classification.

Type a bipolar cells have axons which terminate in the distal third of the IPL. These can be subdivided into:

Type a1, representing 11% of the 72 bipolar cells classified. They have monostratified axonal trees that extend into the distal 1/3 of the inner plexiform layer (Fig. 11). Their axons extend a considerable distance from the cell body, with a horizontal spread of up to 350 µm. This is the widest horizontal spread I measured in any of the bipolar cell classes of the lemon shark. There is little branching in these axons. The axon stem usually leaves the cell body vertically or occasionally at an oblique angle. The cell body is approximately 12.5 µm in diameter and is located in the distal 1/3 of the inner nuclear layer. The dendrites extend 60 µm, but not all of the dendrites were completely stained and thus, this may not represent the total extent of this class of bipolar cell axons.

Landolt's clubs, cylindrical to bulbous in shape, extended from the cell body toward the photoreceptor layer. They terminate just beyond the external limiting membrane.

Type a2: These bipolar cells were the most numerous and composed 38% of bipolar cells. They have multistratified axons that terminate in the distal 1/3 of the IPL. Their axons have many branches which spread from 45 to 80 µm. The axon stem appears to enlarge as it enters the IPL. From this enlargement, branches appear which bifurcate and then send off their own branches. These branches have bulbous expansions at their end (Fig. 11).

The cell body of a2 bipolars is slender (15 µm in diameter) and is located in the distal half of the INL. The dendritic spread is at least 45 µm. Vertical projections come off of the main dendrites. Slender, filamentous to bulbous Landolt's clubs arise from a position slightly OFF-center from the cell body and pass to a point just distal to the external limiting membrane.

Type a3: This type of bipolar cell (5% of the sample) has axon terminals in the distal 1/3 of the IPL. Its axons are multistratified, but do not send out projections as far as the type a2 bipolar cell. There are usually just four projections arising from the axon stem that end in terminal expansions (Fig. 11). The axonal spread is approximately 16 µm. The cell body, located in the middle of the INL, is approximately 11.8 µm in diameter and appears as a tubular expansion of the axonal stem as it travels distally.

The dendritic spread was small and difficult to visualize in these preparations due to precipitate in the outer plexiform and distal inner nuclear layer. These cells also ended with a filamentous to bulbous Landolt's club that projected through the ELM.

Type a4: A fourth type of bipolar cell with monostratified axons terminating in the distal 1/3 of the IPL was seen only occasionally (2%). Its axons were very long (135 µm) and spread in opposite directions (Fig. 11). The ovoid nucleus was located in the distal half of the INL. The cell bifurcated at its distal end and then branched into finer processes. No Landolt's club was present.

Cells whose axons terminated in the middle of the inner plexiform layer were termed Type b bipolar cells. Two forms of Type b cells were found.

Type b1: These cells represented 14% of the cells classified. Their axons were monostratified with a spread of 12- to 80 µm (Fig. 12). Their terminals ended in bulbous expansions. The cell body was located in the middle of the iNL. There was no Landolt's club. The dendrites ran horizontally for a distance

between 50 and 100 µm and then turned towards the photoreceptors.

Type b2: These cells made up 5% of the bipolar cells classified. They were multistratified with axons that terminated in the middle of the IPL (Fig. 12). The axons ran obliquely from the axon stem for a distance of 138 µm. Branches appear towards the end of the axon. The cell body, located in the distal 1/3 of the INL is funnel shaped, being approximately 11 µm in diameter. Dendrites appear to come off the outer margins of the part of the cell body nearest to the photoreceptors and spread out for a short distance.

Type c bipolar cells had axons that terminated in the proximal 1/3 of the inner plexiform layer. Two Type c bipolar cells were described.

Type c1: These bipolar cells were monostratified, and had their axons terminate in the proximal 1/3 of the inner plexiform layer, and represented 14% of the sample (Fig. 13). There was little branching of their axons which have a spread of 90 to 170 µm. A single axons stem bifurcates when it reaches the proximal part of the IPL. The cell nucleus is in the middle of the inner nuclear layer. I did not see a Landolt's club in any cell whose axons terminated in the proximal part of the IPL. Dendrites arose horizontally from the distal part of the perikaryon and traversed a distance from 50 to 100 µm.

Type c2: A second type c bipolar cell occurred in 11% of the sample. This cell wasmultistratified and had a spread of about 60 µm (Fig. 13). The axon terminals were highly branched. The ovoid cell body was located in the middle of the INL. A short stalk ran vertically towards the outer plexiform layer from the perikaryon. Dendrites arose from this stalk and extended horizontally for a distance of approximately 70 µm.

Interplexiform Cells

Cells which have their perikaryon in the inner nuclear layer and send processes to both outer and inner plexiform layer are, by definition, bipolar cells. However, there is another cell type located in the INL that sends processes to both outer and inner plexiform layers, termed the interplexiform cells. Interplexiform cells differ morphologically from bipolar cells in the location of their perikarya, which are located at the proximal edge of the inner nuclear layer among the amacrine cells. Interplexiform cells also differ from bipolar cells in having multiple processes coming off the cell body and going towards the inner plexiform layer. The processes that arise from the cell body and pass to the OPL separates the interplexiform cells from the amacrine cells, which have processes only in the IPL. Using the Golgi stain, I classified three varieties of interplexiform cells in the lemon shark retina.

The first type had a spherical perikaryon approximately 15 µm in diameter (Fig. 14). It was located along the proximal border of the INL. Axons arose from the proximal margin of the perikaryon, entered the IPL and traversed horizontally in opposite directions for a distance of 240 µm. A single dendrite arose out of the distal edge of the perikaryon and entered the outer plexiform layer.

A second variation of interplexiform cell had axons that branched (Fig. 14). Cells of this type had a single axonal stem which originated from the perikaryon then bifurcated at the proximal 1/3 of the IPL.

A third type of interplexiform cells in the lemon shark retina, sent highly branched processes form its cell body (Fig. 14). This type terminated in both the distal and proximal 1/3 of the IPL. A single dendrite, stouter than in the two previous variations transversed the inner nuclear layer. Finer dendrites came off this dendrite stem just before it entered the OPL.

Amacrine Cells

The amacrine cell body is located along the proximal margin of the INL. It has no axons but the dendrites terminate in the inner plexiform layer. The perikarya are spherical to ovoid and 7-15 µm in diameter. With the Golgi stain, the cell body, and the processes projecting from it can be visualized.

One type of amacrine cell I found in the lemon shark retina was monostratified with an ovoid cell body 7-10 µm in diameter, and located in the proximal 1/3 of the INL (Fig. 15). It has a single process coming off the proximal border of the perikaryon. This traverses the IPL obliquely until it reaches the proximal 1/3 of that layer.

A second type of monostratified amacrine cell also has an ovoid nucleus, 15 µm in diameter located in the proximal third of the INL (Fig. 15). It has processes coming off of opposite sides of the perikaryon. These processes are thicker than those of the previous cell type. They proceed obliquely from the cell body to the middle of the IPL then travel horizontally.

A third amacrine cell type has a spherical cell body 10 µm in diameter (Fig. 15). It has a single, thick process originating from the proximal edge of the perikaryon. The process then proceeds to the proximal 1/3 of the inner plexiform layer where it bifurcates, sending the two processes horizontally in opposite directions.

Ganglion Cells

The ganglion cells are third order neurons whose axons leave the retina to form the optic nerve. For the most part they are widely interspaced in the ganglion cell layer and among the nerve fiber layer. Ganglion cells of the lemon shark vary in size and shape. There are two classes of ganglion cells. The first type is the small ganglion cell, found in the ganglion cell layer. It measures

between 8 and 10 µm in diameter and has an irregularly shaped, eccentrically located nucleus. Nissl substance, or ribosomal endoplasmic reticulum, can be seen in sections stained with toluidine blue.

I observed other small spherical ganglion cells, approximately 10 µm in diameter, in the middle of the inner plexiform layer. These should be called 'displaced ganglion cells' because they were not restricted to the ganglion cell layer.

A second type fo ganglion cell is the giant ganglion cell. These cells vary in size from 20 to 30 µm in diameter. They have spherical nuclei with a deeply staining nucleolus. The cells are found not only in the ganglion cell layer, but in intermediate positions in the middle of the inner plexiform layer.

Additionally, giant ganglion cells were seen in the proximal margin of the inner nuclear layer along with amacrine cells. These displaced giant ganglion cells are similar to those found in Mustelus by Stell and Witkovsky (1973). They are semilunar in shape and flattened at the base. Figure 15 shows a displaced giant ganglion cell with part of one of its processes entering the inner plexiform layer. A Golgi stained preparation of the same type of cell (Fig. 15) shows the lateral extent of the dendritic spread.

The axons of ganglion cells of most vertebrates are non-myelinated until they exit the eye to pass through the lamina cribosa and enter the optic nerve. There they become myelinated. Elasmobranchs in general, and lemon sharks in particular, have myelinated axons throughout the nerve fiber layer (Fig. 17).

Electrophysiology

During the course of this study, 99 cells, or units, were studied: 63% (62) were OFF-units, 18% (18) were ON-units and 19% (19) were ON-OFF units.

The complete experimental protocol took 6-7 hours. Because of the length of time for the entire protocol, complete data were not obtained for every unit.

Complete and partial data were taken on 83% (82) of the cells studied, while 17% (17) of the cells were only classified as to type of unit.

Spontaneous Activity

Three types of spontaneous activity were recorded. The first was a high frequency burst of spike activity. These were large spikes whose amplitude decreased until the spikes disappeared. This activity resulted from lowering the electrode too fast, resulting in injury to the cell. The high frequency firing is the so-called 'injury potential.'

The second type of spontaneous activity was in the form of a continuous train of regularly occurring spikes. The rate of firing was 1-2 spikes per second and the size of the spikes was 250-300 μvolts. A small spot of light centered on the electrode had no effect on the discharge. Such activity has been reported in the frog from 'unhealthy' preparations (Barlow, 1953). However, another explanation is that the appropriate stimulus was not used, i.e. the proper feature necessary to excite this cell was not used.

The third type of activity was recorded from healthy preparations. This spontaneous activity was usually encountered as soon as the electrode touched the retinal surface. The discharge consisted of 4-7 ($\bar{x} = 6$) spikes occurring in a burst every 12-15 seconds. These bursts of spikes appeared to be characteristic of spontaneous activity in the retina of the lemon shark.

Size of Receptive Field

All data for measuring the size of the receptive field center (RFC) were collected without background light. I used the area-sensitivity method (Stell et al., 1975) for determining the size of the ganglion cell RFC. The light intensity (neutral density value) needed to obtain a criterion response (1-2 spikes) for spots of white light of increasing diameter centered on the electrode was determined

by observing the oscilloscope screen and listening to the audio monitor for the criterion response. For a typical OFF-unit, as the diameter of the light spot was increased the threshold decreased up to a specific size. Further increases in the diameter of the spot had no effect on threshold. The point where an assymtope is reached is the receptive field center size. In all of the units tested, there was no rise in threshold with very large stimuli.

The size of ganglion cell RFC's varies from 0.85 mm to 1.45 mm in diameter (x = 1.12 mm, N = 18). Hueter (personal communication) has shown that 1 mm on the retina represents 6.04 degrees of visual angle. Thus, the receptive field center size in degrees of visual angle varies from 5.13 to 8.76 degrees with a mean of 6.76 degrees of visual angle.

OFF-Units

As stated the majority of cells (63%), were OFF-center cells. These cells could be 'held' for longer periods than any of the other cell types.

Dark Adapted OFF-Units

When all of the dark adapted spectral sensitivity data were plotted on one graph, the individual curves fell roughly into two groups based on sensitivity.

The first group of dark adapted OFF-units had higher sensitivities. The mean ($\pm$1 SEM) spectral sensitivity curve for this group is shown in Figure 18.

The solid curve is the Dartnall nomogram curve for a vitamin A1 based pigment with a λmax at 522 nm. The nomogram curve gives only a fair fit to the data. The curve formed by the experimental data seems wider at the blue end of the spectrum than the nomogram curve. This suggests that more than one pigment is contributing to the makeup of the spectral sensitivity curve.

Because the computer program that fits the experimental data to the Dartnall nomogram was written to give equal weight to all data points, the

computer could not fit the data to one leg of the nomogram curve. Therefore, the Dartnall nomogram curve was fitted by eye to the left leg of the curve (Fig. 18). A λmax of 504 nm is obtained. This emphasizes the difference on the right side of the curve, and suggests an additional pigment.

The second group of dark adapted spectral sensitivity curves corresponds to OFF-units with low sensitivities. When a stimulus of low intensity was flashed, no response was obtained from any of these cells. Only after the intensity of the flash was increased by approximately 2-3 log units, was a response evoked. The spectral sensitivity curves (means, ±1 SEM) are shown in Figure 20. The solid curve represents the Dartnall nomogram placed by the computer at a λmax of 544 nm. There is a reasonably good fit between the data and the nomogram curve. This suggests that a single visual pigment contributes to the makeup of this curve.

Light Adapted OFF-Units

After the dark-adapted spectral-sensitivities were determined the retina was light adapted with a white light background and thresholds were followed until they stabilized. It required approximately 20 minutes for the thresholds to attain this stable level. Thereafter, the thresholds for different wavelengths were determined. With a steady background light, the test stimulus was flashed, until threshold was found for a particular wavelength. This was repeated for each interference filter.

Figure 21 is a graph of the (means, ±1 SEM) normalized values, of light adapted OFF-units. The solid curve is a Dartnall nomogram curve placed by the computer at a λmax of 546 nm. The nomogram curve fits the data well. The shift of λmax from 522 to 546 nm following light adaptation is termed the Purkinje shift.

Chromatic Adaptation OFF-Units

To determine whether there was more than one pigment contributing to the curve of spectral sensitivity in the light adapted preparation, the OFF-units were chromatically adapted. Two filters were used: blue-green, and yellow. Other filters were used for specific conditions and these will be described later. The adapting light was turned on and the thresholds followed until stable. Thresholds to test stimuli were then determined for each wavelength, and the resulting data plotted as before. Figure 22 shows the mean normalized spectral sensitivity of OFF-unit ganglion cells using a blue-green background. The fit between the data points and the Dartnall nomogram curve (solid curve) placed by the computer (λmax = 544 nm) is good. This suggests that there is no cone pigment at the longer wavelengths. This is comparable to the earlier ERG work on the lemon shark (Cohen et al., 1977), which showed a reduced sensitivity in the red end of the spectrum following light adaptation. The reduced sensitivity at the red end of the spectrum has been reported for other elasmobranchs (Gruber and Cohen, 1978), that possess retinas with rod and cone photoreceptors. It represents a situation unlike that found in the bony fish which are well known for having strong sensitivity in the red end (Easter, 1975). Chromatic adaptation with a yellow filter produced the results shown in Figure 23. The Dartnall nomogram fitted the data best if the λmax was placed at 547 nm; and the fit was good.

A peculiar response was seen in some OFF-units. With an intense stimulus (3 log units above threshold), a short latency OFF response appeared, followed by a second, long latency, burst of spikes. The second burst was delayed by up to 60 seconds after the stimulus. Similar second bursts of activity with long latencies have been reported for the frog (Chino and Starr, 1975).

ON-Units

ON-center units were more difficult to isolate and could not be recorded for more than one hour. They composed the lowest percentage (18%) of all cells.

Dark Adapted ON-Units

Thresholds of ON-center units in the dark adapted state were generally lower than those of OFF-units. It was not unusual to record threshold intensities 2 to 3 log units lower than for the OFF-units under similar conditions.

The mean (±1 SEM) dark adapted spectral sensitivity for ON-units is shown in Figure 24. The solid curve is the Dartnall nomogram curve fit by the computer at a max of 522 nm. As with the dark adapted OFF-units, this curve does not match the peak spectral sensitivity for the extracted pigment of 501 nm, and has a slightly higher sensitivity than expected in the blue-green region of the spectrum.

Light Adapted ON-Units

Of the 18 ON-units, only one unit was held long enough to study the effects of white light and chromatic adaptation. The light adapted spectral sensitivity curve of this cell is shown in Figure 24. The λmax of this curve as calculated by the computer is at 547 nm. There was a shift in the λ max from 522 nm to 547 nm upon light adaptation. This implies that ON-units have input from two systems, probably rods and cones. The fit of the data to the nomogram curve is fairly good.

Chromatic Adaptation ON-Units

The cell was first exposed to a red background (Kodak wratten #92) and thresholds were followed until stable. The spectral sensitivity was then determined and the resultant curve shown in Figure 26. The computer

determined λmax was 544 nm. According to the shape of the spectral sensitivity curve only one pigment system exists.

The presence of a light orange background (Kodak wratten #23) also failed to change the λmax from the peak of 544 nm (Fig. 27).

ON OFF Units

These cells are characterized by responding with spikes at the onset and offset of the stimulus. They occurred in 21% of the sample.

Dark Adapted ON OFF Units - Off Component

Data from the off component of the ON OFF center cells fell into two categories: high and low sensitivity. The spectral sensitivity data for the low sensitivity cells are shown in Figure 27. The solid curve is the Dartnall nomogram curve placed at a λmax of 544 nm. The fit is good, suggesting the presence of only one pigment.

The spectral sensitivity curve for the high sensitivity units in the dark adapted state is shown in Figure 29. These data have been normalized as explained earlier. The λmax was at 522 nm. The fit was good, but the peak of the curve did not match the peak found for the extracted pigment which was 501 nm (Bridges, 1965). This suggests that more than one pigment is contributing to the makeup of the dark adapted spectral sensitivity curve. One of the pigments probably originates from the rods, while the other may originate from the cones.

If the short wavelength contribution to the curve is from the rods, adaptation with white light will raise the rod thresholds high enough so that only the cones will operate. This will result in the spectral sensitivity curve moving horizontally to a new λmax at the red end of the spectrum. Chromatic adaptation will be needed to bring out the cone input to these cells as explained

earlier (see Methods and Materials, Procedure).

Light Adapted ON-OFF Units - Off Component

The spectral-sensitivity curve for the light-adapted state is shown in Figure 30. The λmax is placed at 544 nm. There is a good fit of the data to the curve. The peak sensitivity shifted from 522 nm to 544 nm during light adaptation. This suggests that for the high sensitivity cells, two pigments contribute to the dark adapted spectral sensitivity; and one of them probably originates in the rods.

Chromatic Adaptation ON-OFF Units - Off Component

To decide if more than one pigment is associated with the low sensitivity cells, they were chromatically adapted with a yellow filter. This should depress the sensitivity in the yellow to red portion of the spectrum. When this filter was used on cell number 47, the peak of the spectral sensitivity curve was placed at 544 nm (Fig. 31). From this datum, it appears that only one pigment is present and that its peak is at 544 nm.

ON-OFF Units - On Component

The on component of the ON-OFF units had, as with the ON-units a lower threshold than OFF units under dark-adapted conditions.

To obtain separate spectral-sensitivity data for the on and the off component of the ON-OFF units, meant that twice as much data had to be recorded from one cell. This in effect doubled the time needed to record from a cell to complete the protocol. However, cells could not be held for this increased period of time. As a result, complete data, including results from dark, light and chromatically adapted states, for the on component of the ON-OFF units are lacking.

Dark Adapted ON-OFF Units - On Component

The spectral sensitivities of the on component of dark adpated ON-OFF units were similar to those of the ON-units. Peak spectral sensitivity was placed at 519 nm (Fig. 32). The fit of the curve to the data is fairly good, but again the peak does not match that of VP501, extracted from the lemon shark retina by Bridges (1965).

Light Adapted ON-OFF Units - On Component

The peak spectral sensitivity of the on component of the ON-OFF units in the light adapted state moved peak to 535 nm (Fig. 33).

Chromatic Adaptation ON-OFF Units - On Component

Use of a yellow background produced a spectral sensitivity curve with a λmax of 544 nm (Fig. 34). The fit was fair.

Surround

To determine if an antagonistic surround was present, the retina was stimulated with annular stimuli of various sizes. An annular stimulus consists of a ring of light. The center of the ring is dark.

The presentation of annular stimuli with either white light or particular wavelengths of light, did not evoke a response, or at best evoked only a very weak one. To bring out the surround response, I continuously illuminated the receptive field center with a small spot of white light, while stimulating the surround with an annulus of white light. Figure 35 shows the effects of stimulating a cell first with a small spot of light and then with both a small spot of light an an annulus. Stimulating the cell with a spot of light elicits an ON-response, while presentation of the annulus evokes an OFF-response, thus demonstrating the presence of a surround.

To determine whether color opponent mechanisms were present, I stimulated the retina with large diameter spots of 460 nm, 540 nm, and 610 nm light. A color opponent cell should respond to light stimulating both the center and surround of its receptive field with an ON and OFF response. This is because the center has a different spectral sensitivity from the surround. Therefore, the center and surround would each respond, either with an ON or an OFF response, only to that part of the spectrum to which it is sensitive to. However, for all wavelengths, the sign of the response of lemon shark ganglion cells was the same. Spectral sensitivity using large diameter spots gave the same λmax as that found using small spot stimuli.

With the use of an annular stimulus, I determined spectral sensitivities for four (1 ON and 3 OFF) units. In the cases tested, the λmax of the surround appeared to be the same as the λmax of the center. Although no color opponent units were found, it is difficult to conclude that such cells do not occur in this retina.

A few cells that I originally classified as OFF-units had ON-OFF responses when stimulated with an annulus. However, the spectral sensitivities had the same λmax. I did not record enough of this type of unit to make a detailed study of the rod and cone inputs.

Miscellaneous Cells

During the course of this study I found 4 cells that changed their sign from OFF units to ON-OFF units upon chromatic adaptation. This type of response has also been reported by Demonasterio, Gouras and Tolhurst (1975) for cells of the rhesus monkey. Those were color opponent cells since their responses had different spectral sensitivities. In the lemon shark cells, however, the on and off components responded to all wavelengths of light, and the spectral sensitivity curves all had the same λmax, making them spectrally non-opponent cells.

DISCUSSION

Possible Sources of Error

Anatomy

The Golgi stain is a method of selectively staining neuronal cells. The method is very capricious (a term inevitably used by adherents of the Golgi technique). This means that not every cell takes up stain. In fact, only a small proportion of the cells in any given retina become stained. This is an advantage, since if all cells stained, the detail of single cells would be lost. One problem with the Golgi method, is that cells do not necessarily take up the stain throughout their entire set of process. Thus, it is possible to miss types of cells, or parts of cells. The distances of axonal spans and dendritic arborizations therefore, should be viewed as minimum values, unless otherwise stated. In practice I only classified lemon shark retinal cells that were totally stained by the Golgi method.

Electrophysiology

One potential source of error for these electrophysiological experiments (and other studies using this type of electrode) may be a sampling bias introduced through the use of tungsten microelectrodes with large tips. For example, the large number of OFF-center cells encountered in this study may be due to a sampling of larger cells by the tungsten electrodes due to their relatively large diameter tips. Stone (1973) has shown that electrodes with lower resistances and therefore larger tip diameters, record preferentially from larger cells and that electrodes with lower resistances and smaller tip diameters select from smaller cells. The use of the tungsten electrodes might therefore skew the percent of cells sampled to those with large cell bodies.

The selection of larger cells was partially confirmed in this study when I used glass microelectrodes with resistance of 10-20 megohms. Recording extracellularly, three out of four cells were of the ON-center variety. Also, I noticed that tungsten electrodes which appeared to have finer tips when examined under a microscope would inevitably produce more ON-center cell records.

Discussion of Results

Anatomy

In this study I have confirmed that the visual cell population of the lemon shark upon examination by light and electron microscopy consists of rods and cones. Based upon light microscopy, Gruber et al. (1963) first reported the presence of cones in the retina of the lemon shark. My work extends the early study to the ultrastructural level.

Photoreceptor cells were divided into two types on the basis of morphology. One type, the cone was conically tapering, while the second type was cylindrically shaped and termed a rod. Additional criteria have been added over the years as studies on different retinas have progressed utilizing the electron microscope. I have shown that lemon shark photoreceptors meet additional ultrastructural criteria for division into two cell types. For example, cones of the lemon shark have their plasma membrane continuous with the lamellae of the outer segment, while rods do not. Cones have synaptic terminals that are flattened basally with numerous invaginating synapses. Rods have smaller, spherically shaped terminals with fewer invaginations. The cones have more numerous and more densely packed mitochondria in the inner segment than the rods.

My description of the lemon shark photoreceptors generally agrees with

that of Gruber et al. (1963). Differences in measurements may be attributable to differences in amount of shrinkage between paraffin and plastic embedded material. While the rod and cone nuclei could be differentiated in this study, they could not in the earlier study (Gruber et al., 1963). Again, this may be due to differences in embedding and staining material.

The one difference that stands out between the two studies is the rod to cone ratio. Gruber et al. (1963) reported a ratio of 12 rods to 1 cone. Whie similar ratios were found in the lemon shark retina during this study, a lower ratio of 5 rods to 1 cone was found in the dorsal part of the retina. This ratio makes it one of the lowest for elasmobranchs studied. Gruber et al. (1975) found a ratio of 4:1 for the great white shark Carcharodon carcharias, and 5:1 for the thresher shark Alopias vulpinus. Additionally, they found rod:cone ratios of 8:1 for the blue shark Prionace glauca, 10:1 for the white tip shark Carcharinus longimanus, and the Mako shark Isurus oxyrinchus, and 13:1 for the sand-bar shark Carcharhinus milberti. These sharks are all active predators. In contrast the rod to cone ratio for the smooth dogfish Mustelus canis, is 100:1 (Stell and Witkovsky, 1973). This animal is a bottom feeder and subsists on a diet of mostly crustacea (Bigelow and Schroeder, 1948).

The lower rod to cone ratios appear to predominate in those sharks that have active predatory life styles, where vision probably plays an important role. The large number of cones seen in these animals would extend the period of time over which they could hunt as well as increase their visual acuity which would be important to a predatory animal.

The horizontal cells of the lemon shark are massive cells arranged in three layers. I have shown the presence of membrance specializations, called gap junctions, between horizontal cells of the same layer. Gap junctions between horizontal cells have been reported in Mustelus manazo and Dasyatis akajei

(Yamada and Ishikawa, 1965) as well as in Mustelus canis (Stell and Witkovsky, 1973). Kaneko (1971) demonstrated that an electrical current passed through an electrode into one horizontal cell could be recorded in the adjacent cell. When procion dye was injected it leaked into the next cell, presumably through the gap junction. Because the horizontal cells are electrically connected to one another, Werblin and Dowling (1969) believed that they govern lateral interaction in the retina and possibly contribute to the surround mechanism of the receptive field.

The bipolar cells described here are similar to those found in the retina of Mustelus canis (Stell and Witkovsky, 1973). However, I have described certain cells in the retina of the lemon shark retina that did not fit into their classification system.

I found two additional classes of Type a bipolar cells. Type a3 had a multistratified axon terminal with very short projections that terminated in bulbous expansions. Stell and Witkovsky (1973) found bulbous terminal expansions only on their Type b bipolar cells. The second class of Type a bipolar cell (a4) I found in the lemon shark retina had long monostratified axon terminals (135 μm). The length of the Type a4 bipolar cell axons did not approach the length found for the monostratified bipolar cell Type a1 (400-600 μm) of Stell and Witkovsky (1973). It is possible that Type a4 cells had longer axon terminals that did not stain, however, the shape of the nucleus, as well as its lack of a Landolt's club separates it distinctly from the Type a1 bipolar cell.

While Stell and Witkovsky (1973) found one bipolar cell with axons terminating in the middle of the IPL, I found an additional variety that was multistratified and terminated in the middle of the IPL. I called this Type a2 bipolar cell.

The additional bipolar cell reported here may be accounted for by the greater numbers of cone photoreceptor cells in the lemon shark and may possibly

represent cone bipolar cells. Electron microscopy of serially sectioned material could answer this question.

Bipolar cells were thought to be the only units that sent processes to both plexiform layers (Boycott et al., 1975). In recent years however, another cell has been described that has its perikaryon located in the inner nuclear layer among the amacrine cells, and has connections to both outer and inner plexiform layers. These are the interplexiform cells. They have been described in the retinas of cat, dolphin, goldfish, New World monkeys and rabbits (Gallego, 1971; Dawson and Perez, 1973; Ehinger, Falck and Laties, 1969; Boycott et al., 1975; and Oyster and Takahashi, 1977). They were unknown in elasmobranchs until now, although star shaped cells that might fit the description of flat-mounted interplexiform cells were seen (Neumayer, 1897). In goldfish and New World monkeys interplexiform cells contain the neurotransmitter dopamine (Ehinger et al., 1969; Dowling and Ehinger, 1975). Electron microscopic analysis of synaptic terminals in goldfish retina show that these cells only receive input from amacrine cells of the inner plexiform layer. They are presynaptic to horizontal and bipolar cells and thus represent a centrifugal pathway, i.e. opposite the normal direction of flow, for information to pass from inner to outer plexiform layers (Dowling and Ehinger, 1975). In cat retina, the interplexiform cells are both pre- and postsynaptic in the inner plexiform layer and only presynaptic in the outer plexiform layer (Kolb and Famiglietti, 1976). However, cat interplexiform cells are presynaptic in the outer plexiform layer only to bipolar cells, not to both bipolar and horizontal cells as in the goldfish. While goldfish and monkey interplexiform cells contain dopamine, cat and rabbit interplexiform cells contain neither dopamine nor any biogenic amine. This demonstrates that morphologically similar cells employ different neurotransmitters.

The present study has conclusively established for the first time, the

presence of interplexiform cells in an elasmobranch retina. Information about synaptic connections, neurotransmitters and ultimately their function can form the basis of interesting future studies.

The stratification found in bipolar cell axons applies equally well to ganglion cell dendrites. I found in addition, ganglion cell bodies at all levels of the inner plexiform and ganglion cell layers. In addition, displaced ganglion cells were found in the proximal part of the inner nuclear layer. While only a few ganglion cell bodies stained with the Golgi method, their cell processes stained very well. These processes appeared to be stratified into sub-types so that specific ganglion cell processes would synapse only in specific regions of the inner plexiform layer and with specific cell sub-types. This has been suggested by Cajal's (1892) drawings and has been found to be true in Mustelus (Witkovsky and Stell, 1973).

Electrophysiology

Receptive Field Size

I measured the receptive field sizes for two reasons. First, knowledge of the size for the center of the receptive field allowed me to choose the appropriate spot diameter for stimulating the receptive field center (RFC) only. Second, I could compare the size of the RFC in the lemon shark to the RFC size in other animals.

I measured receptive fields whose size ranged from 0.85 mm to 1.45 mm in diameter (5.13 to 8.76 degrees of visual angle). This agrees with the results of Stell et al. (1970, 1971, 1975) who found receptive fields of 1-2 mm. No indication was given as to how these sizes relate to visual angle.

Receptive field sizes have been correlated with size of ganglion cell dendritic spread (Stell et al., 1975). I found dendritic fields of giant ganglion

cells of 1 mm in Golgi stained material of lemon shark retina, thus verifying anatomically the electrophysiolgoical data for receptive field size. This also suggests that the cells I recorded from were the giant ganglion cells.

Dark Adaptation

The rods, containing the pigment rhodopsin, mediate vision primarily at night (Rodieck, 1973). The action spectrum of the dark adapted retina should follow the absorption spection of rhodopsin. Bridges (1965) has extracted the visual pigment from the retina of the lemon shark and showed that it was a homogeneous, vitamin A1 based retinene with a wavelength of maximal absorption (λmax) at 501 nm.

The dark-adapted spectral sensitivity recorded from the ganglion cells did not match the wavelength of maximal absorption of 501 nm. OFF-center, ON-center and the off component of the ON-OFF center cells had a λmax of 522 nm, while the ON component of the ON-OFF center cells had a λmax of 519 nm. The difference between the 519 nm and the 522 nm peak spectral sensitivities can probably be explained on the basis of experimental error, i.e. the error due to the accuracies of the equipment. For example, the half amplitude bandwidth of the interference filters is 10 nm. Therefore, a difference between results of as much as $\pm$5 nm is within reason and could be attributed to the bandwidth of the interference filters.

A mismatch between the dark-adapted spectral sensitivity and the absorption spectrum has been previously reported for the lemon shark. Cohen et al. (1977) using the ERG to determine spectral sensitivity, found a λmax of 530 nm in the dark adapted state of the intact animal. By using the eyecup and aspartate-treated isolated retina, they showed that neither absorption by the preretinal media, nor spectral reflectance from the tapetum lucidum could

account for the 30 nm difference between the maximum absorption and the peak of the spectral sensitivity.

There are a number of possibilities which might explain why the dark adapted spectral sensitivity did not match the peak of the visual pigment absorption curve.

First, the mismatch between pigment λmax and peak dark-adapted spectral sensitivity could be interpreted as incomplete dark adaptation of the retina. However, the animal was dark adapted for at least one hour prior to the removal of the eye. The eyecup was then given an additional 30 minutes of dark adaptation before the experiment began. Based on previous experiments (Gruber, 1967; Cohen et al., 1977) this should have been adequate for the eye to become dark adapted. In addition, further dark adaptation had no effect on the peak of the spectral-sensitivity curve. A second possibility is that the 519-522 nm peak found by recording from ganglion cells in the dark-adapted state might represent a pure cone response, with no rod input. This could be tested by light adaptation. If the peak of the spectral sensitivity curve in the dark-adapted state is due to pure cone input, light adaptation should have no effect on the point of maximum sensitivity, since the threshold for the cones would have been reached in the dark-adapted state. Further light adaptation woudl thus have no effect on the sensitivity.

If upon light adaptation however, the λmax does shift to the red end of the spectrum, it would mean that a second pigment, with a different sensitivity was contributing to the makeup of the spectral-sensitivity curve in the dark-adapted state, but not in the light-adapted state. As will be discussed in the next section, the peak of the spectral sensitivity curve in the dark adapted state did shift towards the red end of the spectrum upon light adaptation. This implies that the 519-522 nm response is not due to a single cone pigment.

A third possibility, and the one most likely to explain these results is that the ganglion cells of lemon sharks receive input from both rods and cones and that both systems are operating under dark-adapted conditions. The resulting rod-cone interaction could produce a spectral-sensitivity curve that is a composite of both systems, shifting the peak away from the λmax of the rod pigment. Cohen et al. (1977) believed rod-cone interaction to be the explanation for the mismatch of the ERG determined spectral sensitivity and the λmax of the pigment. Witkovsky et al. (1975) citing the large number of cones in the retina of the carp, attributed the lack of agreement between the peak of the spectral sensitivity curve and the peak of the absorption spectrum of the pigment, to rod-cone interaction in the scotopic state.

Gouras (1965) and Gouras and Link (1960) have shown that cones strongly influence the ganglion cells of dark-adapted monkeys. While cones were shown to be less sensitive than rods, they were found to respond much faster. Where rod and cone signals converge on the same ganglion cell, the first to arrive, inhibits the action of the second response for a short time.

For the rod-cone hypothesis to be credible it must be shown that the cones can operate under scotopic conditions. Nelson (1977) recording intracellularly from cat cones has shown that the cones respond to light stimuli well within scotopic light intensities.

Under scotopic conditions I found a second class of cells in the lemon shark retina that had lower sensitivities under dark adapted conditions than the previously described cells. This group was found among OFF-center cells and the off component of the ON-OFF center cells. The peak of the spectral sensitivity curve was at 544 nm. Further dark adaptation failed to shift the peak of this curve, suggesting that the cell lacked a rod input. Only after the stimulus was raised 2-3 log units was I able to evoke a response from these cells, implying that

this group of cells had only cone inputs. If the low sensitivity group of cells has only cone input, light adaptation should not shift the peak of the spectral sensitivity curve.

Light Adaptation

A background of white light shifted the peaks of the spectral sensitivity curve from a λmax of 519-522 in the dark adapted state to a λmax of 544 nm for the ON-center cells, and off component of the ON-OFF center cells. The OFF center units had a λmax of 546 nm in the light adapted state. The difference between the 544 nm and 546 nm peak is within experimental error. The 535 nm λmax in the light adapted state for the on component of the ON-OFF center cells, while shifted from the peak found in the dark adapted state does not coincide with the 544 nm peak found for all other light adapted cells. I believe that this may have resulted from data being taken before the cell was fully light adapted. If this is true, the rod photoreceptors may still have been responding and contributing to the spectral sensitivity curve. This would result in the peak of the curve not matching that of a curve obtained from cells fully light adapted, having contributions only from cones. The peak of the light adapted spectral sensitivity curve for the lemon shark ganglion cells conicides closely with a λmax of 541 nm found using the ERG (Cohen et al., 1977).

Chromatic Adaptation

I have shown that the peak of the spectral sensitivity curve, in the light-adapted state is at 544-546 nm. The ultimate basis for the response is the absorption spectrum of a visual pigment. Because the responses occur in the light adapted state, I believe that they originate in the cone photoreceptors. The light-adapted spectral-sensitivity curve may however, be the result of several cone classes, each having a different spectral system. The spectral sensitivity

curve would therefore not represent the absorption spectrum of a single cone pigment, but would represent the combined absorption spectrums of several cone classes. To determine if the 544-546 nm peak is a result of one or more cone classes, I chromatically adapted the retina with wide band cut on and cut off filters.

Chromatic adaptation using a blue green filter failed to change the point of maximum sensitivity for either OFF center cells or the ON center cells, from the light adapted λmax of 544 nm. This indicates that a blue green pigment does not influence the 544 nm spectral peak. This is because the 544 nm peak remained the same under conditions of blue green adaptation, when the influence of a blue green pigment would be supressed. In addition, the 544 nm peak remained the same under light adapted conditions, in the absence of a blue green background, when a blue green pigment could exert an influence.

To determine if a pigment in the yellow region of the spectrum affected the spectral sensitivity, the retina was chromatically adapted with a yellow filter. The λmax for the OFF center cells occurred at 547 nm while that for the ON center cells and the off response of the ON-OFF center cells was at 544 nm. I believe that it is possible that the 3nm difference between the 547 and 544 nm peaks can be attributed to experimental error.

This series of experiments shows that there is no pigment that absorbs light maximally in the yellow region of the spectrum because the peak of the sensitivity curve remained the same with and without the yellow background.

One set of experiments were done on the ON center units using first a red filter and then an orange filter. These filters transmit more light in the red end of the spectrum. The peak of the spectral sensitivities with both the red and orange backgrounds were at 544 nm. Thus, no red pigment system was present. This substantiates earlier findings on elasmobranchs in general (Gruber and

Cohen, 1978) and the lemon shark in particular (Cohen et al., 1977), which showed a very low sensitivity to the red portion of the sepctrum.

The results of the chromatic-adaptation experiments closely follows the results of the light-adapted experiments. Taken together, the results from these two conditions indicate that there is only one pigment system, with a λmax of 544-546 nm, operating under bright light conditions.

Chromatic adaptation requires very high intensity backgrounds to completely bleach a pigment system. The light stimulus used in these experiments may not have been as intense as requied for full chromatic adaptation. Therefore, additional pigment systems, with lower sensitivities may be present.

If another pigment system different from the 544-546 nm system were present, I believe that it would have a peak sensitivity of 490-500 nm. Behavioral determination of the spectral sensitivity of the lemon shark, using the nictitating membrane response (Gruber, 1969), showed a slight drop in the sensitivity curve between 510 and 520 nm. A similar drop was seen in the ERG determined spectral sensitivity (Cohen et al., 1977). The drop also appeared in the spectral sensitivities recorded from ganglion cells in the present study. Different light sources and optical systems, as well as different personnel were used in the behavioral, ERG, and ganglion cell spectral sensitivity experiments. Yet, a decrease in sensitivity between 510-520 nm was still observed in all the studies. This rules out discrepancies resulting from calibration errors within each optical system, or differences in methodologies. The data presented in this study on the lemon shark ganglion cells fails to explicitly prove the existence of a 490-500 nm pigment system. Similarly, early experiments on the goldfish failed to show a blue mechanism in spite of the fact that a blue cone pigment had been identified with the microspectrophotometer (Daw, 1968; Adams and

Afanador, 1971). Later research on the goldfish, however, found such a mechanism (Beauchamp and Lovasik, 1973).

Color Vision

According to the Duplicity Theory, cones operate only under photopic conditions. Only then, can wavelengths be distinguished, thus, cones are the photoreceptors responsible for color discrimination. For color vision to work, there must be a minimum of two systems having different spectral sensitivities.

From the results of this work the lemon shark retina contains the required two systems having different spectral sensitivities. The cones constitute one spectral system, while the rods constitute the second spectral system.

Trezona (1970) has suggested that rods play a role in color vision in humans and that they contribute to a blue mechanism. Tilton (1977) suggested that the rods contribute to color vision across the entire spectrum.

From the electrophysiological results of this study, the rods and cones function together only at low light levels. At higher intensities, only the cones seem to function, resulting in the retina having only one spectral system operating. This therefore, negates any color vision function. However, only behavioral testing can determine if an animal possess color vision (Gruber, 1978).

Using a behavioral (nictitating membrane) response, Gruber (1969) suggested the presence of hue discrimination in one lemon shark. He further suggested that additional experiments were needed using larger numbers of subjects. In a two choice color discrimination experiment, Gruber (personal communication) has not been able to show the presence of color vision in the lemon shark after more than 4000 trials. However, the task may have been too difficult for the lemon shark to learn.

Visual Pathways

It appears that the ON and OFF responses are a result of the maintenance of separate pathways. The ON-OFF response seems to be formed by a combination of the separate ON and OFF response paths. This is seen in part from the analysis of the rod and cone inputs to the ganglion cells. The results from the ON and OFF center cells are mirrored in the on and off component of the ON-OFF center cells. Recently the anatomical basis for separate ON and OFF center pathways have been demonstrated in the carp and cat (Famiglietti, Kaneko and Tachibano, 1977; Famiglietti and Kolb, 1976; Nelson, Famiglietti and Kolb, 1978). The inner plexiform layer was shown to be divided into two sublamina. Intracellular recordings of bipolar, amacrine and ganglion cells, followed by injection of dye revealed that OFF-center responses were confined to processes that terminated in sublamina A, nearest to the amacrine cells, while ON-center responses were confined to those processes that terminated in sublamina B, closest to the ganglion cells. A cell with processes overlapping into both layers was found to be an ON-OFF type of cell (Nelson et al., 1978). Intracellular recording with dye injection can confirm these results for the lemon shark, and would constitute an area for future research. The finding of bipolar cell axon terminals that were stratified in the IPL however, provides an anatomical basis for the existence of separate ON and OFF pathways in the lemon shark retina.

CHAPTER FIVE

SUMMARY OF RESULTS

1) The morphology of the lemon shark's retina was studied utilizing both light and electron microscopy. Special staining methods such as impregnation of neurons by the Golgi method were used to isolate single neurons which then allowed me to describe and classify specific neuron types.

2) The retina was shown to possess both rod and cone photoreceptors. They occurred in a ratio of up to 5 rods :1 cone. The photoreceptors were morphologically typical of vertebrate photoreceptors even at the ultrastructural level.

3) The horizontal cells were massive cells arranged in three layers. Horizontal cells of the same layer were connected by gap junctions as well as at points of adhesion called zonula adherentia. The gap junctions have been shown in other animals to be points of low electrical resistance (Kaneko, 1972).

4) Bipolar cells were classified according to the location of their axon terminals in the inner plexiform layer. Bipolar cell axons were found to terminate in distal, middle, and proximal layers of the IPL.

5) A class of cells, previously undescribed for elasmobranchs had perikarya that were situated among the amacrine cells in the inner nuclear layer, and that sent processes to both the outer and inner plexiform layers. This type of cell is known as an interplexiform cell. Three types of interplexiform cell were described.

6) Both regular and giant ganglion cells were found in the lemon shark retina. Ganglion cells were found not only in the ganglion cell layer, but in the inner plexiform and inner nuclear layer. These were termed 'displaced ganglion cells.'

7) Action potentials were recorded extracellularly from retinal ganglion cells. Three modes of discharge were recorded; ON-center units discharged only when a light stimulus was turned on; OFF-center units discharged only at the offset of a light stimulus; and ON-OFF center units responded with a discharge at both the on and offset of a light stimulus.

8) The spatial region of the retina over which a unit responds (receptive field) was found to have a size ranging from 0.85 mm to 1.45 mm in diameter which corresponds to 5.13 to 8.76 degrees of visual angle.

9) A weak antagonistic region, concentric to the center of the receptive field was found that gave opposite sign responses when stimulated with a ring or annulus of light.

10) Spectral sensitivities of receptive field centers showed the presence of two classes of OFF-center units. One class had higher thresholds and was found to have input only from one cone type which had a peak spectral sensitivity around 547-nm. The second OFF-center units had lower thresholds and had inputs from rods and cones.

11) The ON-center units had inputs from both rods and cones. The λmax of the cone input for these units was found to be at 547 nm.

12) The on-component of the ON-OFF units had both rod and cone inputs, while the OFF component, as with the OFF-center units, were composed of two classes of units, those with just cone input and those with both rod and cone input.

13) Pure rod spectral sensitivities were not found in any dark-adapted unit. Spectral sensitivity curves of dark adapted units were found with a peak of 519-522 nm which suggested both rod and cone input under dark adapted conditions.

Figure 1. Experimental Chamber. The chamber is constructed of solid brass and coated with silicone rubber. The eyecup is placed on the platform. A silver-silver chloride electrode is placed under the eyecup and serves as the indifferent electrode. Elasmobranch Ringer's solution fills the reservoir and the moat surrounding the platform. A mixture of 95% oxygen and 5% carbon dioxide flows through an air stone which is placed within the fluid filled reservoir. During the experiment a plexiglass cover encloses the top of the chamber. A hole in the cover allows the electrode and stimulus to pass through.

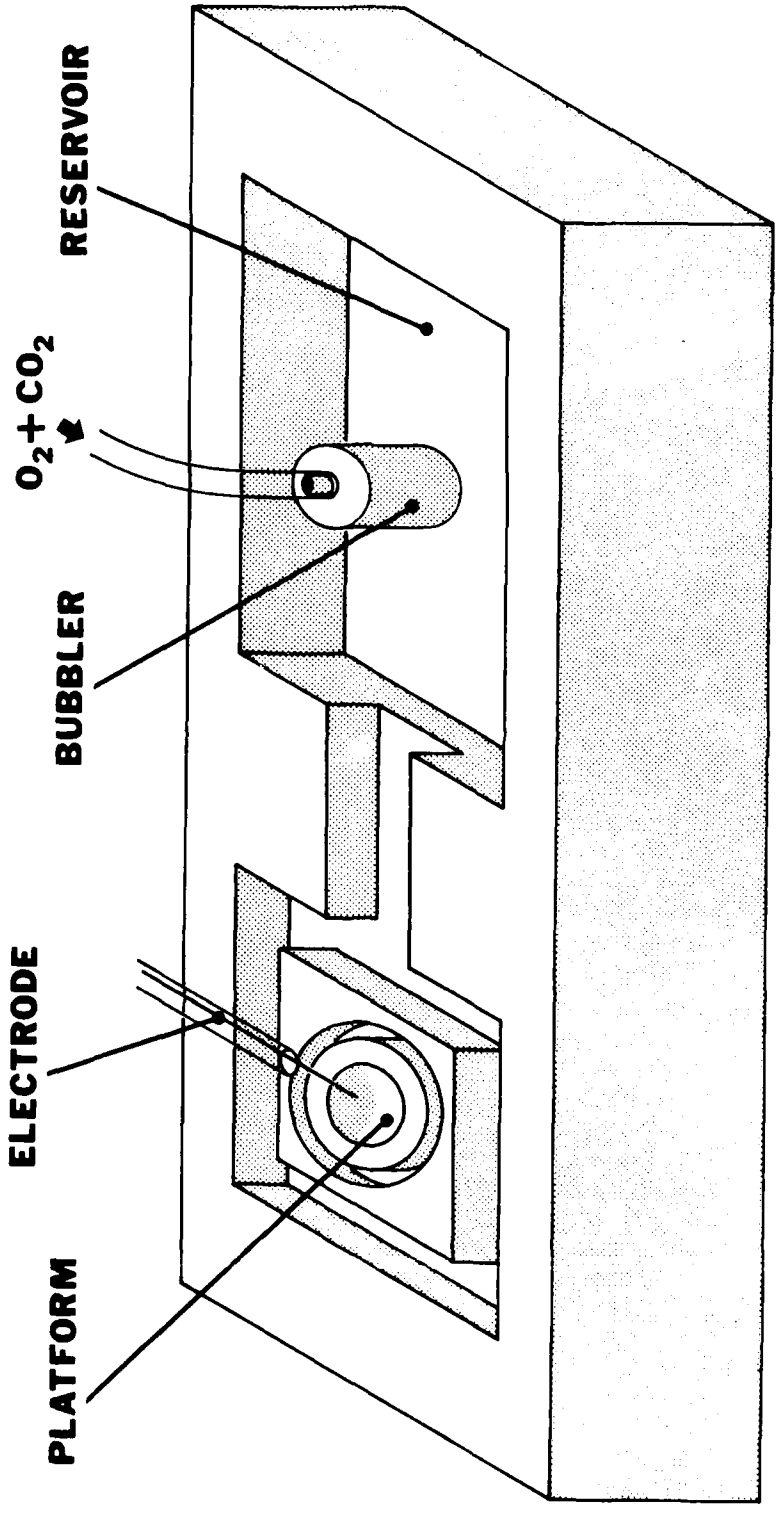
RESERVOIR
$O_2 + CO_2$
BUBBLER
ELECTRODE
PLATFORM

Figure 2. Diagram of optical system. Two channel optical system used in the electrophysiological experiments. A single, 150 watt tungsten-halogen bulb proved both test and adapting beams. Abbreviations: S-light source L_{1-5}-lenses; HF-heat filters; Sh-shutters; Ap-apertures; IF-interference filters; NDF-neutral density filters; MC-mixing cube; M_{1-4}-mirrors.

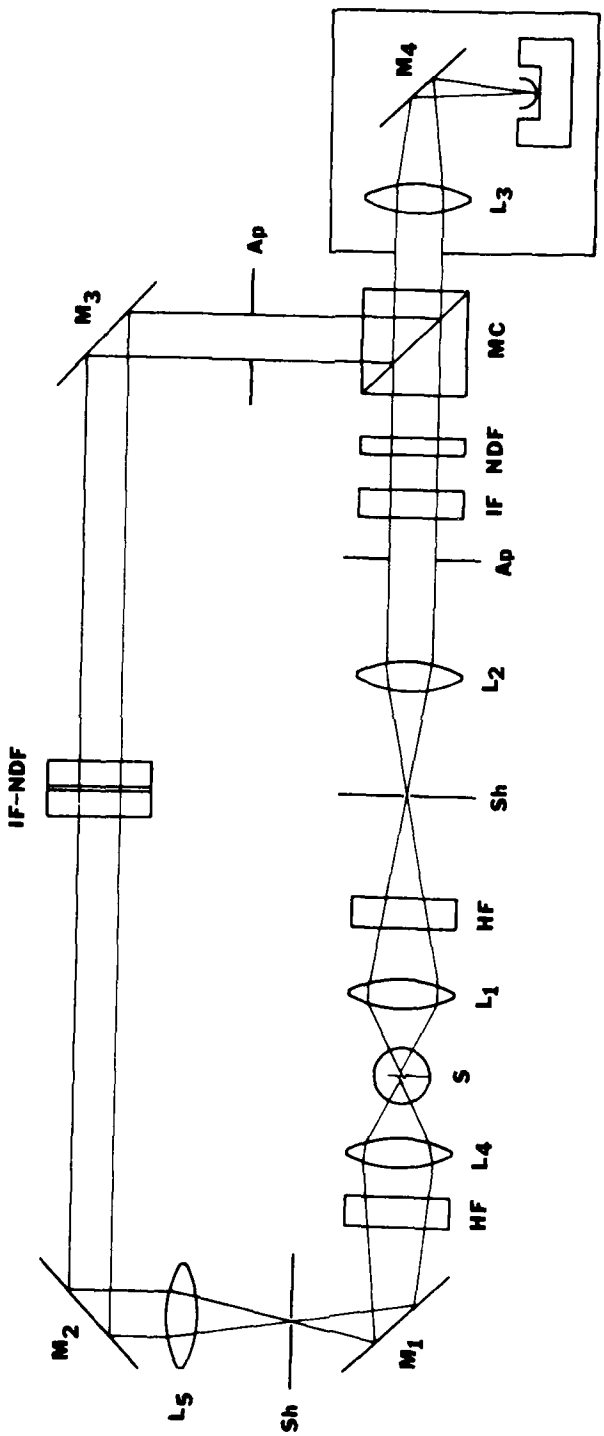
M4
L3
Ap
M3
MC
IF NDF
Ap
L2
IF-NDF
Sh
HF
L1
S
L4
HF
M2
M1
L5
Sh

Figure 3. Spectral radiance of lamp. Spectral output of the 150 watt, tungsten-halogen bulb used in the optical system. The spectral radiance was measured at different wavelengths with a radiometer which utilized a PIN photodiode. The output of the lamp at 610 nm was 2.47×10^{12} photons/cm^2.

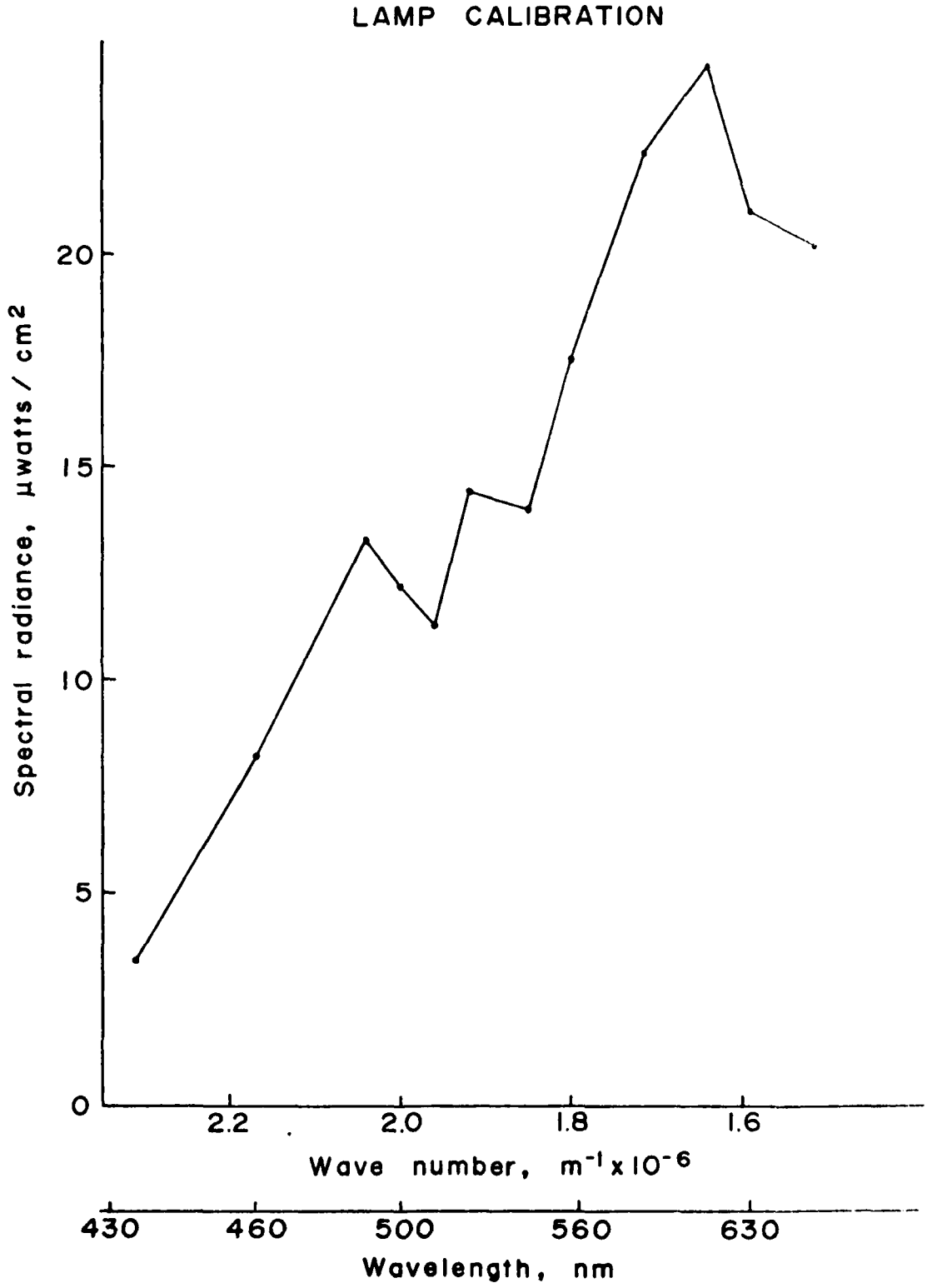
LAMP CALIBRATION
Spectral radiance, μwatts / cm²
0
5
10
15
20
2.2
2.0
1.8
1.6
Wave number, m⁻¹ x 10⁻⁶
430
460
500
560
630
Wavelength, nm

Figure 4. Effect of correction procedure on raw data. Curve A represents uncorrected neutral density threshold values from an OFF-center cell in the dark adapted state. Curve B is the raw data corrected for differences in the energy of a quantum at each wavelength. Curve C is the data corrected for differences in quantal output in the blue and red end of the spectrum.

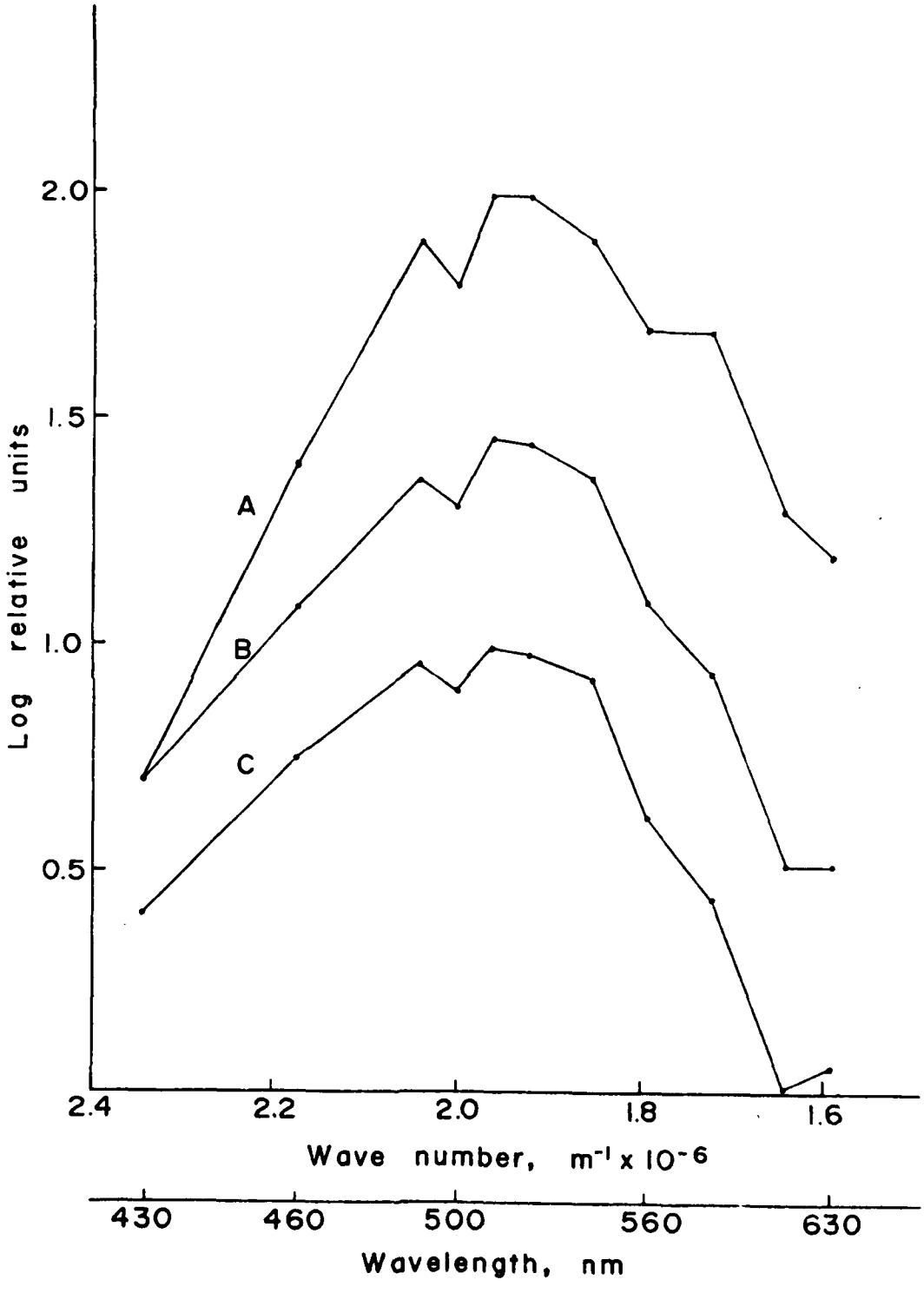
2.0
1.5
1.0
0.5
Log relative units
A
B
C
2.4
2.2
2.0
1.8
1.6
Wave number, m⁻¹ x 10⁻⁶
430
460
500
560
630
Wavelength, nm

Figure 5. Upper photo: Two micron thick section of lemon shark retina. Note the two types of photoreceptors. In the optic nerve layer, myelinated nerve fibers can be seen. Phosphate buffered gluteraldehyde fixation. Stained with toluidine blue.

Lower photo: Enlargement of photoreceptor layer clearly showing rods and cones.

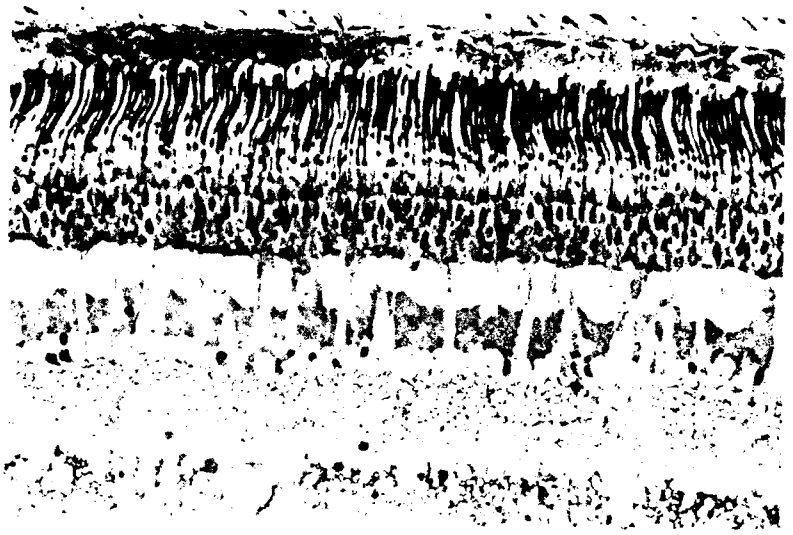

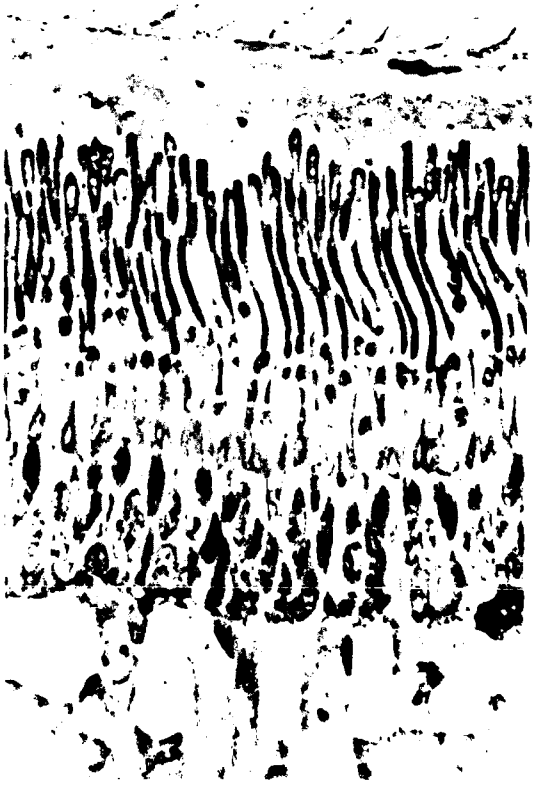

Figure 6. Electron micrograph of rod outer segments from the lemon shark retina. The lamellae are evident as is the plasma membrane which completely encloses the rod outer segment. Fixed in phosphate buffered gluteraldehyde. Postfixed with 1% OsO_4. Stained with lead citrate and uranyl acetate.

Figure 7. Electron micrograph of a cone photoreceptor. Mitochondria are densely packed in the inner segment and the lamella are open to the extracellular space, which is characteristic of cones.

Figure 8. Two photoreceptor synaptic terminals can be seen in this electron micrograph. The cone terminal (left) is larger than the rod terminal (right). The cone terminal is flattened basally and has several synaptic inclusions and is termed a pedicle. The rod terminal or spherule is smaller than the cone terminal and is spherically shaped with fewer synaptic inclusions than the pedicle.

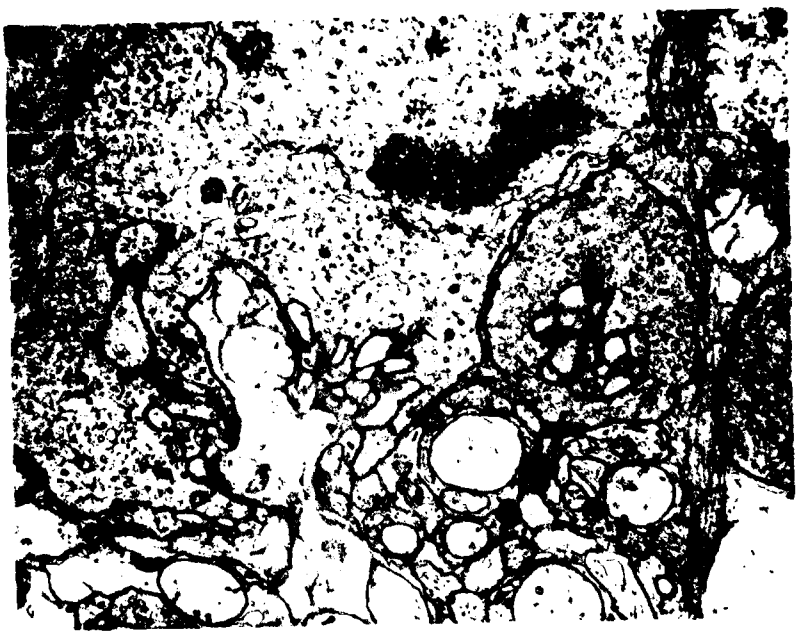

Figure 9. Golgi stained section of a horizontal cell in the lemon shark retina. Dendritic processes can be seen extending towards the photoreceptor cells.

Figure 10. Electron micrograph of horizontal cells of the lemon shark. These cells appear to interdigitate. Thickenings along the membrane are membrane specializations termed gap junctions where the membranes from two adjacent cells join. These represent points of low electrical resistance.

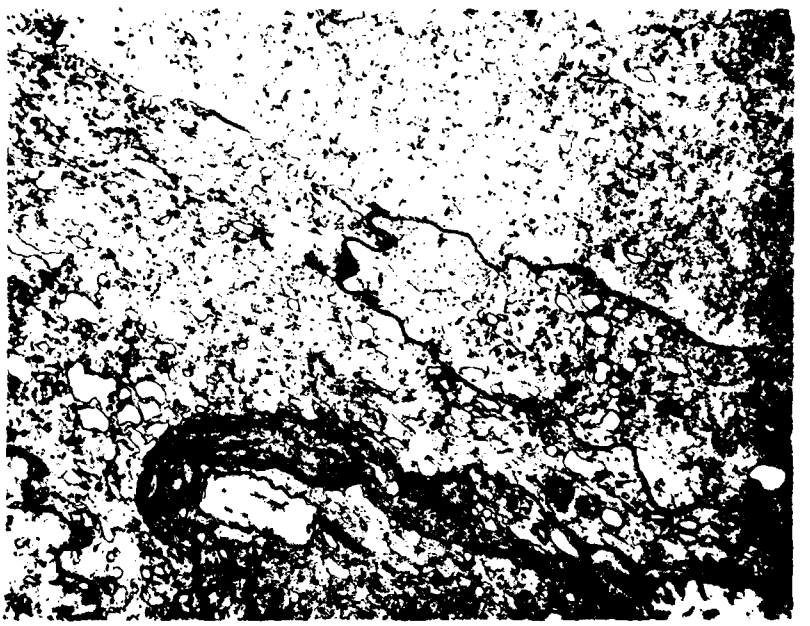

Figure 11. Type a bipolar cells. These bipolar cells have axons which terminate in the distal 1/3 of the inner plexiform layer.

A: Golgi stained type a1 bipolar cell.

B: Type a2 bipolar cell. These cells are multistratified and also possess a Landolt's club.

C: Two adjacent type a3 bipolar cells. These cells are multistratified, but have a smaller axonal spread than the type a2 bipolar cells. These cells also possess a Landolt's club.

D: Camera lucida drawing of a type a4 bipolar cell. These cells are monostratified with long axonal processes, but without a Landolt's club.

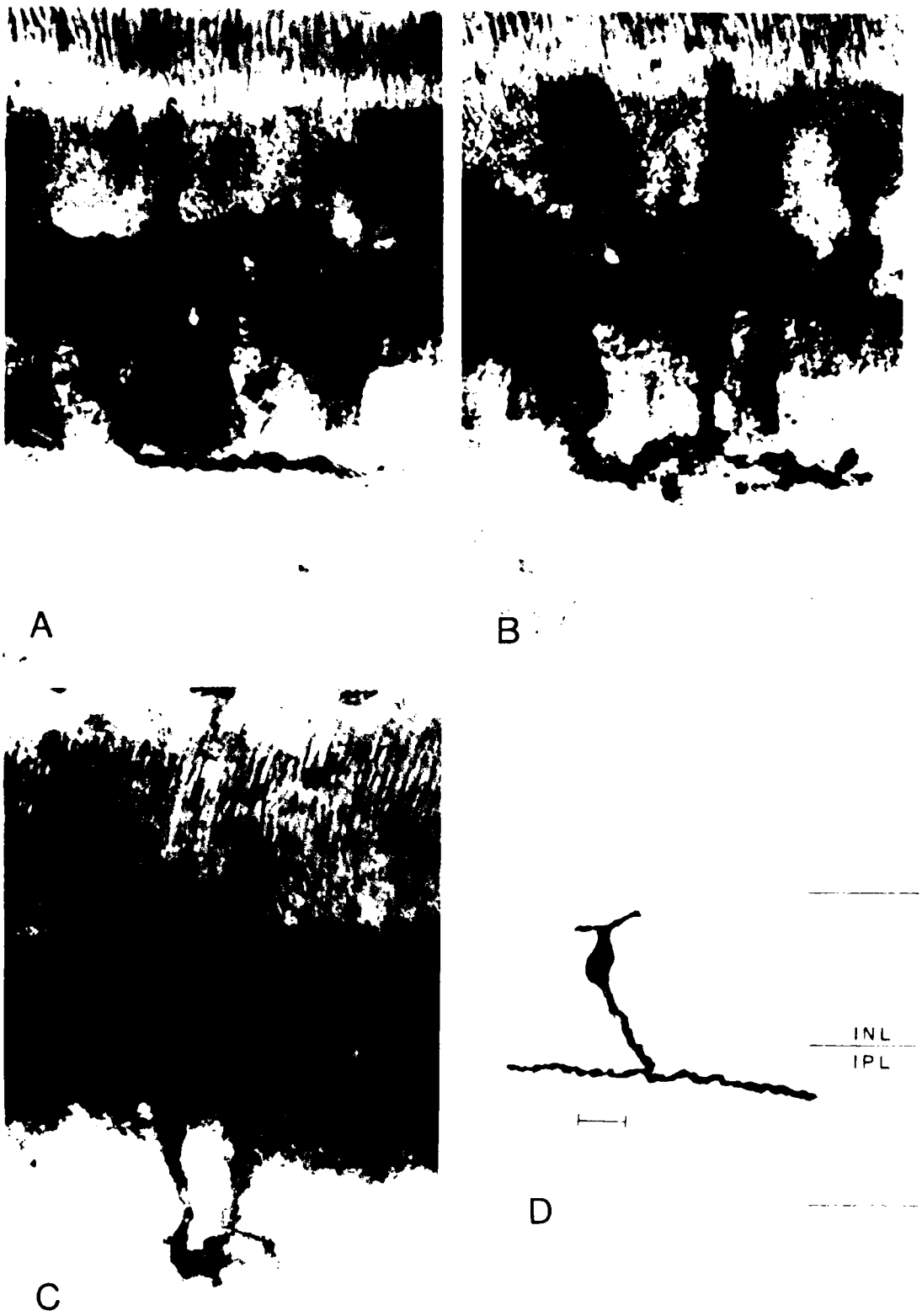
A
B
C
D
INL
IPL

AD-A083 177 ROSENSTIEL SCHOOL OF MARINE AND ATMOSPHERIC SCIENCE --ETC F/G 6/3
FUNCTIONAL ORGANIZATION OF THE RETINA OF THE LEMON SHARK (NEGAP--ETC(U)
MAY 80 J L COHEN NU0014-75-C-0173
UNCLASSIFIED UM-RSMAS-80002 NL

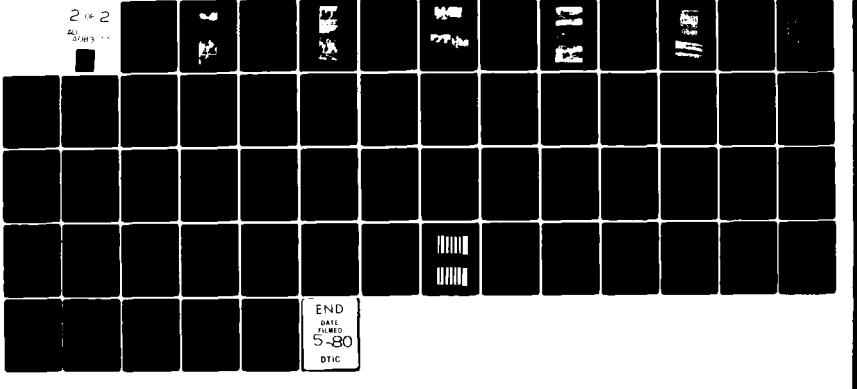

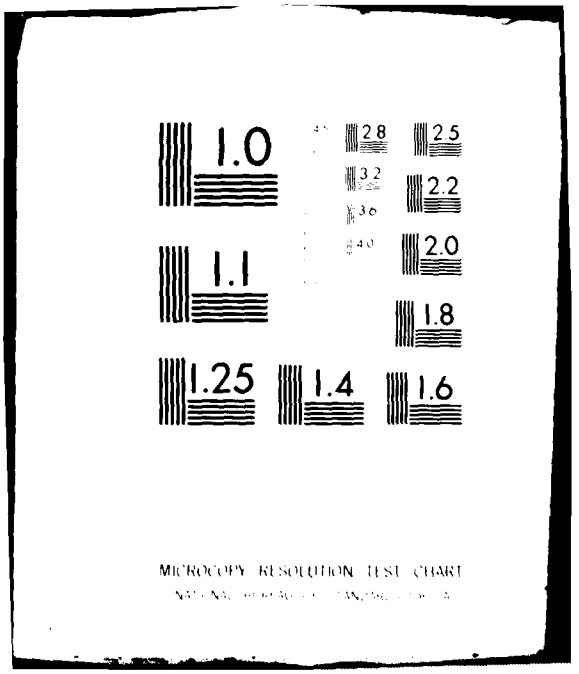
1.0
2.8
2.5
3.2
2.2
3.6
4.0
2.0
1.1
1.8
1.25
1.4
1.6
MICROCOPY RESOLUTION TEST CHART

Figure 12. Type b bipolar cells. Upper photo: Photomicrograph of Golgi stained type b1 bipolar cell. These cells are monostratified. Axons terminate in the middle of the inner plexiform layer.

Lower photo: Type b2 bipolar cells. These cells are multistratified with their axons terminating in the middle of the inner plexiform layer. The dark process crossing over this cell represents an axon from an adjacent (type a) bipolar cell. Type b bipolar cells do not possess a Landolt's club.

Figure 13. Type c bipolar cells. Upper photo: Type c1 bipolar cell. These cells are monostratified with axons terminating in the proximal 1/3 of the inner plexiform layer.

Lower photo: Type c2 bipolar cell. These cells are multistratified with axons terminating in the proximal 1/3 of the inner plexiform layer. Landolt's clubs were never found on type c bipolar cells.

Figure 14. Golgi stained photomicrographs of lemon shark interplexiform cells. These cells have their cell bodies located along the proximal border of the inner nuclear layer among the amacrine cells. They send processes to both plexiform layers.

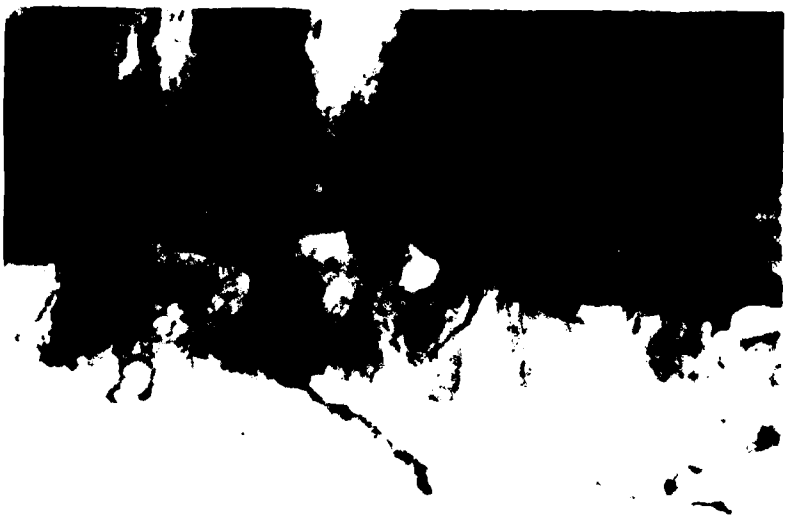

Figure 15. Amacrine cells. Upper: Photomicrograph of Golgi stained amacrine cell from lemon shark retina. This cell has one process which follows the distal border of the inner plexiform layer.

Middle drawing: A second type of Golgi stained amacrine cell from the lemon shark. Two processes leave the cell body and obliquely enter the inner plexiform layer to terminate in the middle of the IPL.

Lower: A third type of amacrine cell in the lemon shark. A single thick process leaves the cell body, proceeds to the proximal 1/3 of the inner plexiform layer and divides into many finer processes.

INL

IPL

Figure 16. Upper: Light micrograph of a displaced giant ganglion cell in the retina of the lemon shark. This cell is located in the proximal portion of the inner nuclear layer. Part of a process can be seen coming from the cell body and entering the inner plexiform layer. Fixed in phosphate buffered gluteraldehyde and stained with toluidine blue.

Lower: Golgi impregnated displaced giant ganglion cell. This is the same type of cell as that shown in the photo above. Here the extensive processes can be clearly seen.

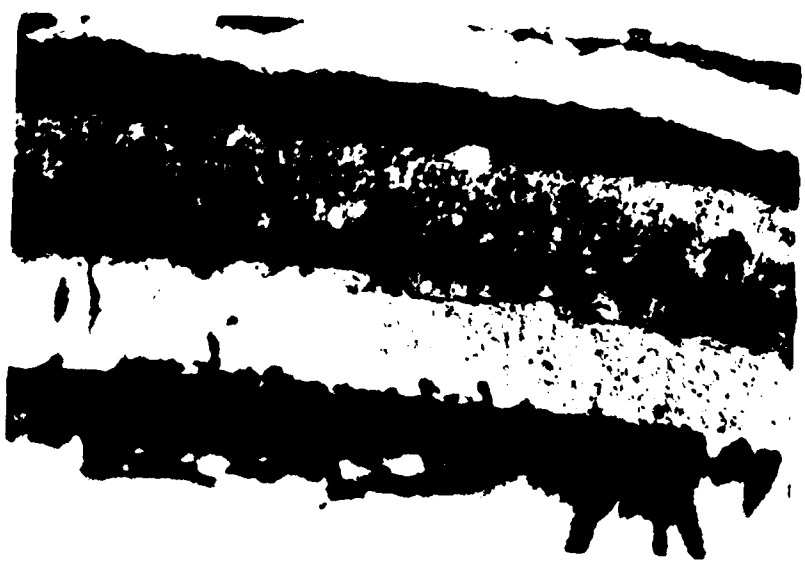

Figure 17. Electron micrograph of the nerve fiber layer in the lemon shark retina. Numerous myelinated nerve fibers can be seen.

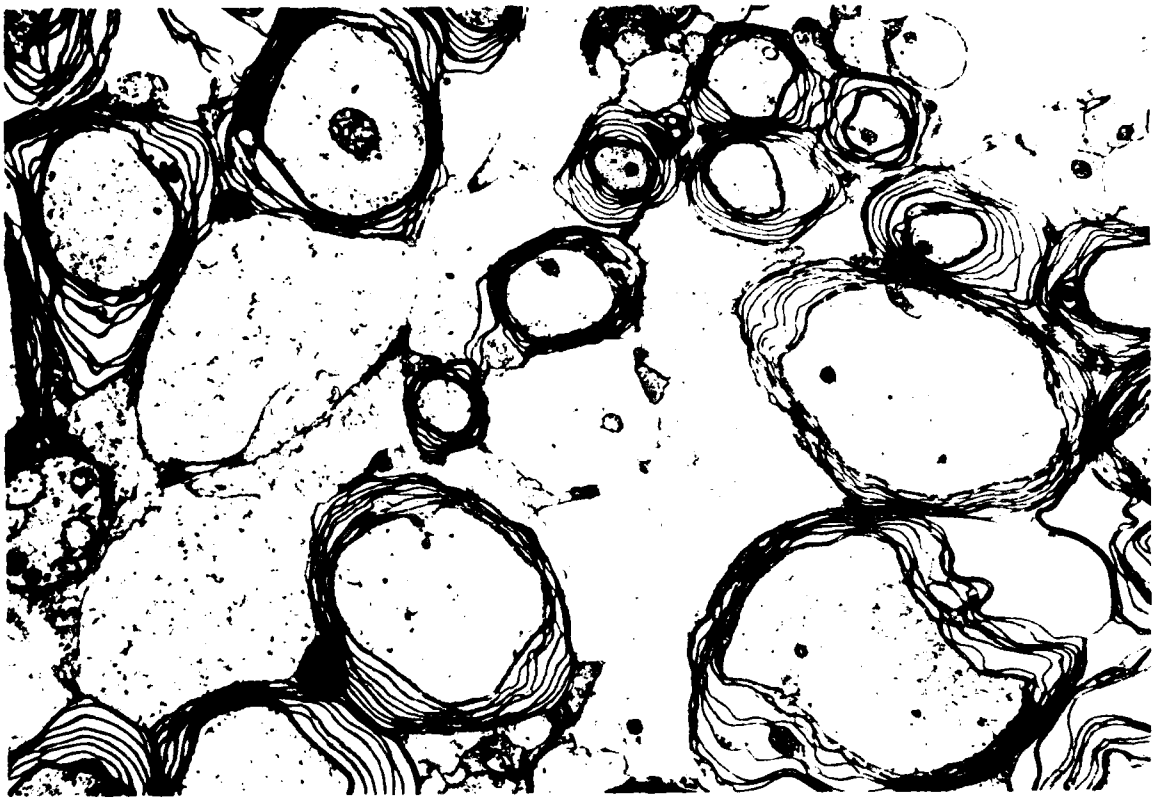

Figure 18. Spectral sensitivity of dark adapted OFF-center cells. The data represents the high sensitivity cells. Filled circles represents mean data. Vertical bars are $\pm$ 1 standard error of the mean (S.E.M.). The solid curve represents the Dartnall nomogram curve placed at a λ max of 522 nm.

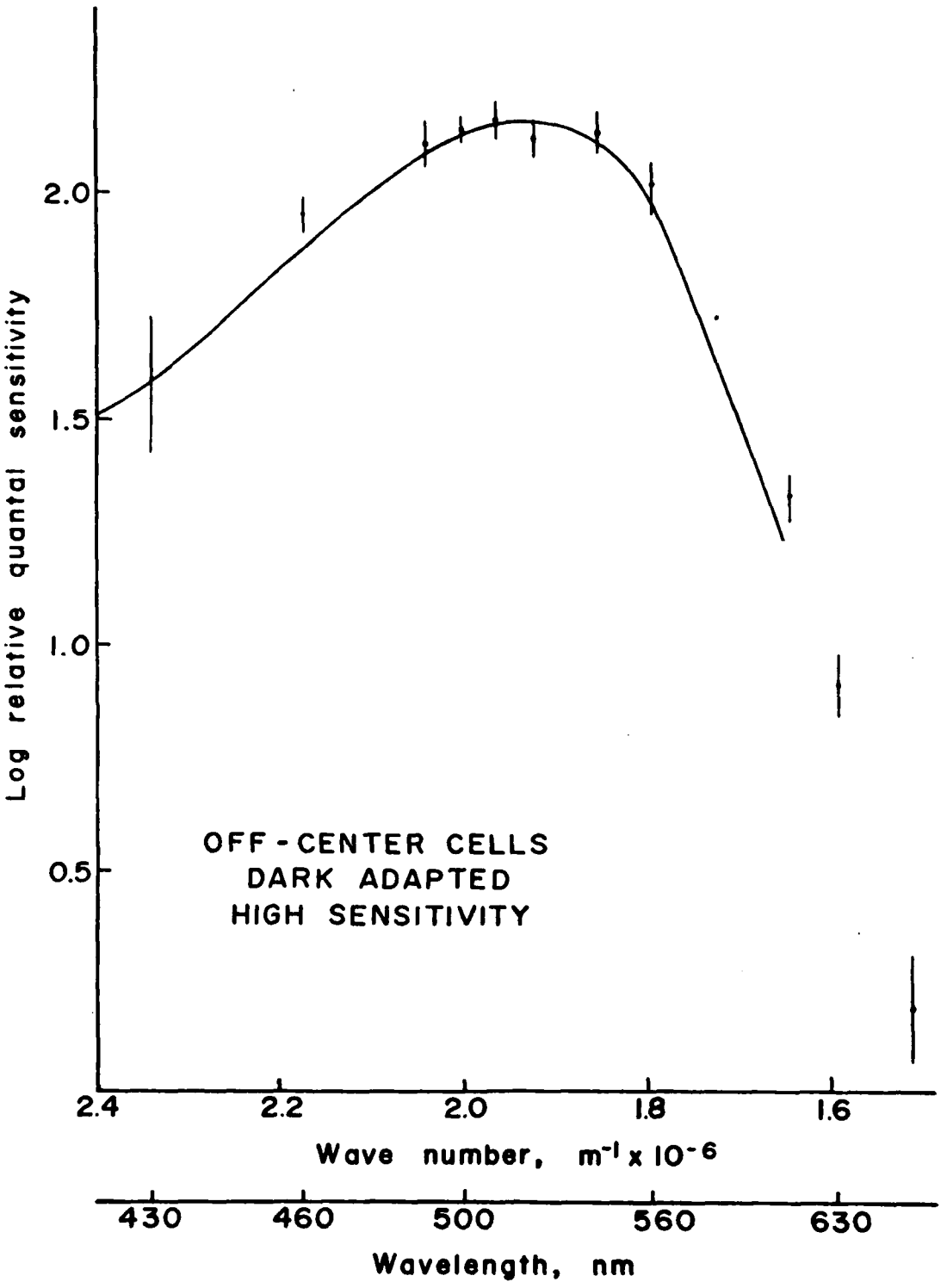
Log relative quantal sensitivity
2.0
1.5
1.0
0.5
OFF-CENTER CELLS
DARK ADAPTED
HIGH SENSITIVITY
2.4
2.2
2.0
1.8
1.6
Wave number, m⁻¹ x 10⁻⁶
430
460
500
560
630
Wavelength, nm

Figure 19. Spectral sensitivity of dark adapted OFF-center cells. These data are from the high sensitivity cells shown in the previous figure except that the Dartnall nomogram curve (solid curve) has been fitted by eye to the left leg of the data at the λmax of 504 nm.

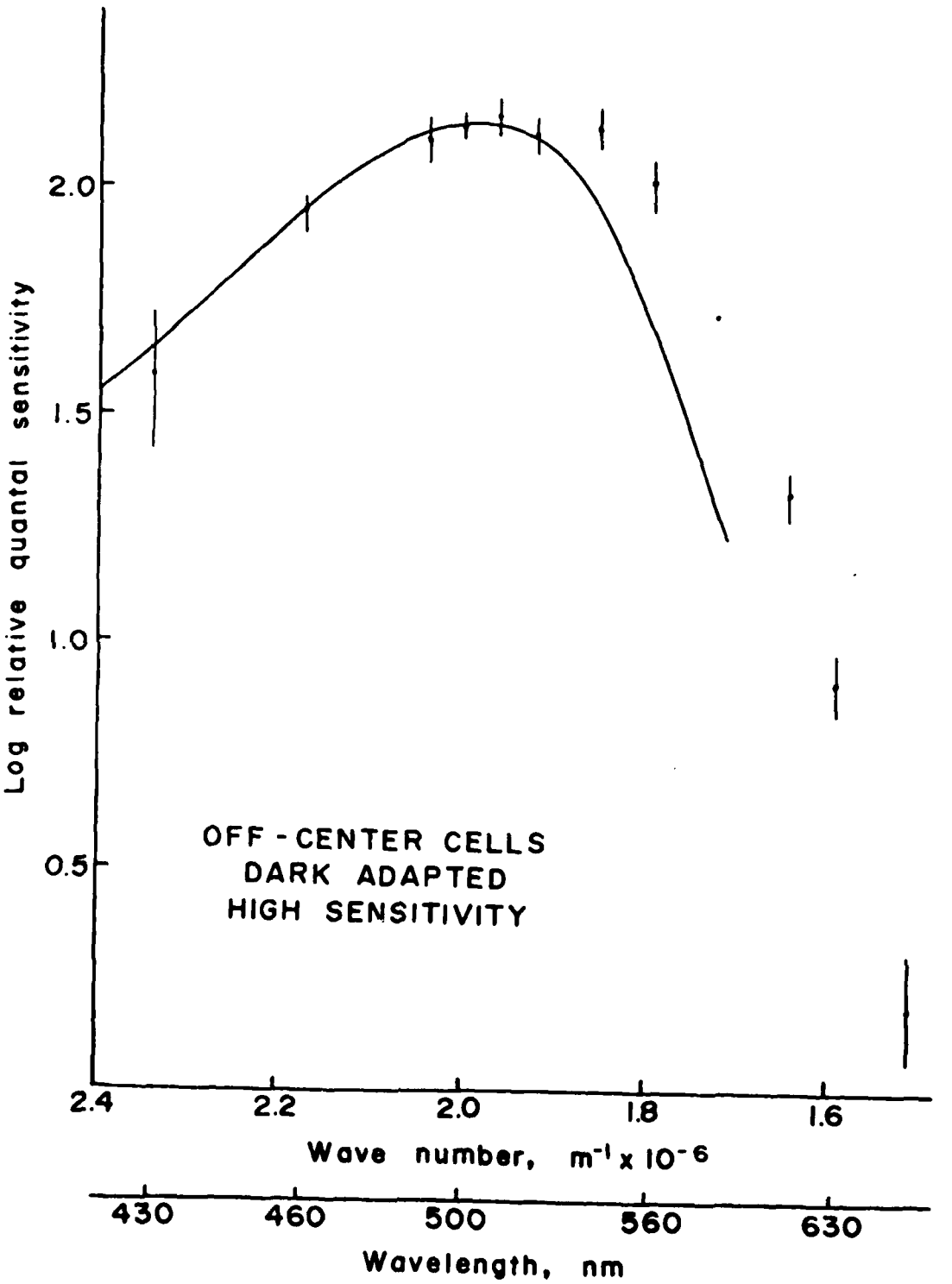
Log relative quantal sensitivity
2.0
1.5
1.0
0.5
OFF-CENTER CELLS
DARK ADAPTED
HIGH SENSITIVITY
2.4
2.2
2.0
1.8
1.6
Wave number, m⁻¹ x 10⁻⁶
430
460
500
560
630
Wavelength, nm

Figure 20. Dark-adapted spectral sensitivity of OFF-center cells. The data represents the mean, $\pm$ 1 standard error of the mean for the low sensitivity cells. The solid curve is the Dartnall nomogram curve placed at a λmax of 544 nm.

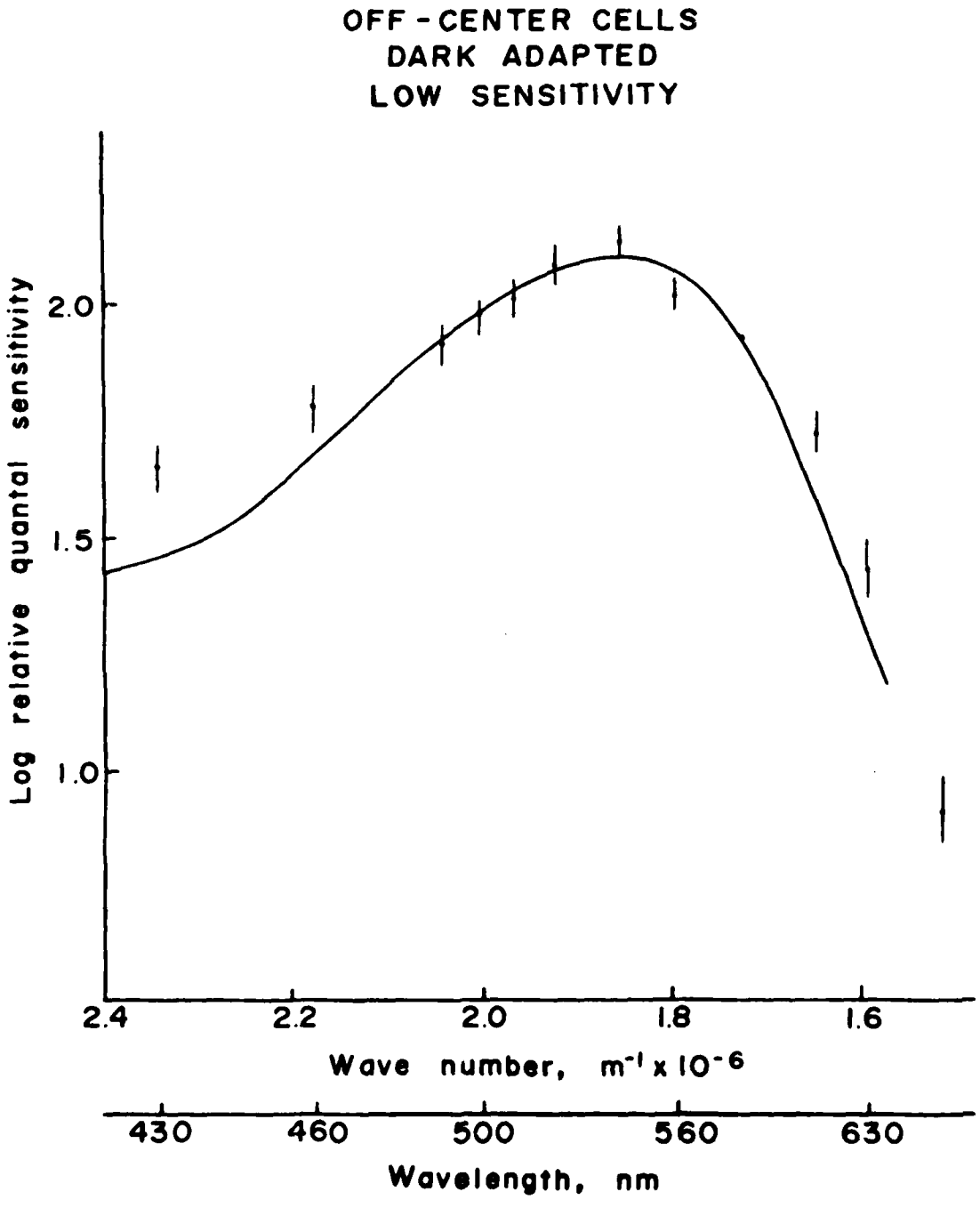
OFF-CENTER CELLS
DARK ADAPTED
LOW SENSITIVITY
Log relative quantal sensitivity
2.0
1.5
1.0
2.4
2.2
2.0
1.8
1.6
Wave number, m⁻¹ x 10⁻⁶
430
460
500
560
630
Wavelength, nm

Figure 21. Light-adapted spectral sensitivity for OFF-center cells. The data represents the means ($\pm$ 1 standard error of the mean) for OFF-center cells with a white light background. The retina was stimulated with 0.67 mm diameter spots of light. The solid curve is a Dartnall nomogram with the peak of the curve placed at 546 nm.

OFF-CENTER CELLS
LIGHT ADAPTED

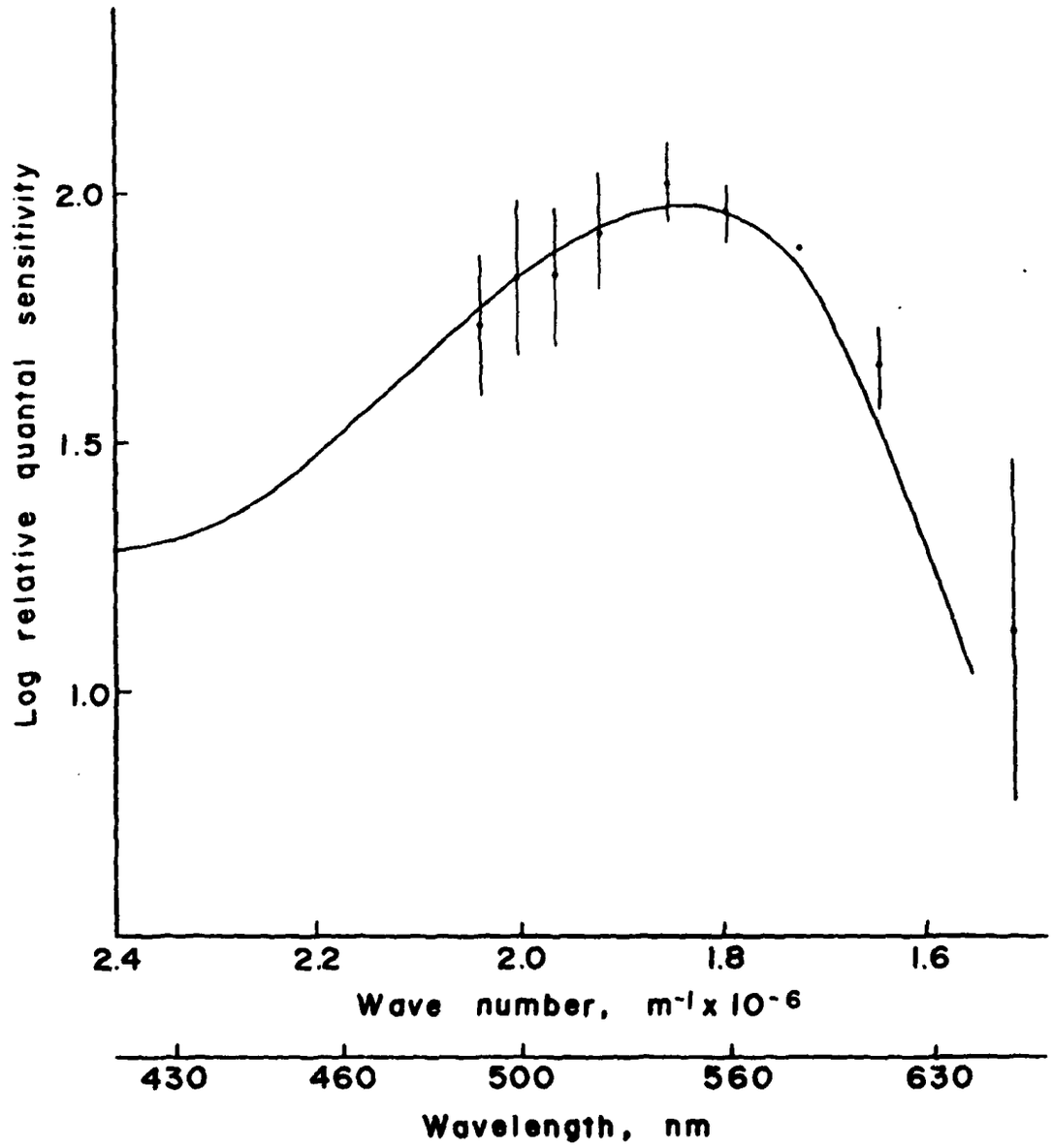

Figure 22. Spectral sensitivity of OFF-center cells with a blue-green background (Bausch & Lomb filter #90-1-570). Filled circles represent the mean, bars are $\pm$ 1 standard error of the mean. All data are normalized to 580 nm. The solid curve is the Dartnall nomogram curve placed at a peak sensitivity of 544 nm.

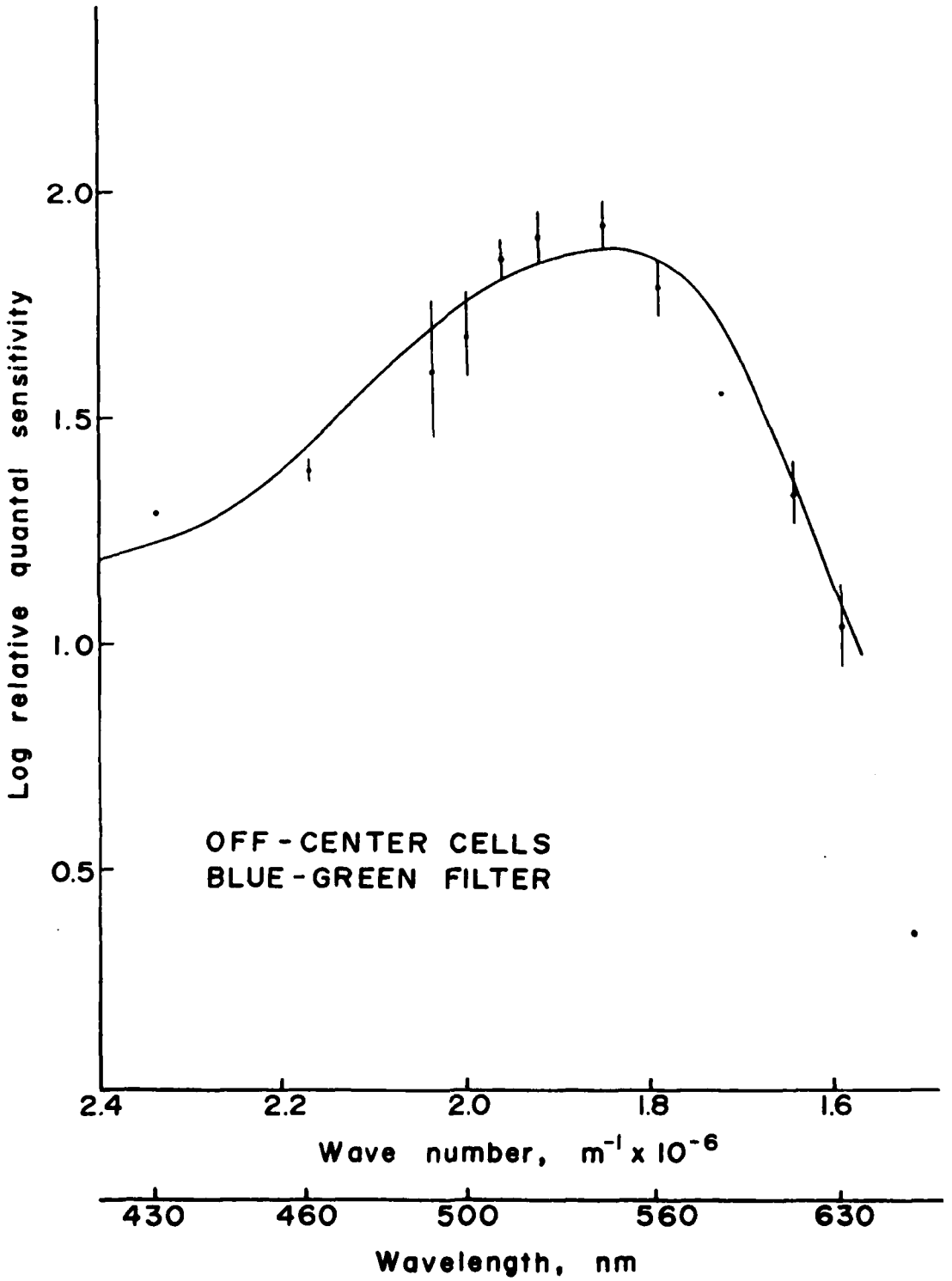
Log relative quantal sensitivity
2.0
1.5
1.0
0.5
OFF-CENTER CELLS
BLUE-GREEN FILTER
2.4
2.2
2.0
1.8
1.6
Wave number, m⁻¹ x 10⁻⁶
430
460
500
560
630
Wavelength, nm

Figure 23. Spectral sensitivity of OFF-center cells with a yellow background (Bausch & Lomb filter #90-2-520). The filled circles are the mean, vertical bars are $\pm$ 1 standard error of the mean. All data has been normalized to 580 nm. The solid curve is the Dartnall nomogram curve fitted to a peak sensitivity of 547 nm.

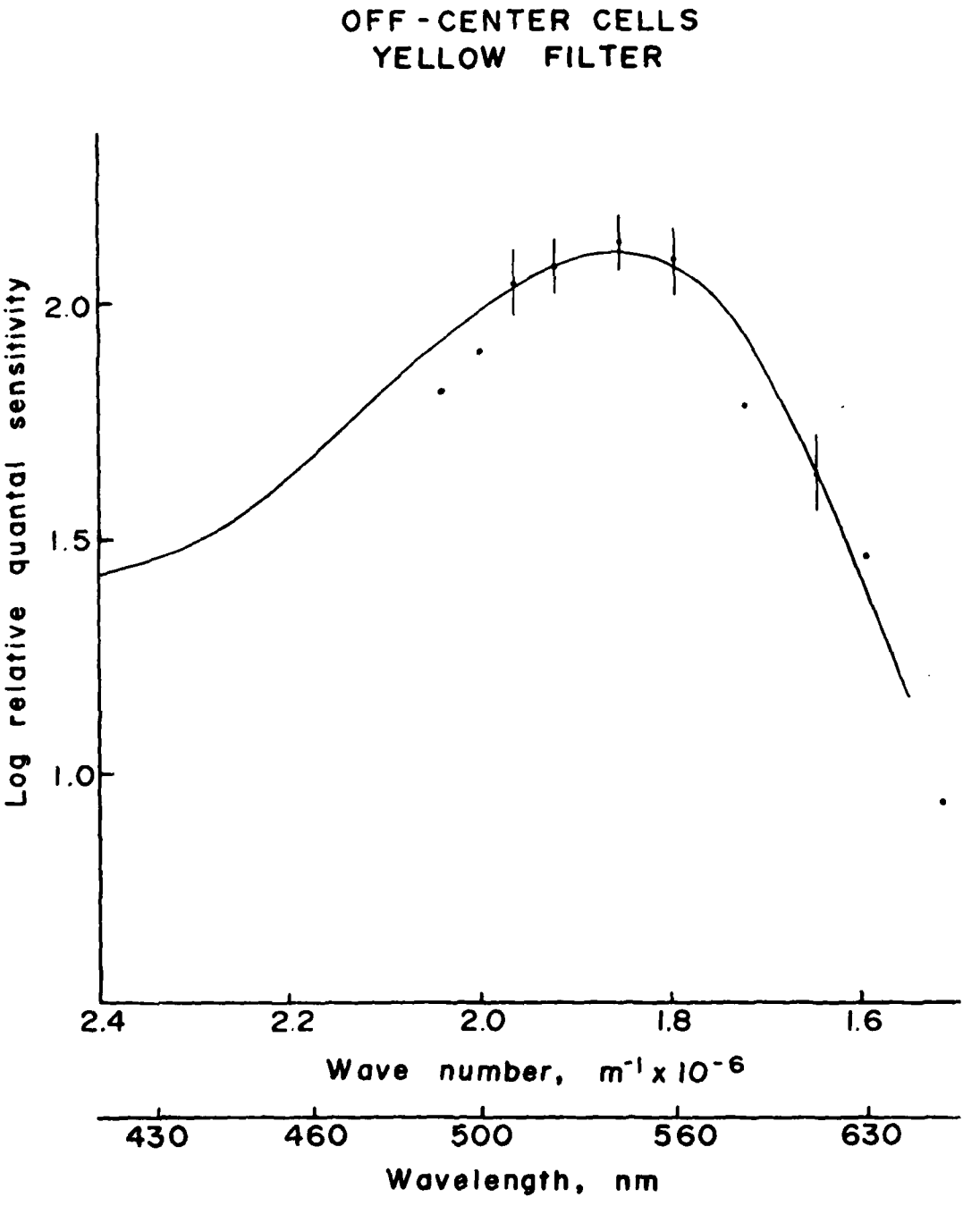
OFF-CENTER CELLS
YELLOW FILTER
Log relative quantal sensitivity
2.0
1.5
1.0
2.4
2.2
2.0
1.8
1.6
Wave number, m⁻¹ x 10⁻⁶
430
460
500
560
630
Wavelength, nm

Figure 24. Spectral sensitivity of dark adapted ON-center cells. The filled circles are the mean of the data. Vertical bars represent $\pm$ 1 standard error of the mean. The stimulus was a spot of light 0.67 mm in diameter. All data has been normalized to 580 nm. The solid curve is the Dartnall nomogram placed at a λmax of 522 nm.

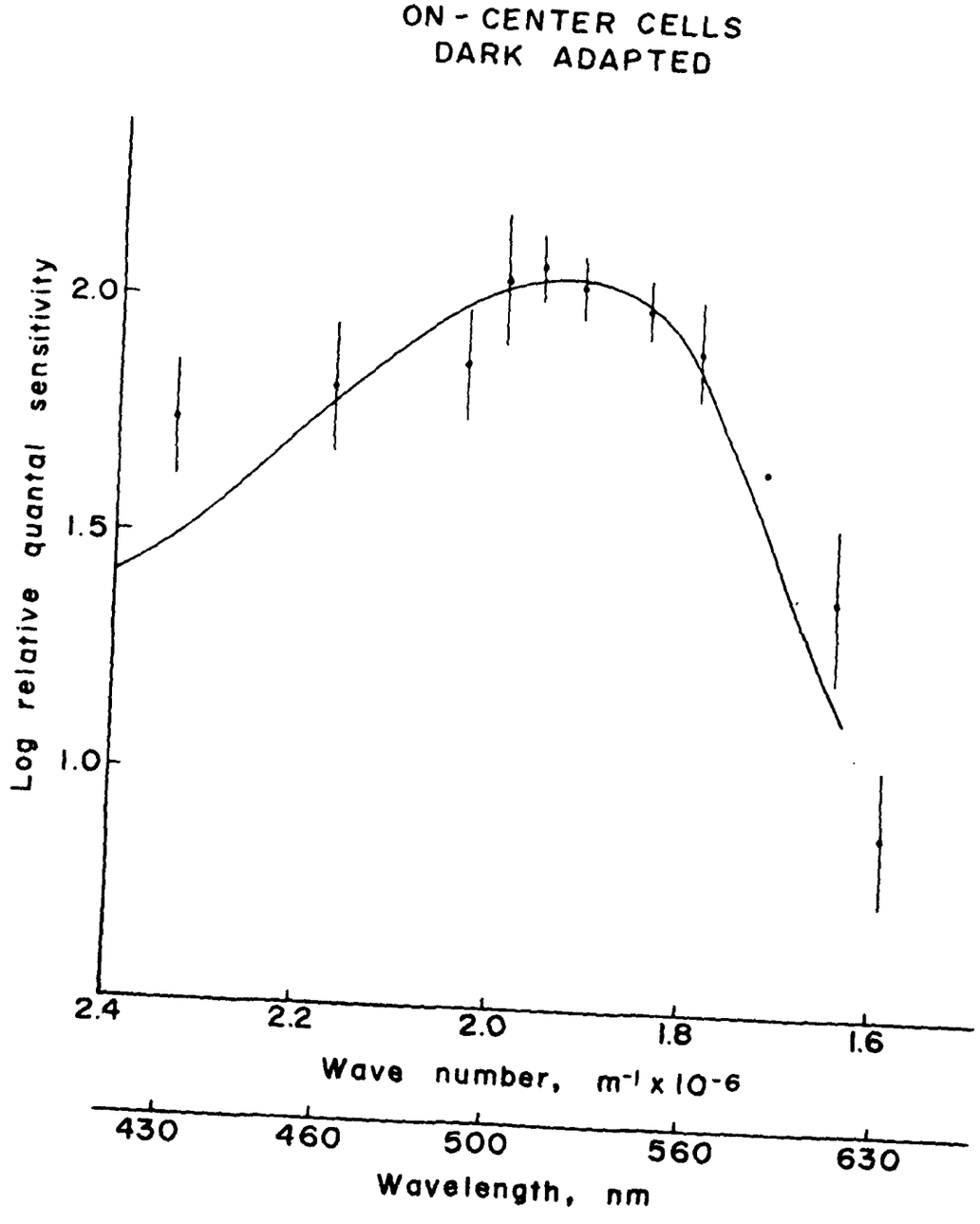
ON - CENTER CELLS
DARK ADAPTED
Log relative quantal sensitivity
2.0
1.5
1.0
2.4
2.2
2.0
1.8
1.6
Wave number, m⁻¹ x 10⁻⁶
430
460
500
560
630
Wavelength, nm

Figure 25. Spectral sensitivity for light adapted ON-center cell. The filled circles represent data from a single experiment. The retina was adapted with a white light background (2.1 mm in diameter) and stimulated with a 0.67 mm spot. The solid curve is the Dartnall nomogram placed at a λmax of 547 nm.

ON-CENTER CELLS
LIGHT ADAPTED

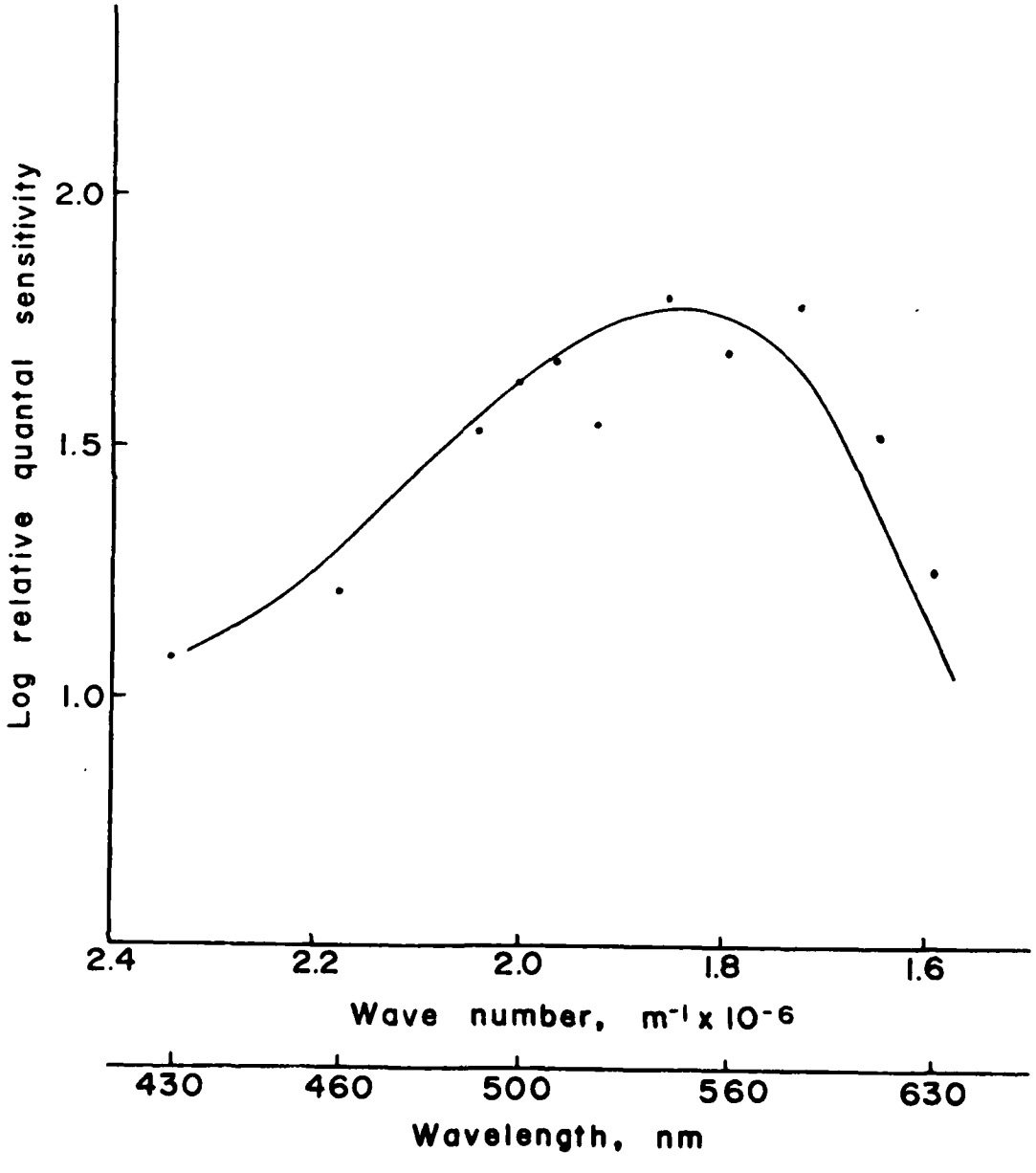

Figure 26. Spectral sensitivity for an ON-center cell with a red background (Kodak wratten #92). The filled circles represent data from a single experiment. The retina was adapted with a 2.1 mm spot of red light. The stimulus was a 0.67 mm spot of light of different wavelengths. The solid curve is the Dartnall nomogram placed at a λmax of 544 nm.

ON-CENTER CELLS
RED FILTER

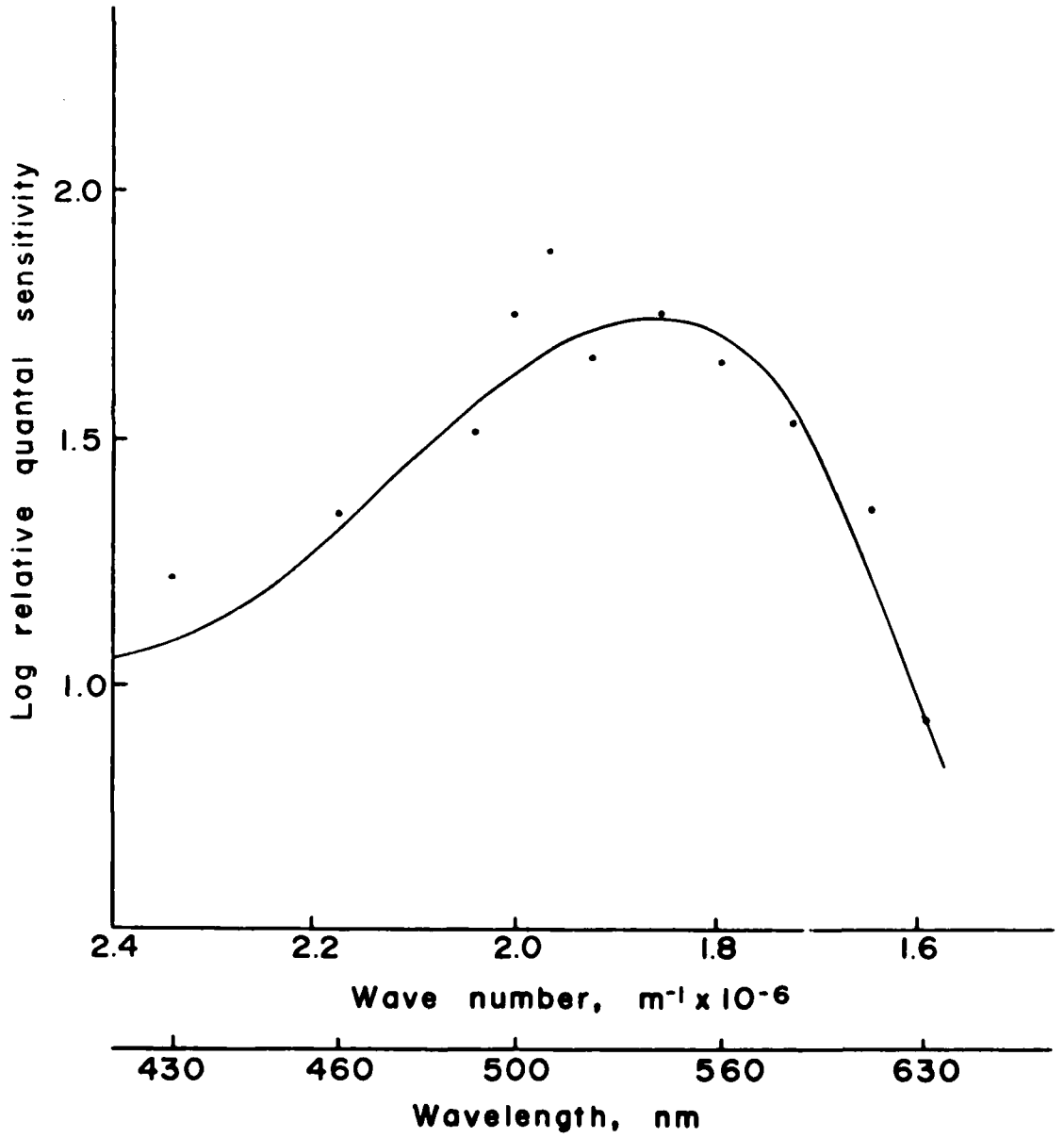

Figure 27. Spectral sensitivity for an ON-center cell with an orange background (Kodak wratten #23). The filled circles represent data from a single experiment. The cell was adapted with an orange background (2.1 mm in diameter) and stimulated with 0.67 mm spots of light. The solid curve is the Dartnall nomogram with a peak sensitivity of 544 nm.

ON-CENTER CELLS
ORANGE FILTER

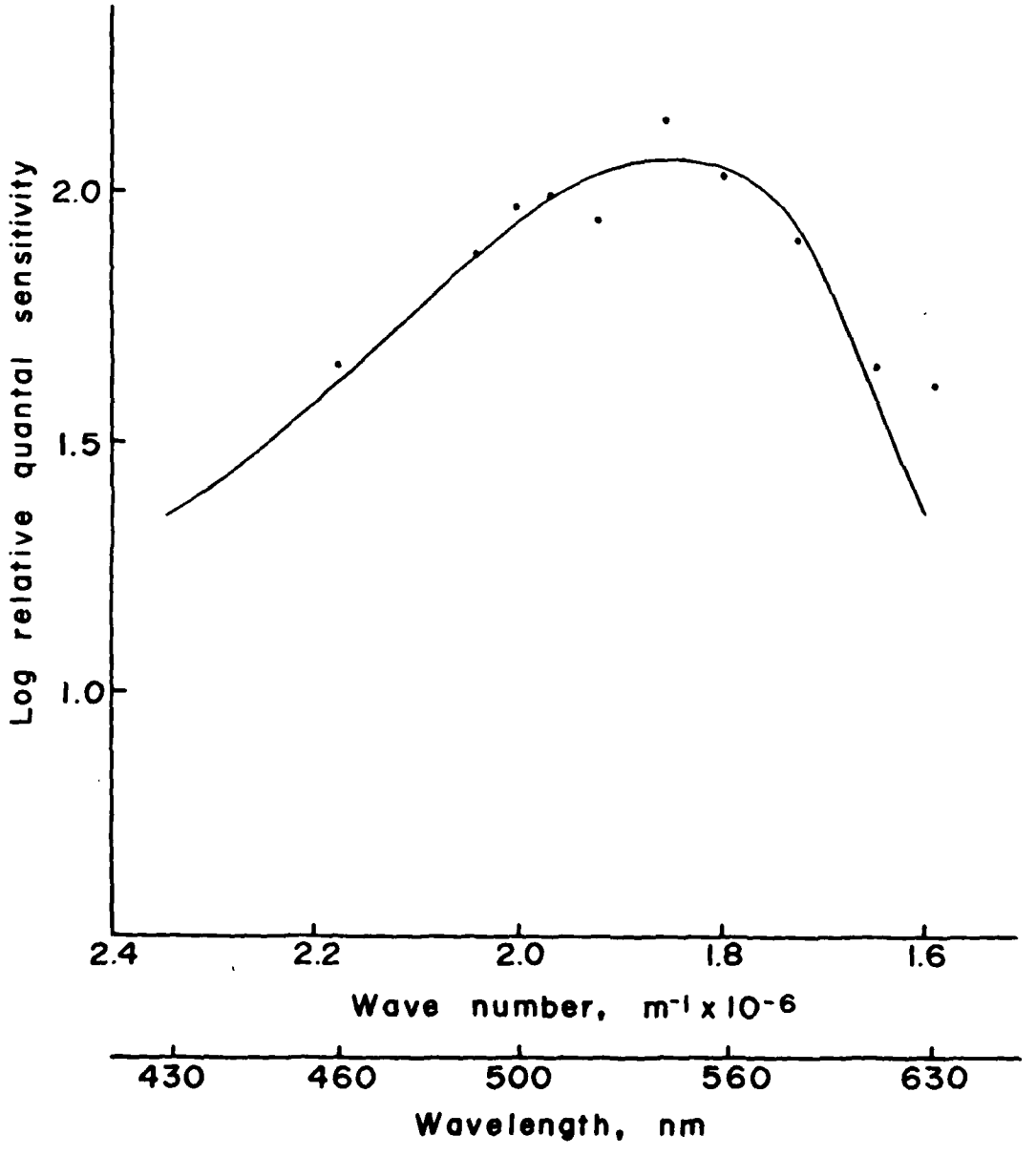

Figure 28. Spectral sensitivity for the off component of ON-OFF center cells in the dark-adapted state. The data are for the low sensitivity cells. The filled circles represent the mean of the data. The vertical bars are $\pm$ 1 standard of the mean. All data has been normalized to 580 nm. The solid curve is the Dartnall nomogram placed at a λmax of 544 nm.

ON-OFF-CENTER CELLS: OFF COMPONENT
DARK ADAPTED
LOW SENSITIVITY

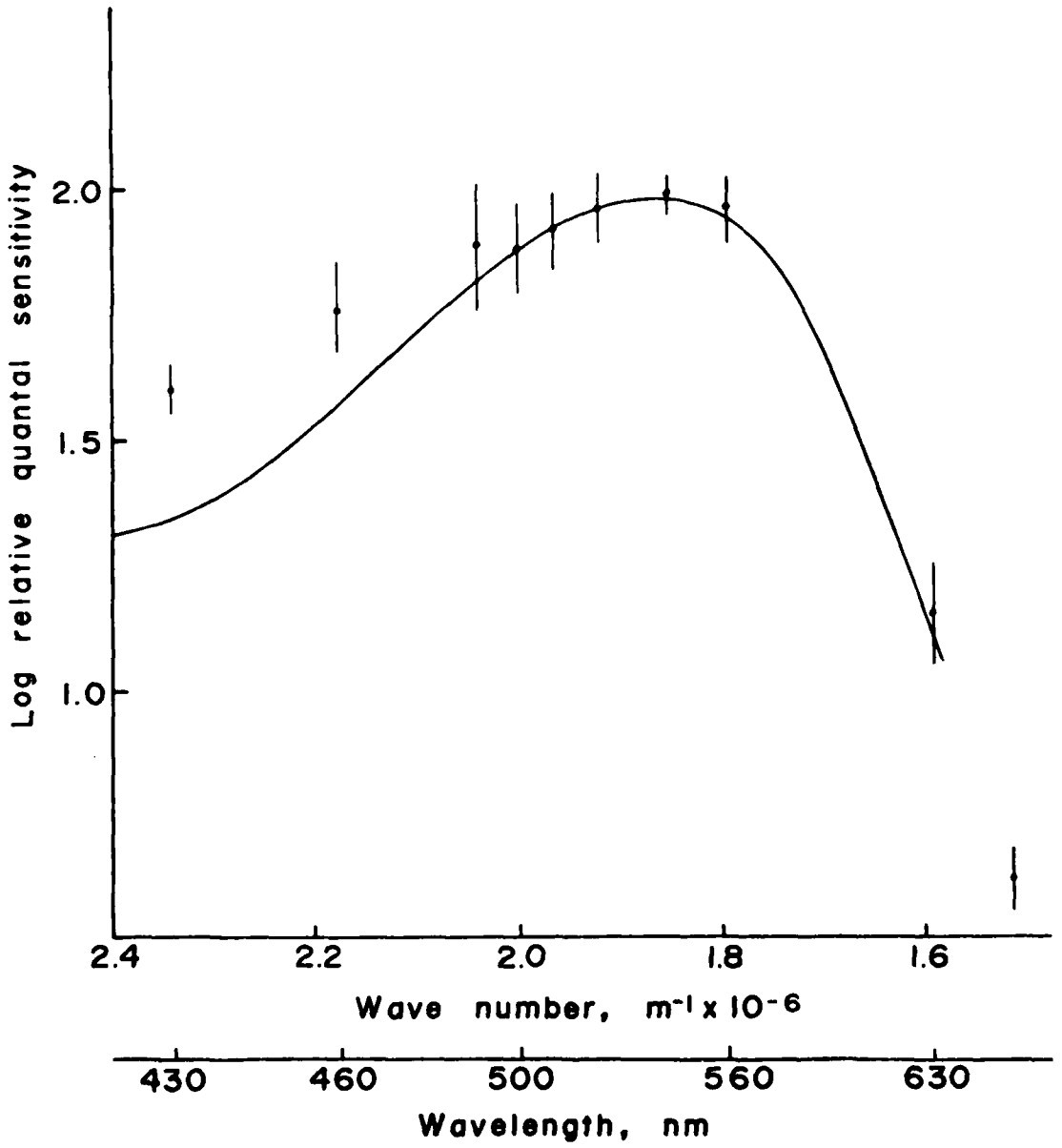

Figure 29. Spectral sensitivity for the off component of the ON-OFF center cells in the dark adapted state. The filled circles represent the mean of the data. The vertical lines are $\pm$ 1 standard error of the mean. The data is from the high sensitivity cells. The solid curve is the Dartnall nomogram placed at a λmax of 522 nm.

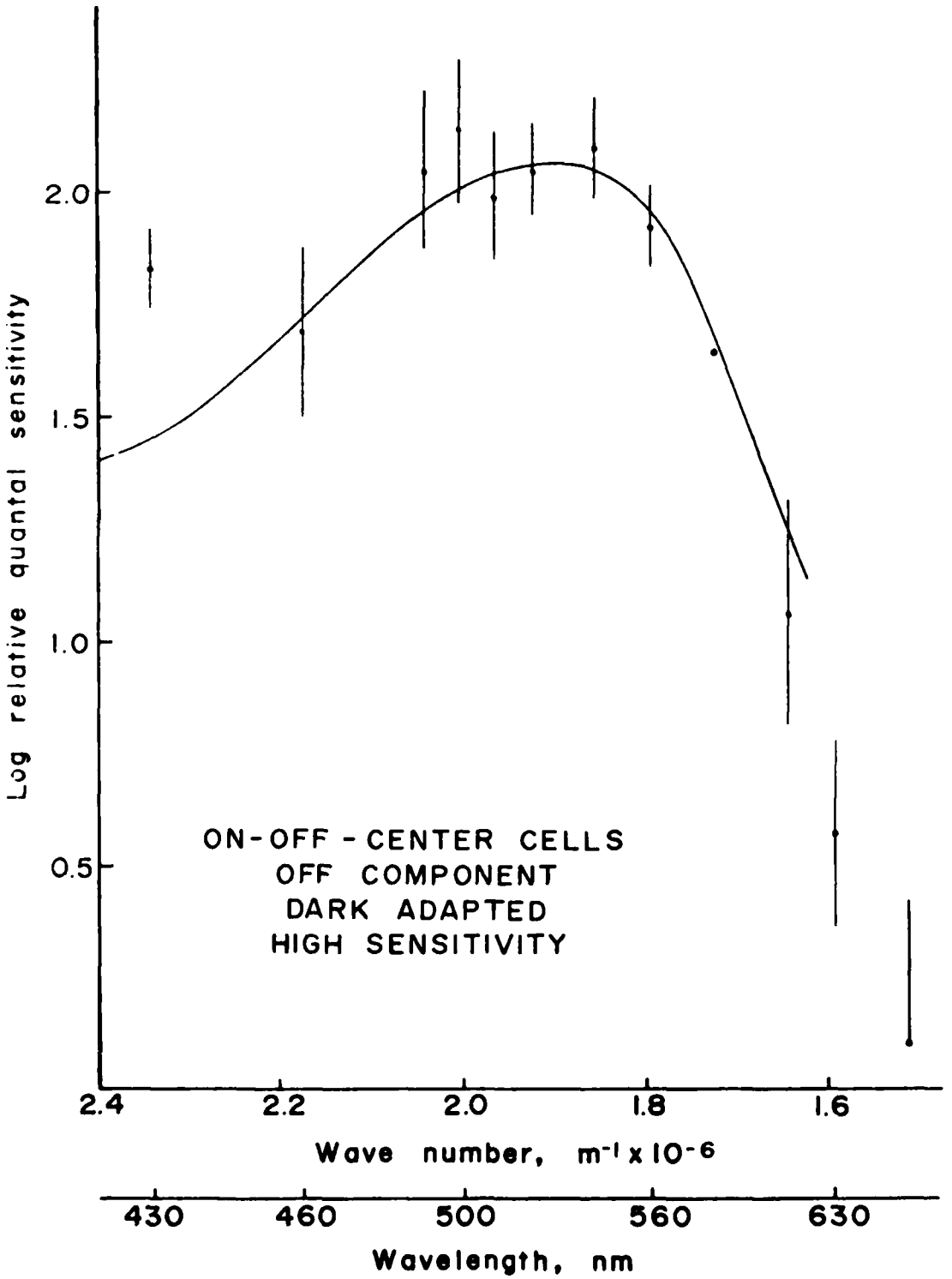
Log relative quantal sensitivity
2.0
1.5
1.0
0.5
ON-OFF-CENTER CELLS
OFF COMPONENT
DARK ADAPTED
HIGH SENSITIVITY
2.4
2.2
2.0
1.8
1.6
Wave number, m⁻¹ x 10⁻⁶
430
460
500
560
630
Wavelength, nm

Figure 30. Spectral sensitivity for the off component of the ON-OFF center cells in the light adapted state. The retina was adapted with a white light background (2.1 mm in diameter) and stimulated with a 0.67 mm spot. The data has been normalized to 580 nm. The solid curve is the Dartnall nomogram placed at a λmax of 544 nm.

ON-OFF-CENTER CELLS: OFF COMPONENT
LIGHT ADAPTED

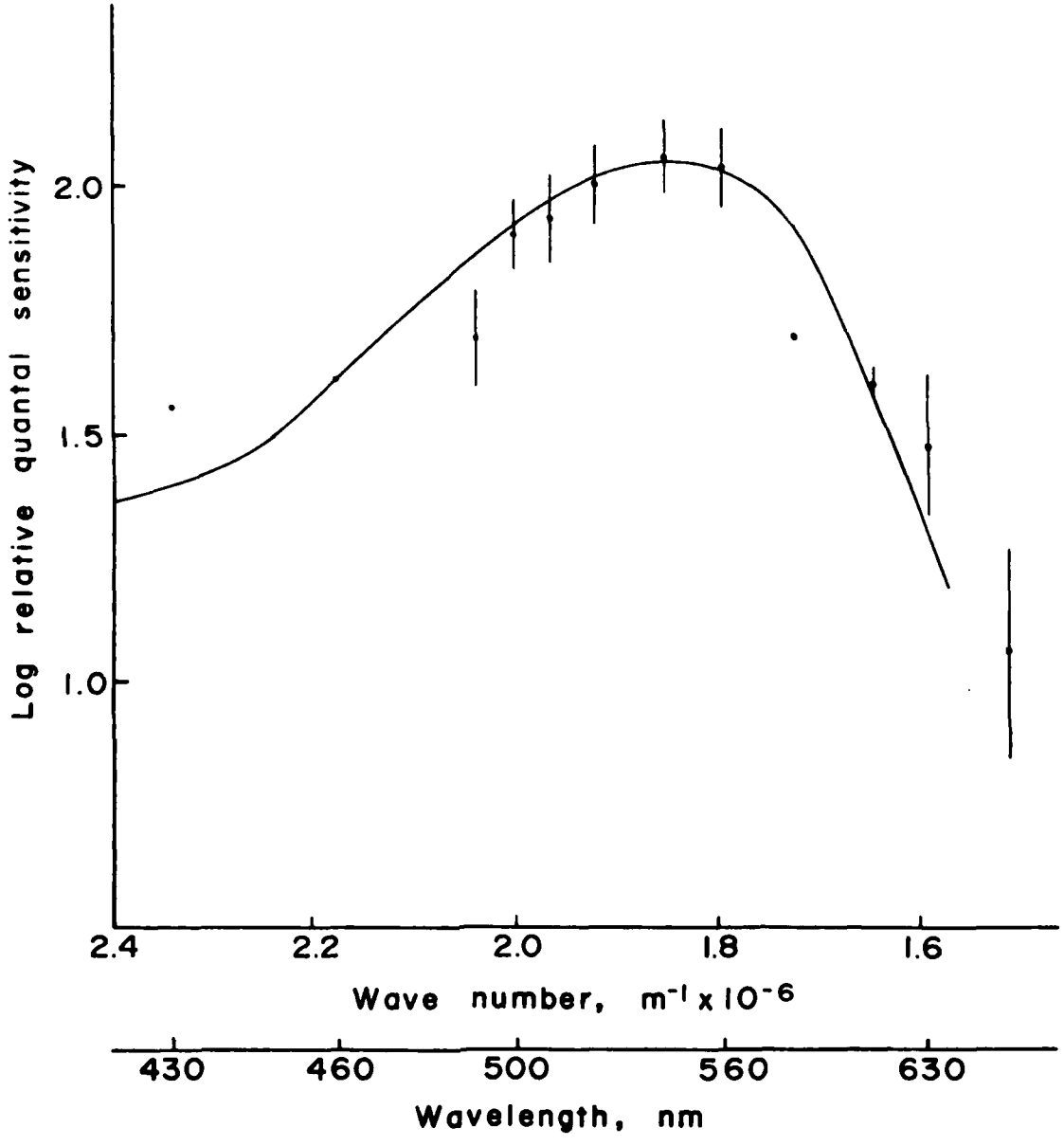

Figure 31. Spectral sensitivity for the off component of an ON-OFF center cell with a yellow background (Bausch & Lomb filter #90-2-520). The solid curve is the Dartnall nomogram curve placed at a λmax of 544 nm.

ON-OFF-CENTER CELLS: OFF COMPONENT
YELLOW FILTER

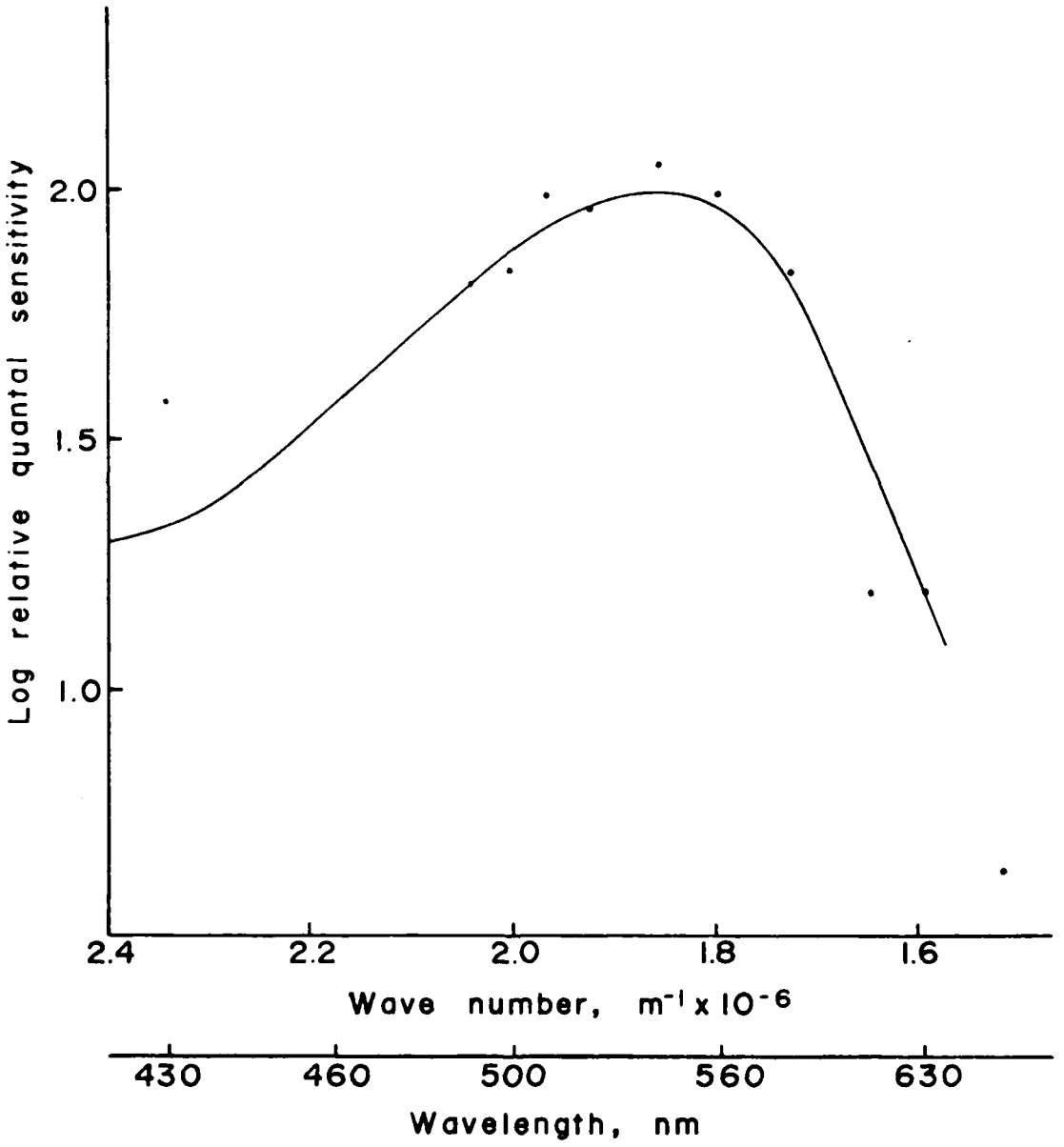

Figure 32. Spectra sensitivity of the on component of ON-OFF center cells in the dark adapted state. The data represents the mean, $\pm$ 1 standard error of the mean. All the data has been normalized to 580 nm. The solid curve is the Dartnall nomogram placed at a λmax of 519 nm.

ON-OFF-CENTER CELLS: ON COMPONENT
DARK ADAPTED

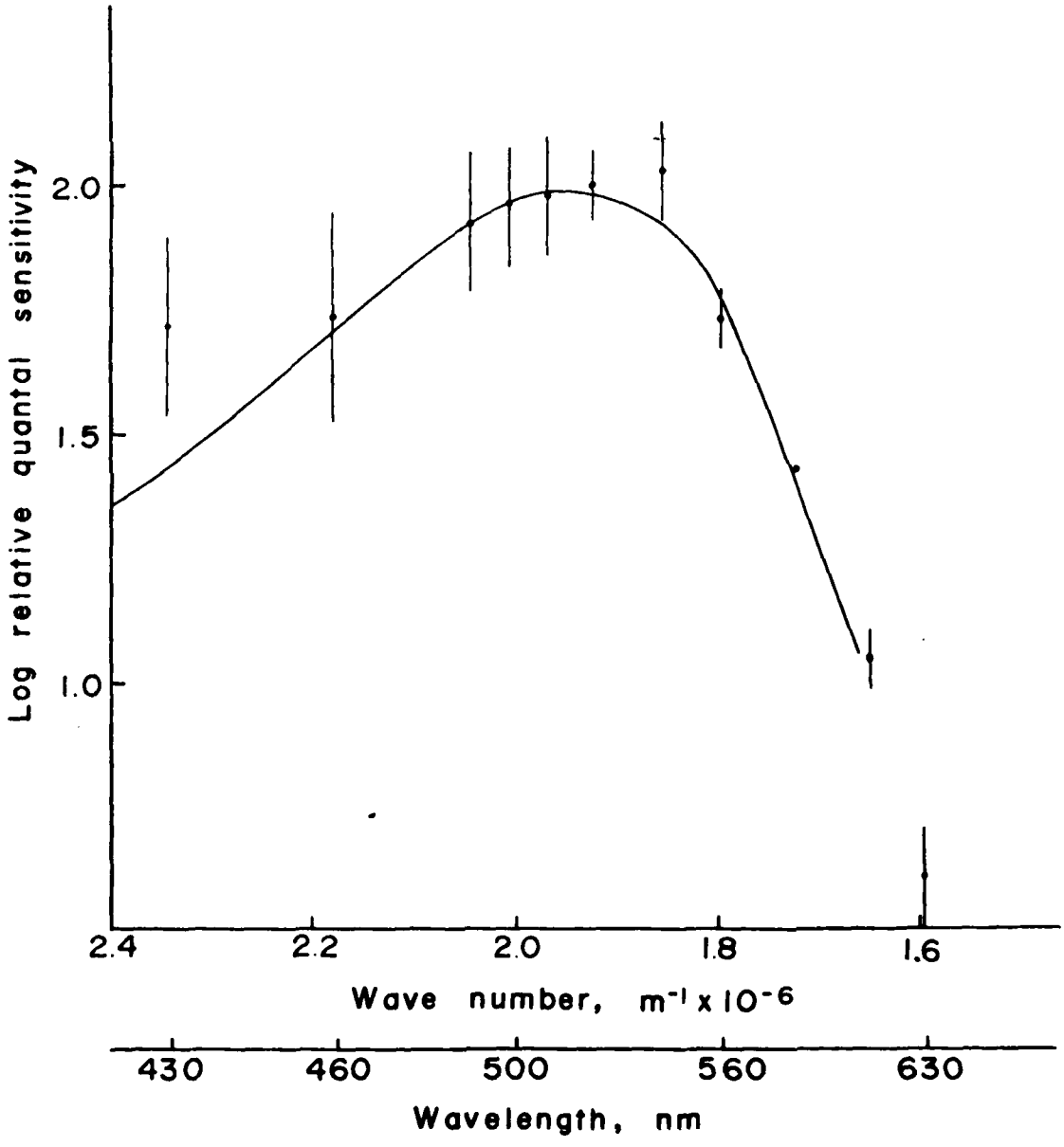

Figure 33. Spectral sensitivity for the on component of ON-OFF center cells in the light adapted state. The retina was adapted with a white light background (2.1 mm in diameter) and stimulated with 0.67 mm spots of light. The filled circles represent the mean of the data. Vertical bars are $\pm$ 1 standard error of the mean. All the data has been normalized to 580 nm. The solid curve is the Dartnall nomogram placed at a λmax of 535 nm.

ON-OFF-CENTER CELLS: ON COMPONENT
LIGHT ADAPTED

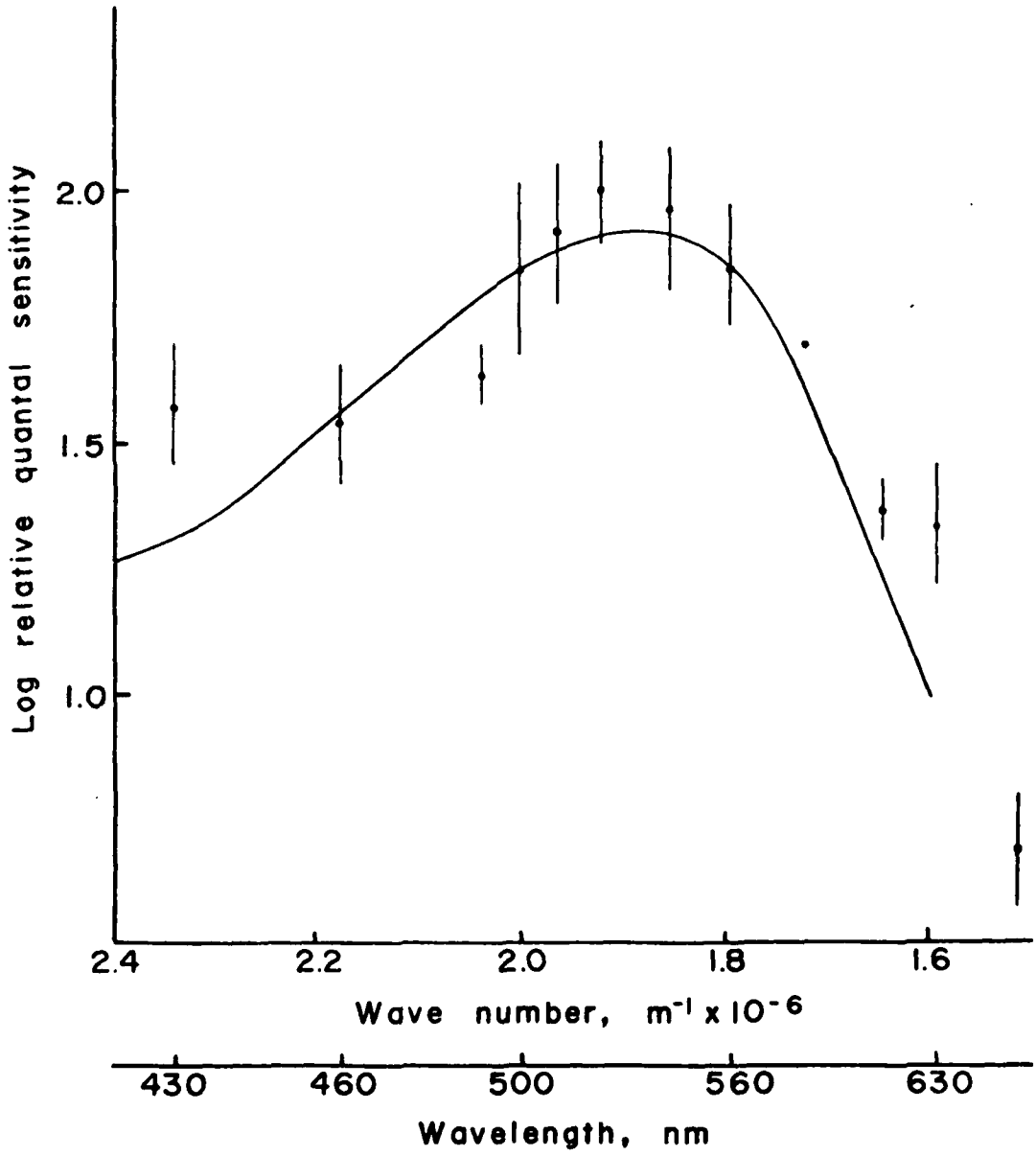

Figure 34. Spectral sensitivity of the on component of ON-OFF center cells with a yellow background (Bausch & Lomb filter #90-2-520). The retina was adpated with a yellow background (2.1 mm in diameter) and stimulated with 0.67 mm spots of light. The filled circles represent the mean of the data. Vertical bars are $\pm$ 1 standard error of the mean. All the data has been normalized to 580 nm. The solid curve is the Dartnall nomogram placed at a λmax of 544 nm.

ON-OFF-CENTER CELLS: ON COMPONENT
YELLOW FILTER

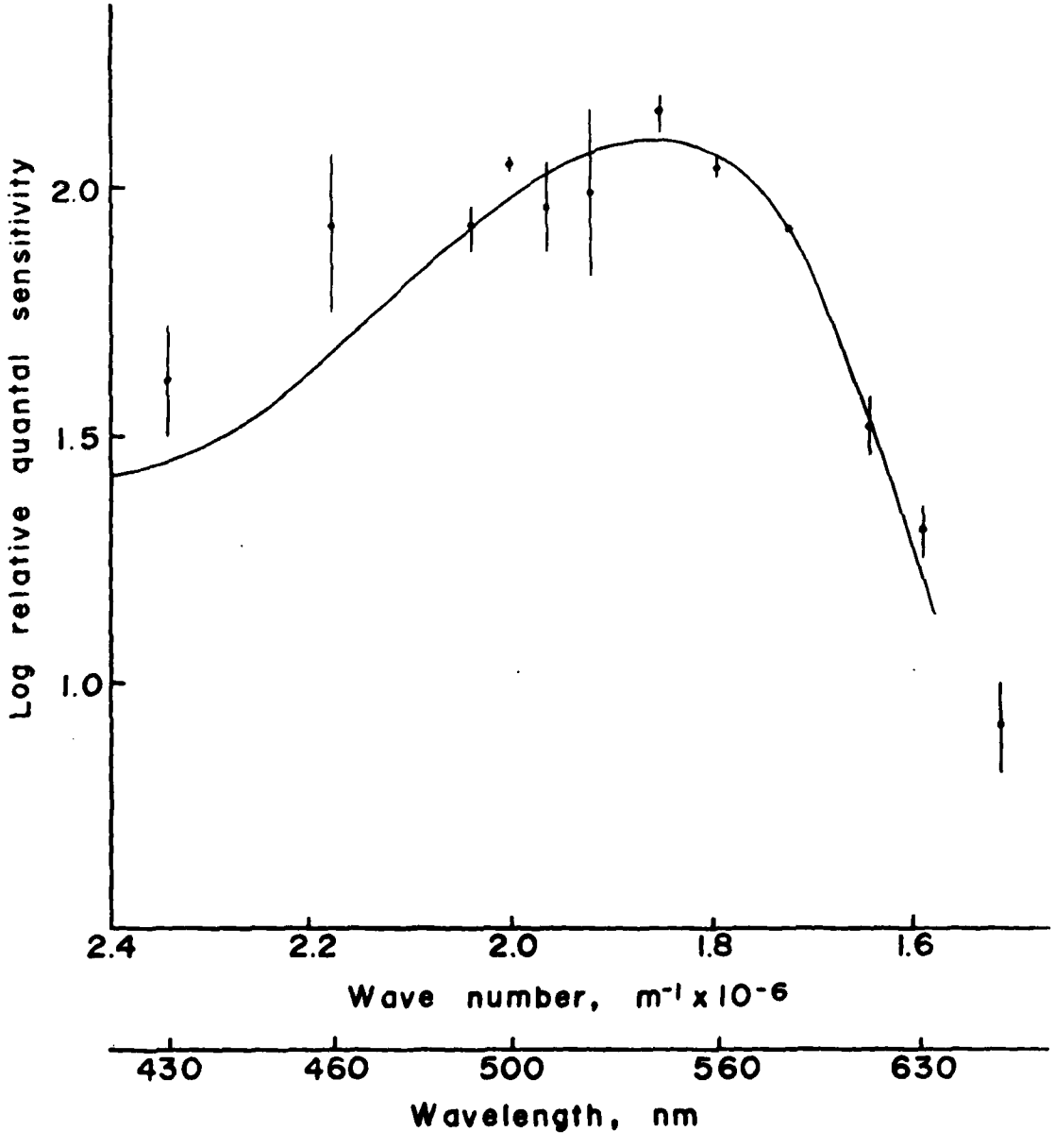

Figure 35. Antagonistic surround. The left hand column represents the response of an ON-center cell to a small spot (0.67 mm in diameter) of white, blue (460 nm) and red (610 nm) light, one second in duration. The response is "on" to all the stimuli. The right hand column is the responses of the same cell to an annular stimulus. A small spot (0.67 mm in diameter) of white light is continuously on. The response of the cell is "off" to all annular stimuli. Time marker is one second. Amplitude is 50 μvolts/div.

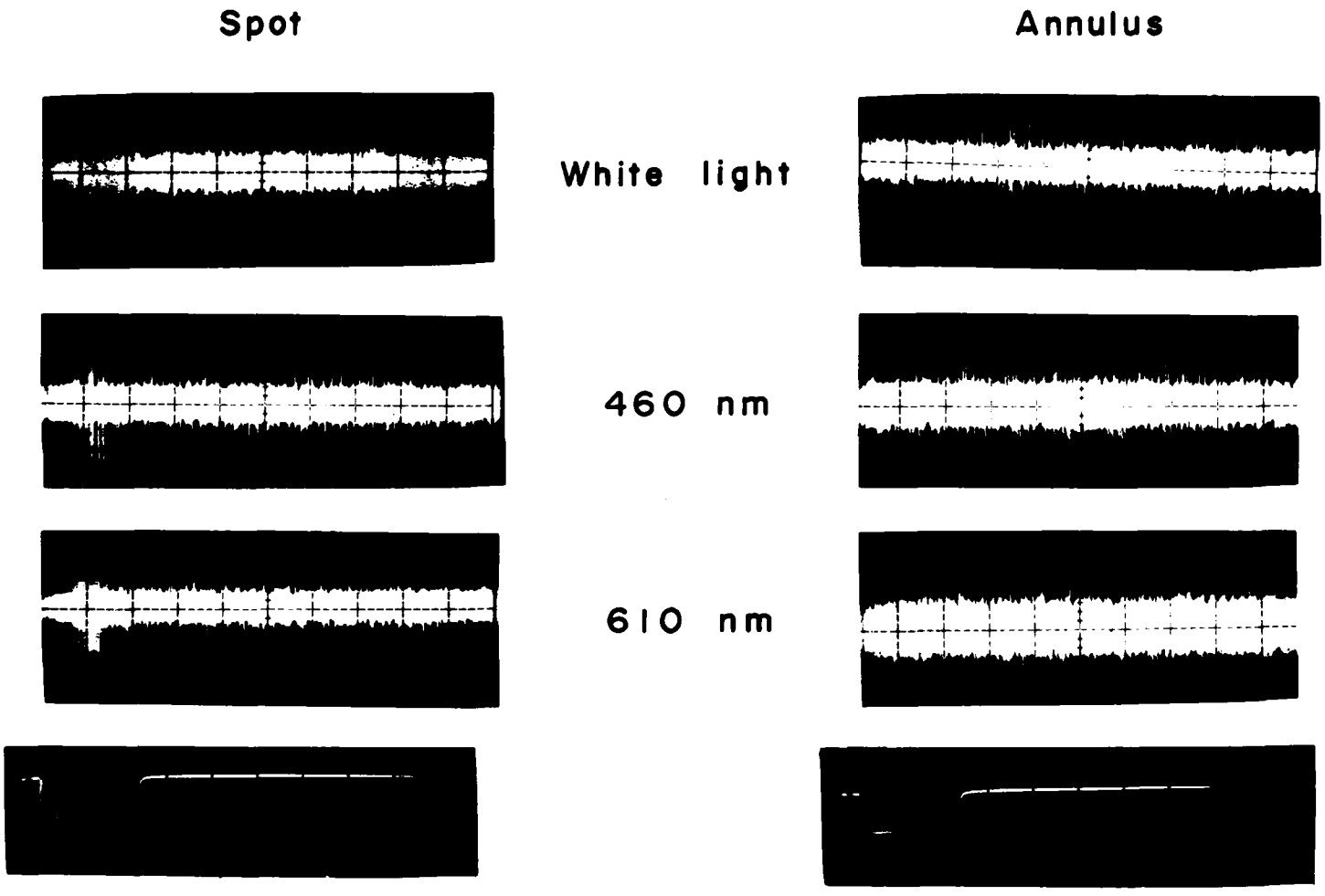
Spot
Annulus
White light
460 nm
610 nm
1 sec
1 sec

REFERENCES

Adams, A.J. and A.J. Afanador. 1971. Ganglion cell receptive field organization at different levels of light adaptation. Am. J. Optometry and Am. Acad. Optometry, 48: 889-896.

Ali, M.A. and M. Anctil. 1974. Retinas of the electric ray (Narcine brasiliensis) anc the freshwater stingray (Paratrygon motoro). Vision Res., 14: 587-588.

Ali, M.A. and M. Anctil. 1976. Retinas of Fishes. An Atlas. Springer-Verlag, Berlin.

Ali, M.A. and H.J. Wagner. 1975. Distribution and development of retinomotor responses. Vision in Fishes. Plenum Press, New York.

Anctil, M. and M.A. Ali. 1974. Giant ganglion cells in the retina of the hammerhead shark (Sphyrna lewini). Vision Res., 14: 903-904.

Barlow, H.B. 1953. Summation and inhibition in the frog's retina. J. Physiol., 119: 69-88.

Beauchamp, R.D. and J.V. Lovasik. 1973. Blue mechanism response of single goldfish optic fibers. J. Neurophysiol., 36: 925-939.

Bigelow, H.G. and W.C. Schroeder. 1948. Fishes of the Western North Atlantic Pt. 1., Lancelets, Cyclostomes and Sharks. Memoir #1. Sears Found. for Mar. Res., Yale University, New Haven.

Boycott, B.B. and H. Kolb. 1973. The connexions between bipolar cells and photoreceptors in the retina of the domestic cat. J. Comp. Neur., 148: 91-114.

Boycott, B.B., J.E. Dowling, S.K. Fisher, H. Kolb and A.M. Laties. 1975. Interplexiform cells of the mammalian retina and their comparison with catecholamine containing retinal cells. Proc. R. Soc. Lond., B191: 353-368.

Bridges, C.D.B. 1965. The groupings of fish visual pigments about preferred positions in the spectrum. Vision Res., 5: 223-238.

Cajal, S.R.y. 1892. La retine des vertebres. Cellule, 9: 121-225. Engl. transl. The Structure of the Retina (transl. S.A. Thorpe and M. Glickstein). C.C. Thomas. Springfield.

Chino, Y.M. and J.F. Sturr. 1975. The time course of inhibition during the delayed response of the ON-OFF ganglion cell in the frog. Vision Res., 15: 185-191.

Cohen, J.L., S.H. Gruber and D.I. Hamasaki. 1977. Spectral sensitivity and Purkinje shift in the retina of the lemon shark, Negaprion brevirostris (Poey). Vision Res., 17: 787-792.

Copenhagen, D.R. and W.G. Owen. 1976. Functional characteristics between rods in the retina of the snapping turtle. J. Physiol., 259: 251-282.

Daw, N.W. 1968. Colour-coded ganglion cells in the goldfish retina: extension of their receptive fields by means of new stimuli. J. Physiol., 197: 567-592.

Dawson, W.W. and J.M. Perez. 1973. Unusual retinal cells in the dolphin eye. Science, 181: 747-749.

DeMonasterio, F.M. and P. Gouras. 1975. Functional properties of ganglion cells of the rhesus monkey retina. J. Physiol., 251: 167-195.

DeMonasterio, F.M., P. Gouras and D.J. Tolhurst. 1975. Concealed colour opponency in ganglion cells of the rhesus monkey retina. J. Physiol., 251: 217-229.

Dowling, J.E. 1970. Organization of vertebrate retinas. Invest. Opthal., 9: 655-680.

Dowling, J.E. and B.B. Boycott. 1966. Organization of the primate retina: Electron Microscopy. Proc. Roy. Soc. Lond., B166: 80-111.

Dowling, J.E. and B. Ehinger. 1975. Synaptic organization of the amine containing interplexiform cells of the goldfish and cebus monkey retinas. Science, 188: 270-273.

Dowling, J.E. and H. Ripps. 1970. Visual adaptation in the retina of the skate. J. Gen. Physiol., 56: 491-520.

Dowling, J.E., J.E. Brown and E. Major. 1966. Synapses of horizontal cells in rabbit and cat retinas. Science, 153: 1639-1641.

Dunn, R.F. 1973. The ultrastructure of the vertebrate retina. The Ultrastructure of Sensory Organs. Elsevier, New York.

Easter, S.S., Jr. 1975. Retinal specializations for aquatic vision: Theory and facts. Vision in Fishes. Plenum Press, New York.

Ehinger, B., B. Falck and A.M. Laties. 1969. Adrenergic neurons in teleost retina. Z. Zellforsch. Mikrosk. Anat., 97: 285-297.

Famiglietti, E.V., Jr. and H. Kolb. 1976. Structural basis for ON and OFF center responses in retinal ganglion cells. Science, 194: 193-195.

Famiglietti, E.V., Jr., A. Kaneko and M. Tachibana. 1977. Neuronal architecture of on and off pathways to ganglion cells in carp retina. Science, 198: 1267-1269.

Gallego, A. 1971. Horizontal and amacrine cells in the mammal's retina. Vision Res. Suppl., 3: 33-50.

Gilbert, P.W. 1961. The visual apparatus of sharks and its probable role in predation. Abstr., Xth Pacific Sci. Congr., Honolulu.

Gilbert, P.W. 1963. The visual apparatus of sharks. Sharks and Survival. D.C. Heath and Co., Lexington.

Gold, G.H. and J.E. Dowling. 1979. Photoreceptor coupling in retina of the toad, Bufo marinus. I. Anatomy. J. Neurophysiol., 42: 292-310.

Gouras, P. 1965. Primate retina duplex function of dark adapted ganglion cells. Science, 147: 1593-1594.

Gouras, P. 1968. Identification of cone mechanisms in monkey ganglion cells. J. Physiol., 199: 533-547.

Gouras, P. and K. Link. 1966. Rod and cone interaction in dark-adapted monkey ganglion cells. J. Physiol., 184: 499-510.

Gruber, S.H. 1969. The physiology of vision in the lemon shark, Negaprion brevirostris (Poey): a behavioral analysis. Ph.D. dissertation, Unversity of Miami, Coral Gables, Florida.

Gruber, S.H. 1979. *Mechanisms of color vision: An ethologist's primer.* The Behavioral Significance of Color. Garland STP Press, New York.

Gruber, S.H. and J.L. Cohen. 1978. Visual system of the elasmobranchs: state of the art 1960-1975. Sensory Biology of Sharks, Skates, and Rays. U.S. Government Printing Office, Washington, D.C.

Gruber, S.H., D.I. Hamasaki and C.D. Bridges. 1963. Cones in the retina of the lemon shark (Negaprion brevirostris). Vision Res., 3: 397-399.

Hamasaki, D.I. and S.H. Gruber. 1965. The photoreceptors of the nurse shark, Ginglymostoma cirratum and the sting ray, Dasyatis sayi. Bull. Mar. Sci., 15: 1051-1059.

Hartline, H.K. 1938. The response of single optic nerve fibers of the vertebrate eye to illumination of the retina. Am. J. Physiol., 121: 400-415.

Hartline, H.K. 1940a. The receptive fields of optic nerve fibers. Am. J. Physiol., 130: 690-699.

Hartline, H.K. 1940b. The effects of spatial summation in the retina on the excitation of the fibers of the optic nerve. Am. J. Physiol., 130: 700-711.

Hubel, D.H. 1957. Tungsten microelectrode for recording from single units. Science, 125: 549-550.

Hubbell, W.L. and M.D. Bownds. 1979. Visual transduction in vertebrate photoreceptors. Ann. Rev. Neurosci., 2: 17-34.

Kaneko, A. 1971. Electrical connexions between horizontal cells in the dogfish retina. J. Physiol., 213: 95-105.

Kolb, H. and E.V. Famiglietti, Jr. 1976. Rod and cone pathways in the retina of the cat. Invest. Ophthal., 15: 935-946.

Kuffler, S.W. 1953. Discharge patterns and functional organization of mammalian retina. J. Neurophysiol., 16: 37-68.

Lasansky, A. 1971. Synaptic organization of cone cells in the turtle retina. Phil. Trans. Roy. Soc., B 262: 365-381.

Lettvin, J.Y., H.R. Maturana, W.S. McCulloch and W.H. Pitts. 1959. What the frog's eye tells the frog's brain. Proc. Inst. Radio Engrs., 47: 1940-1951.

Maturana, H.R., J.Y. Lettvin, W.S. McCulloch and W.H. Pitts. 1960. Anatomy and physiology of vision in the frog (Rana pipiens). J. Gen. Physiol., 43, suppl. 2 (Mechanisms of vision): 129-171.

Michael, C.R. 1968. Receptive fields of single optic nerve fibers in a mammal with an all-cone retina. III. Opponent color units. J. Neurophysiol., 31: 268-282.

Munz, F.W. and W.N. McFarland. 1973. The significance of spectral position in the rhodopsins of tropical marine fishes. Vision Res., 13: 1829-1874.

Naka, K.I. 1976. Neuronal circuitry in the catfish retina. Invest. Ophthal., 15: 926-935.

Naka, K.I. and W.A.H. Rushton. 1968. S-potential and dark adaptation in fish. J. Physiol., 194: 259-269.

Nelson, R. 1977. Cat cones have rod input: a comparison of the response properties of cones and horizontal cell bodies in the retina of the cat. J. Comp. Neur., 172: 109-136.

Nelson, R., E.V. Famiglietti and H. Kolb. 1978. Intracellular staining reveals different levels of stratification for on and off center ganglion cells in cat retina. J. Neurophysiol., 41: 472-483.

Neumayer, L. 1897. Der feinere Bau der Selachier-Retina. Archiv fur

mikroskopische anatomie, 48: 83-111.

Oyster, C.W. and E.S. Takashi. 1977. Interplexiform cells in rabbit retina. Proc. Roy. Soc. Lond., B197: 477-484.

Parthe, V. 1972. Horizontal, bipolar and oligopolar cells in the teleost retina. Vision Res., 12: 395-406.

Peters, A., S.L. Palay and H.deF. Webster. 1976. The Fine Structure of the Nervous System: The Neurons and Supporting Cells. W.B. Saunders Co., Philadelphia.

Pease, D.C. 1964. Histological Techniques for Electron Microscopy. Academic Press, New York.

Purkinje, J.E. 1825. Beobachtungen und Versuche zur Physiologie der Sinne. Zweites Bandchen. G. Reimer, Berlin.

Raviola, E. and R.B. Gilula. 1973. Gap junctions between photoreceptor cells in the vertebrate retina. Proc. Natl. Acad. Sci. USA, 70: 1677-1681.

Rodieck, R.W. 1973. The Vertebrate Retina. Principles of Structure and Function. W.H. Freeman and Co., San Francisco.

Schultze, M. 1866. Aur Anatomie und Physiolgoie der Retina. Arch. Mikr. Anat., 2: 165-286.

Shibkova, S.A. 1971. Retinal ganglion cells in selachia. Arkhiv. Anat. Gist. i Embr., 60: 21-28.

Spekreijse, H., H.G. Wagner and M.L. Wolbarsht. 1972. Spectral and spatial coding of ganglion cell responses in goldfish retina. J. Neurophysiol., 35: 73-86.

Stell, W.K. 1967. The structure and relationships of horizontal cells and photoreceptor-bipolar synaptic complexes in goldfish retina. Am. J. Anat., 121: 410-423.

Stell, W.K. 1972. The structure and morphologic relations of rods and cones in

the retina of the spiny dogfish Squalus. Comp. Biochem. Physiol., 42A: 141-151.

Stell, W.K. 1976. Functional polarization of horizontal cell dendrites in goldfish retina. Invest. Ophthal., 15: 895-908.

Stell, W.K. and P. Witkovsky. 1973a. Retinal structure in the smooth dogfish, Mustelus canis: General description and light microscopy of giant ganglion cells. J. Comp. Neur., 148: 1-31.

Stell, W.K. and P. Witkovsky. 1973b. Retinal structure in the smooth dogfish, Mustelus canis: Light microscopy of photoreceptor and horizontal cells. J. Comp. Neur., 148: 33-45.

Stell, W.K., H.G. Wagner and M.L. Wolbarsht. 1970. Receptive field organization of ganglion cells in the retina of the smooth dogfish, Mustelus canis. Biol. Bull., 139: 437-438.

Stell, W.K., P.B. Detwiler, H.G. Wagner and M.L. Wolbarsht. 1971. Spatial organization and adaptational changes of ON-OFF ganglion cells in Mustelus retina. Biol. Bull., 141: 403-404.

Stell, W.H., P.B. Detwiler, H.G. Wagner and M.L. Wolbarsht. 1975. Giant retinal ganglion cells in dogfish (Mustelus): Electrophysiology of single on-centre units. Vision in Fishes. Plenum Press, New York.

Stone, J. 1973. Sampling properties of microelectrodes assessed in the cat's retina. J. Neurophysiol., 36: 1071-1079.

Tilton, H.B. 1977. Scotopic luminosity function and color mixture data. J. Opt. Soc. Am., 67: 1494-1501.

Tinbergen, N. 1951. The Study of Instinct. Clarendon Press, Oxford.

Toyoda, J.I., T. Saito and H. Kondo. 1978. Three types of horizontal cells in the stingray retina: Their morphology and physiology. J. Comp. Neur., 179: 569-580.

Trezona, P.W. 1970. Rod participation in the "blue" mechanism and its effect on colour matching. Vision Res., 10: 317-332.

Verrier, M.L. 1930. Contribution a l'etude de la vision chez les selachians. Ann. Sci. Natur., 13: 52-63.

Wagner, H.G., E.F. MacNichol, Jr. and M.L. Wolbarsht. 1960. The response properties of single ganglion cells in the goldfish retina. J. Gen. Physiol., 43, part 2, July suppl.: 45-62.

Wagner, H.G., R.G. MacNichol, Jr. and M.L. Wolbarsht. 1963. Functional basis for "on"-center and "off"-center receptive fields in the retina. J. Opt. Soc. Am., 53: 66-70.

Walls, G.L. 1942. The Vertebrate Eye and its Adaptive Radiation. Cranbrook Inst. Science, Bloomfield Hills, Michigan., Reprint Hafner, New York, 1967.

Wang, C.J. 1968. The eye of fishes with special reference to pigment migration. Ph.D. dissertation, Cornell University, Ithaca, New York.

Werblin, F.S. and J.E. Dowling. 1969. Organization of the retina fo the mudpuppy, Necturus maculosus. II. Intracellular recording. J. Neurophysiol., 32: 339-355.

Witkovsky, P. 1965. The spectral sensitivity of retinal ganglion cells in the carp. Vision Res., 5: 603-614.

Witkovsky, P. and W.K. Stell. 1973. Retinal structure in the smooth dogfish, Mustelus canis: Light microscopy of bipolar cells. J. Comp. Neur., 148: 47-59.

Witkovsky, P., F.E. Dudek and H. Ripps. 1975. Slow PIII component of the carp electroretinogram. J. Gen. Physiol., 65: 119-134.

Wyszecki, G. and W.S. Stiles. 1967. Color Science. Concepts and Methods, Quantitative Data and Formulas. John Wiley, New York.

Yamada, E. and T. Ishikawa. 1965. The fine structure of the horizontal cells in some vertebrate retinae. Cold Spring Harb. Symp. Quant. Biol., 30: 383-392.

SECURITY CLASSIFICATION OF THIS PAGE *(When Data Entered)*

REPORT DOCUMENTATION PAGE		READ INSTRUCTIONS BEFORE COMPLETING FORM
1. REPORT NUMBER	2. GOVT ACCESSION NO.	3. RECIPIENT'S CATALOG NUMBER
4. TITLE *(and Subtitle)* Functional Organization of the Retina of the Lemon Shark (Negaprion brevirostris, Poey): An Anatomical and Electrophysiological Approach.		5. TYPE OF REPORT & PERIOD COVERED 1979-1980 6. PERFORMING ORG. REPORT NUMBER
7. AUTHOR(s) Joel L. Cohen		8. CONTRACT OR GRANT NUMBER(s) N00013-75-C-0173
9. PERFORMING ORGANIZATION NAME AND ADDRESS Rosenstiel School of Marine and Atmospheric Science University of Miami, 4600 Rickenbacker Causeway Miami, Florida 33149		10. PROGRAM ELEMENT, PROJECT, TASK AREA & WORK UNIT NUMBERS NR 083-060
11. CONTROLLING OFFICE NAME AND ADDRESS Commander Ronald C. Tipper Biological Oceanography (Code 484), Department of Navy, ONR, NSTL Station, Mississippi 39524		12. REPORT DATE 1980 13. NUMBER OF PAGES 144
14. MONITORING AGENCY NAME & ADDRESS *(if different from Controlling Office)*		15. SECURITY CLASS. *(of this report)* Unclassified 15a. DECLASSIFICATION/DOWNGRADING SCHEDULE

16. DISTRIBUTION STATEMENT *(of this Report)*

Approved for public release, distribution unlimited

17. DISTRIBUTION STATEMENT *(of the abstract entered in Block 20, if different from Report)*

Approved for public release, distribution, unlimited.

18. SUPPLEMENTARY NOTES

19. KEY WORDS *(Continue on reverse side if necessary and identify by block number)*

vision, retina, shark biology, sensory biology, Negaprion brevirostris

20. ABSTRACT *(Continue on reverse side if necessary and identify by block number)*

The retina of the lemon shark (Negaprion brevirostris) was studied by both anatomical electrophysiological techniques. Light and electron microscopy reveal the normal complement of retinal cells found in other vertebrate retinas. The finding of both rod and cone photoreceptor cells was confirmed with the use of the electron microscopic. The interplexiform cell, was described for the first time in an elasmobranch.

DD FORM 1 JAN 73 1473 EDITION OF 1 NOV 65 IS OBSOLETE
S/N 0102-LF-014-6601

SECURITY CLASSIFICATION OF THIS PAGE *(When Data Entered)*

20. Action potentials recorded from the ganglion cells revealed three types of responses: ON, OFF and ON-OFF.

The ON center cells inputs had inputs from both rods and cones. Two classes of OFF center cells were found. One class had input only from one cone type while the second class had input from both rods and cone.

The on component of the ON-OFF units had both rod and cone inputs, while the off component, as with the OFF center units were composed of two classes of units, those with just cone input and those with both rod and cone input.